College of Engineering

Virginia Polytechnic Institute and State University

Blacksburg, Virginia 24061

VPI-E-82-24 SEPTEMBER 1982

ASSESSMENT OF LATERAL AND TORSIONAL STIFFNESS CHARACTERISTICS OF MEDIUM RISE CONCRETE BUILDINGS

by

M. Mirtaheri[1] and P. R. Sparks[2]

Department of Engineering Science and Mechanics

Work supported by:

National Science Foundation Grant No:

CEE-8105784

(1) Graduate Research Assistant

(2) Associate Professor

IOGRAPHIC DATA SHEET	1. Report No. VPI-E-82-24	2.	3. Recipient's Accession No. PB83 101238
Title and Subtitle: Assessment of Lateral and Torsional Stiffness Characteristics of Medium Rise Concrete Buildings			5. Report Date: September 1982 6.
Author(s): M. Mirtaheri and P. R. Sparks			8. Performing Organization Rept. No.
Performing Organization Name and Address: Dept. of Engineering Science and Mechanics College of Engineering Virginia Polytechnic Institute and State University Blacksburg, VA 24061			10. Project/Task/Work Unit No. 11. Contract/Grant No. CEE 8105784
Sponsoring Organization Name and Address: National Science Foundation Washington, D.C. 20550			13. Type of Report & Period Covered: Final June 1981-Sept 1982 14.

Supplementary Notes

Abstracts: Design assumptions for five concrete buildings, each representing a different structural system, were evaluated by comparing theoretical results with experimental data on dynamic characteristics. Initial estimates of the natural frequencies and mode shapes were made by using the TABS-77 program. Model improvements were made by incorporating the effects of "non-structural" partitions and cladding and by considering the efficiency of elevator cores. Improvements were made until theory and experimental results matched for both natural frequencies and mode shapes. Implications of incorrect modelling were investigated for both static and dynamic lateral loadings. This study showed that it is necessary to match both frequencies and mode shapes if an accurate model is desired. Non-structural elements not only add stiffness to the structure but also change the mode shape. Shear lag exists in elevator cores and this should not be neglected. Significant joint rotation can occur in large panel buildings. Considerable inaccuracies are shown to exist in present design practice and this study provides guidance for significantly improving present analytical modelling.

Key Words and Document Analysis. 17a. Descriptors

Building Stiffness
Dynamic Characteristics
Wind Loads
Earthquake Loads
Building Performance
Shear Walls
Shear Lag
Partitions
Vibrator Tests
Full-Scale Testing
Building Natural Frequencies
Building Mode Shapes
System Identification
Computer Analysis

Identifiers/Open-Ended Terms

17c. COSATI Field/Group

18. Availability Statement: Release unlimited	19. Security Class (This Report) UNCLASSIFIED	21. No. of Pages
	20. Security Class (This Page) UNCLASSIFIED	22. Price

ACKNOWLEDGEMENTS

This material is based upon work supported by the National Science Foundation under Grant CEE-8105784. This support is gratefully acknowledged. The authors would also like to acknowledge the assistance provided by Dr. C. Williams of Plymouth Polytechnic, Dr. B. E. Lee of Sheffield University and the staff of the Building Research Establishment in providing information about the buildings investigated.

TABLE OF CONTENTS

LIST OF TABLES

LIST OF FIGURES

CHAPTER I. INTRODUCTION

1.1 Statement of the Problem

The fact that most major buildings are one of a kind imposes certain limitations on the structural design process but as seen by some also bestows certain advantages on the Structural Engineer.

It is normal practice in those areas of engineering where large production runs are made, for example in the aircraft or automotive industries, to incorporate testing of prototypes in the design process. Since the Structural Engineer is not likely to repeat a particular building, he generally feels that it is unecessary to even consider how his structure actually performs. Indeed a request to investigate its performance may plant the seeds of doubt about his competence in the mind of the building owner. Most Structural Engineers, for no good scientific reason, have implicit faith in their designs, particularly in recent years when large computer programs for structural analysis have become available to the profession.

In the days when structural systems were designed by slide rule or desk calculator, the design of a multistoried building was very much an art and the designer was fully aware of both the lack of precision and the lack of accuracy in his work. Accordingly, he combined his calculations with what he knew to be traditionally good practice and used his art to produce a finished design. Now many structural systems are designed with the aid of elaborate computer programs. These programs can produce results which are mathematically very precise but

they probably describe the actual performance of the structure no more accurately than the more traditional methods, since they can be no more accurate than the information fed into the program. Unfortunately, the Engineers using the programs often do not have sufficient experience or information about the performance of actual buildings to feed the computer the proper input. Unless the program is supplied with appropriate descriptions of the properties of all elements comprising the structural system, the output, however precise, cannot represent actual conditions. The very precision of computer output can lull Structural Engineers into a false sense of accuracy, and they may be tempted to reduce the factors of safety accordingly.

Clearly if buildings of the future are to be safe and efficient a knowledge of the accuracy of current analytical procedures is required.

1.2 Current State of Knowledge

Typical of the current structural analysis programs available to the building designer are general purpose three dimensional programs such as STRUDL, STRESS, and TABS. These programs are reasonably sophisticated and are certainly elaborate but, as they are normally used, they neglect all parts of buildings that are considered non-structural. Also they generally assume that each member is fully effective. These shortcomings of the programs could be alleviated somewhat by the programmer for there is some limited information available to enable these factors to be taken into account.

Traditionally the partitions used as infilling for frames and external cladding have been neglected in analysis because including them complicates an already complex problem. Further, it was considered that ignoring any contribution they might have made to the stiffness of the structure was conservative. Over the last thirty years a few papers have appeared indicating serious concern about this neglected portion of the structural systems. As long ago as 1961 Holmes (1) presented a technique for utilizing a notional equivalent strut to replace the effect of infill walls on steel frames. The next year Smith (2) adapted Holmes' work to infill partitions and frames constructed from various materials, and in 1971 Mallick and Garg (3) improved upon the previous publications concerning the effects of infill partitions, by presenting a technique for evaluating the effects of openings such as doors and windows in the infill walls. Each of these techniques was developed and then evaluated through experimental model techniques.

In 1972 Blume (4) performed full-scale tests on two identical four story buildings. He used several different types of materials as infilling for the frames. He showed the effects of each of these materials on the dynamic characteristics of the structure. Blume is one of the few researchers who have performed tests on full-scale buildings.

Gjelsvik (5), in 1974, presented an analysis of steel frames with concrete infill partitions. He analyzed the interaction between the steel frame and the precast concrete panel walls used for infill. His work shows that the strength and rigidity imparted by the infill wall are indeed important to proper analysis of a structural system.

El-Dakhakhni (6,7) in the mid-70's accepted the importance of the contribution of exterior curtain walls or cladding and interior partitions to the structural system and incorporated them in an analysis.

Oppenheim (8) in the early 70's published a number of papers on the effects of cladding on the behavior of tall structures. He states that cladding not only stiffens structures but also can induce high axial forces as a result of changing deflection modes.

Traditionally designers in analysing flat plate buildings have intuitively assumed that only a portion of the slab width will act as a beam element with the columns in frame action. Khan and Sbarounis (9) examined this problem in 1964 and reported an approximation based on a theoretical study for the equivalent effective width of slab to be used as a beam. Their results are available in the form of charts and tables so that if the width-to-span ratio is known for the slab, then the effective width can be easily calculated.

Much has been published on the analysis of shear wall structures starting in the 1940's. Coull and Smith (10) have presented a good review of research in this area. Much of this theory is included in presently available computer programs used in structural design and analysis.

Shear walls are traditionally assumed to be highly efficient ways of providing lateral stiffness and at the same time forming elevator cores and external cladding. Even though these walls often form essentially thin walled members the literature appears not to contain any indication that shear lag might reduce their effective stiffness.

Although rarely used, procedures are available for evaluating the actual lateral and torsional stiffness characteristics of buildings by determining natural frequencies and mode shapes. Starting in the late 1950's Hudson at the California Institute of Technology developed an eccentric mass vibrator system to evaluate the dynamic characteristics of structures using a resonance technique. In general this type of testing system has a number of advantages. Building resonance permits a high response for a low load, the system is easily controllable, and mode shapes can be measured accurately with relatively few devices such as accelerometers.

As data recording techniques improved another method of evaluating building characteristics which had been used as long ago as the 1930's, became attractive. This method simply uses ambient vibrations induced by wind and earth tremors, but the response of the building has to be recorded over a long period of time for statistically meaningful results. This method also requires a large number of accelerometers to remain in place during the observation period, and elaborate spectral analysis equipment is required to evaluate the data. Williams (11) reviewed the above methods and several others such as using the reaction from the force produced by rhythmical motion of one or more human bodies, that produced by sudden release of a cable with a known force in it which had been attached to the structure, and that produced by the explosive reactions from rocket engines. Each of these later methods lacks the controllability of the eccentric-mass vibrator system.

There has been considerable interest in recent years in the use of formal system identification procedures. Baruh (12) provides a good introduction to these procedures. In general these procedures require the identification of large numbers of natural frequencies and mode shapes (eigenvalues and eigenvectors). The approach is principally a mathematical one where an accurate stiffness matrix is sought with little regard to what might physically generate that stiffness matrix. While such methods appear theoretically attractive, it seems not to have been possible to apply them successfully to real building structures since suitable information on higher modes is not available.

When a full set of eigenvectors and eigenvalues is not availavble it is necessary to make an initial estimate of the parameters by some means and use iterative procedures to improve the initial estimates, based on the observed dynamic characteristics of the structure. As Baruh pointed out, this will lead to errors in the higher eigenvalues and eigenvectors. However, for buildings this is of little consequence since they are rarely excited in their higher modes because the spectra of natural loadings, such as wind and earthquakes, contain little energy at higher frequencies.

Goodno and Will (13) in 1978 carried out just this sort of iterative procedure, adjusting an initial estimate of natural frequency to a more accurate value by incorporating cladding-structure interaction effects after the initial trial was completed. The following year, Will, Goodno, and Saurer (14) reported further theoretical justification for the adjustments that had been made to account for cladding

effects. However only frequencies were matched without regard to mode shapes.

1.3 Scope and Purpose of this Study

Although rarely of a quantitative nature the information contained in the literature clearly indicates that one might expect that actual building performance would differ significantly from that assumed in design. Effects of partitions, cladding and so forth are likely to effect principally the lateral and torsional resistance of the structure which is of particular importance in assessing the ability of buildings to resist wind and earthquake loads.

In this thesis use will be made of some of the few published measurements of the lateral and torsional dynamic characteristics of buildings to establish accurate analytical models of the structures.

Recognizing the difficulty inherent in the application of a full system identification approach, the lateral and torsional stiffness characteristics of the buildings will be determined using observed data on their actual fundamental mode shapes and frequencies. Initial estimates of characteristics will be obtained using a TABS-77 program. Improvements will then be made in the analytical models by incorporating 'non-structural' elements or by reducing the efficiency of certain members until the fundametal mode shapes and frequencies are matched. Implications of incorrect modelling at the design stage will then be investigated for both static and dynamic lateral loadings.

The buildings to be studied which are all medium rise and made of reinforced concrete,are as follows:

1. A dormitory building in which the flat slab floors form the framing between the shear walls and columns and extensive blockwork partitions are present.
2. An office building with ribbed floors and flat slab floors, beams framing between shear walls and columns and a few blockwork partitions are present.
3. An office building with similiar ribbed and flat slab floors as in type 2, but with extensive, elaborate, shear-wall cores and no partitions.
4. A university building of the tube-in-tube type with extensive partitions and stiff cladding between closely-spaced exterior columns.
5. A 1/4-scale model of a precast large-panel apartment building, consisting entirely of shear walls and floors with no beams, columns, partitions, or cladding.

CHAPTER II. THEORETICAL CONSIDERATIONS

Several requirements had to be met by any technique used for analysis of the medium rise concrete structures chosen for study. The only practical approach was to use an existing computer program that was capable of meeting the requirements. The selected program had to be able to predict natural frequencies and mode shapes for each structure, and perform both lateral static load analysis and dynamic response analysis. In addition, the selected program had to have sufficient capacity to cope with the buildings under investigation, must have been tested in practice through use in the Structural Engineering profession, must be modern and current, and must, of course, be available. TABS-77 was selected for use but this does not mean that some other program might not have been equally suitable.

2.1 The TABS-77 Program

According to the TABS-77 program manual developed by Wilson, Dovey, and Habibullah (15) at the University of California in Berkeley, many different programs exist for the analysis of three dimensional buildings, and each of them have some strong points and some weak points. TABS-77 was developed to take advantage of the better features of some of these programs and to avoid most of the difficulties encountered in using other derivative programs. It was also specially formulated for standard frame and shear-wall buildings.

TABS-77 utilizes matrix theory for three dimensional linear analysis of building systems. This procedure and program analyses both frame and shear wall structures subjected to both static and earthquake loadings. The program assumes the structure can be idealized as a system of independent frame and shear wall elements, interconnected by floors which act as diaphragms rigid in their own planes. Bending, axial, and shearing deformations are included for each column but axial deformations are neglected for beam elements. TABS-77 does not enforce compatibility with regard to joint displacements at joints which are common to more than one frame. Thus axial deformations in columns common to frames in two directions will not be the same in both frames; however for design purposes, these column axial forces may be added directly to give reasonable results. The formulation includes finite column and beam widths. The program permits consideration of nonsymmetric buildings which have frames and shear walls located arbitrarily in plan.

Of principal interest in matching observed data was the ability of the program to evaluate three dimensional mode shapes and frequencies. Static lateral loading is possible in two directions either together or one at a time. Lateral earthquake loadings in any direction can be specified as time-dependent ground accelerations.

Since this section reviews some of the theoretical background of the TABS-77 program and reference (15) is basic for this task, information from Wilson, Dovey, and Habibullah is used freely throughout the remainder of this section.

The TABS-77 program computes the stiffness of each individual structural element comprising a frame, and then, in order to combine the frame lateral stiffness matrices into a complete structure lateral stiffness matrix, each of the frame stiffnesses is transformed to a common displacement coordinate system which is commonly called the global system. The TABS-77 program utilizes two horizontal translations and one rotation for each story for the global system. The origins of the global displacement coordinates for each story are chosen so that the mass matrix required for dynamic analysis is a diagonal matrix which simplifies the eigenvalue solution. The structure's lateral stiffness is assembled by the addition of components from all frames so that

$$\underline{K} = \sum_i \underline{k}_i$$

For dynamic analysis the mass of each story is assumed to be lumped at each floor level. The equilibrium equations for a structure, including dynamic effects, may be written in the following form:

$$\underline{M}\,\ddot{\underline{r}}_a + \underline{C}\,\dot{\underline{r}} + \underline{K}\,\underline{r} = \underline{P}(t) \qquad (2.1)$$

where $\underline{M}$ = mass matrix

$\underline{C}$ = damping

$\underline{K}$ = stiffness matrix

$\underline{P}(t)$ = applied load vector, which may be time varying

$\underline{r}$ = displacement vector of deformation relative to support motion

$\ddot{r}_a$ = absolute acceleration vector

r and r_a are related in the following fashion

$$r_a = v_g + r \tag{2.2}$$

where v_g is the vector of pseudo-static displacements due to support movement. Also

$$\ddot{r}_a = \ddot{v}_g + \ddot{r} \tag{2.3}$$

The vibration mode shapes represent the solution of the undamped free vibration problem given by

$$M \ddot{r} + K r = 0 \tag{2.4}$$

The eigenvalue problem to be solved is written as

$$K \phi = \omega^2 M \phi \tag{2.5}$$

where ϕ = mode shapes

ω = circular natural frequencies

The mode shapes are normalized such that

$$\phi^T M \phi = I \tag{2.6}$$

then also

$$\underline{\phi}^T \underline{K} \underline{\phi} = \underline{\omega}^2 \tag{2.7}$$

Also, it is assumed that the damping matrix $\underline{C}$ is of a form that is uncoupled by the mode shapes; specifically it is assumed that

$$\underline{\phi}^T \underline{C} \underline{\phi} = [2\zeta_m \omega_m] \tag{2.8}$$

so that ζ_m represents the damping of the m^{th} mode.

The actual displacements, $\underline{r}$, are now expressed as a linear combination of the mode shapes.

$$\underline{r} = [\underline{\phi}_1 \; \underline{\phi}_2 \; \underline{\phi}_3 \cdots \underline{\phi}_N] \begin{bmatrix} Z_1(t) \\ Z_2(t) \\ \vdots \\ Z_N(t) \end{bmatrix} \tag{2.9}$$

i.e. $\underline{r} = \underline{\phi} \; \underline{Z}$

also $\dot{\underline{r}} = \underline{\phi} \; \dot{\underline{Z}}$

and $\ddot{\underline{r}} = \underline{\phi} \; \ddot{\underline{Z}}$

where $Z_m(t)$ represents the response of the m^{th} mode.

The above equations describe the method of attack used by TABS-77 in solving the eigenvalue problem. The program computes periods and

elevation and plan mode shapes. It also calculates the displacement of each frame and evaluates member forces for both static and earthquake loadings.

2.2 Forced Vibration Tests by Eccentric Mass Vibrators

Although the acquisition of full-scale data was not included in this project, it is considered appropriate to include a description of the general methods used to acquire the data. All data used were acquired using eccentric mass vibrators and accelerometers.

A good description of forced vibrations as induced by eccentric mass vibrators was given by Jeary and Sparks (16) in 1979. They state that early vibrator tests were conducted by using single-rotating-mass vibrators. These early researchers relied on the resonances of the tested structures to produce essentially unidirectional responses. For more complex structures the single mass vibrators were unsatisfactory and later tests utilized vibrators with two counter-rotating masses which provided sinusoidally varying unidirectional forces. These two mass vibrators overcame the problem of exciting modes in all directions at the same time which was inherent in the single mass vibrator.

Jeary and Sparks outline the normal procedure for performing a vibrator test. The vibrator is attached to the structure at a suitably high position near the top of the structure. The force from the vibrator is transmitted to the building through its mounting. Testing takes on two distinct aspects. First the investigator searches for resonant frequencies and then detailed measurements are made at

appropriate points so that mode shape can be determined. This sequence is commonly followed for each resonance in turn.

As stated in reference (16) the search for resonant frequencies is initiated by starting the vibrator and setting it to some low frequency, less than the lowest expected resonance frequency but high enough for the vibrator to generate sufficient force for the structure's response to be detected by the monitoring accelerometers. The frequency generated is incrementally increased, and the accelerometers placed strategically around the structure, note the maximum responses.

Next a detailed investigation is made of the mode shape in a given direction. This involves setting the vibrator to a resonant frequency and placing an accelerometer at various locations in turn, to permit a comparison to be made of its response with that of a reference accelerometer placed near the top of the building.

When sufficient data has been collected for each mode shape, the vibrator is stopped suddenly, and the decay of the oscillation is noted for the estimation of the structural damping.

For optimum results there should be no wind while these tests are being conducted. Any wind excitation can introduce undesired response.

According to Jeary and Sparks the results of such testing as is described above can be interpreted on the basis of assuming that the response in each mode is given by the solution to the following differential equation.

$$\ddot{x}_r + 4\pi\zeta_r f_r \dot{x}_r + 4\pi^2 f_r^2 x_r = \frac{F_r}{M_r} \qquad (2.10)$$

where X_r is the modal response,

f_r is the modal frequency,

M_r is the modal mass,

ζ_r is the modal damping,

and F_r is the modal force.

A solution to equation (2.10) in the frequency domain is

$$X_r(f) = |H_r(F)|\ F_r(f) \tag{2.11}$$

where

$$\frac{1}{|H_r(f)|} = 4\pi^2 f_r^2 M_r \left\{ \left[1 - \left(\frac{f}{f_r}\right)^2 \right]^2 + \left[2\zeta_r \left(\frac{f}{f_r}\right) \right]^2 \right\}^{1/2} \tag{2.12}$$

At resonance, in the vibrator tests, the force is sinusoidal and is applied at the frequency, f_r, with a modal amplitude of F_r. The maximum modal displacement response, $\hat{X}_r$, is given by

$$\hat{X}_r = \frac{\hat{F}_r}{8\zeta_r \pi^2 f_r^2 M_r} \tag{2.13}$$

with a maximum acceleration response of

$$\ddot{\hat{X}}_r = \frac{\hat{F}_r}{2\zeta_r M_r} \tag{2.14}$$

Equation (2.14) can be used to determine the modal mass of the structure and from it, using the following relationship, the modal stiffness can be determined:

$$K_r = 4\pi^2 f_r^2 M_r \tag{2.15}$$

It should be observed that if the maximum acceleration response equation, equation (2.14), is used to compute modal mass, then the frequencies in different directions should be well separated, and there should be no coupling between the modes in the various directions, since modal interference can occur. When this happens excitation in one mode might causes some excitation in the other modes. In addition, if the level of excitation induced by the vibrators is low, extraneous excitation resulting from ambient wind or other extrinsic sources may induce intolerable errors. Further, measurements of damping are subject to considerable error.

In many instances it is advantageous to estimate the mass distribution from structural drawings and use equation (2.16) below for the calculation of modal mass.

$$M_r = \int_0^H m(Z)\phi_r^2(Z)dZ \tag{2.16}$$

where m(Z) is the mass per unit height of the building.

When this equation is utilized the only experimental measurements required are the resonant frequencies along with the corresponding relative accelerations of the floors which provide the mode shapes.

2.3 Matching Procedure

The general procedure followed in matching experimental results with the TABS-77 analytical model was to input mass distribution and stiffness parameters in the analytical model. Mass distribution may be well estimated from the structural drawings while stiffness parameters are subject to engineering interpretation. Thus the mass input was held constant and the analytical model was changed by modifying the stiffness parameters. In general the first analytical model was constructed using traditional idealizations for the stiffness parameters. If the resulting model did not closely match the experimental results, then the stiffness parameters were varied in a logical manner and in accordance with theoretical guidelines until not only the frequencies but also the mode shapes were closely matched for each of the structures included in this study.

CHAPTER III. THE RESIDENTIAL NAUTICAL COLLEGE

3.1 Building Location and Geometry

The Residential Nautical College (R. N. C.) building in Plymouth, England, is a dormitory building in which the flat slab floors form the framing between the shear walls and columns. This is an example of a medium-rise concrete building containing extensive blockwork partitions. This eleven story structure is used as accomodation for students. It is situated on the side of a small hill and it is relatively exposed to the wind. On one side only it is faced by some quite tall structures, one of which is about two-thirds the height of the R. N. C.

The R. N. C. is rectangular in section. Figures 3.1, 3.2, and 3.3 show a typical floor plan and two elevations. Figure 3.1 shows that the main shear walls occur at the ends of the structure in the shape of a 'T', and that the elevator shaft is positioned so that it is offset from both the x and y axes. The remainder of the structure is of column and slab construction. In Figure 3.1, column rows A and D are the outside rows with each column 0.3 m by 0.3 m. The interior columns in row B are 0.6 m by 0.3 m while those in row C are 0.45 m by 0.23 m. The floor slab is 0.175 m thick and all floor slabs are of this same thickness.

This building is founded on shillet (a local term used to describe weathered shale), and the column foundations are individual spread footings.

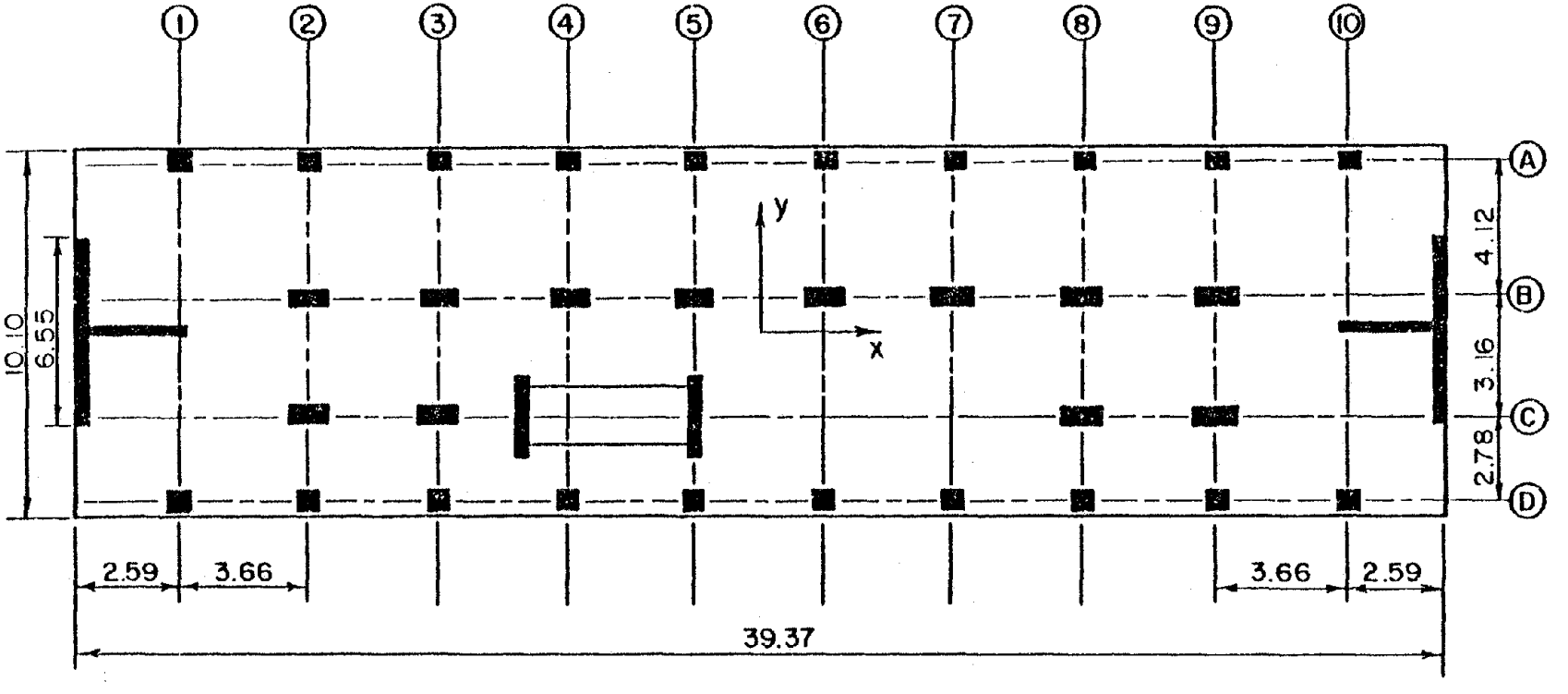

Figure 3.1. Typical Plan View of the Residential Nautical College (All Dimensions in Meters).

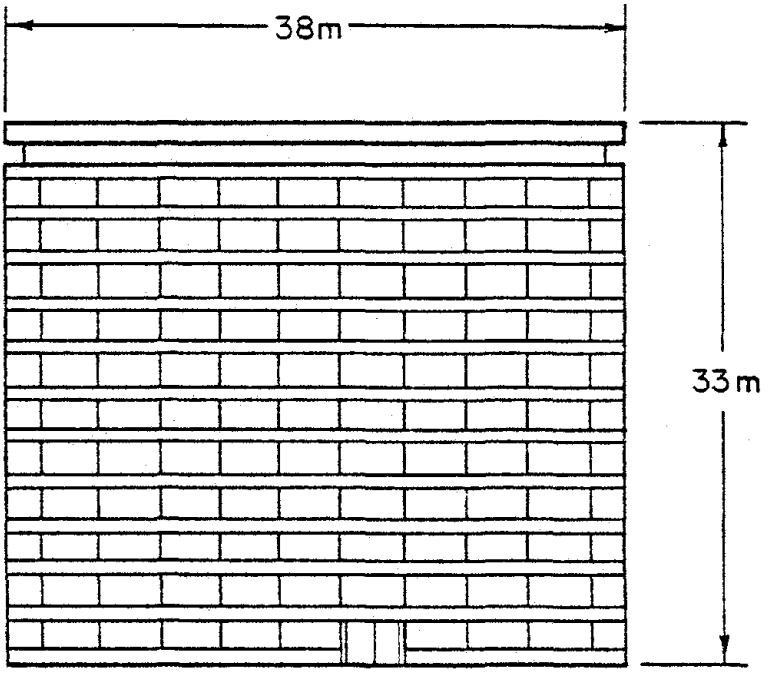

Figure 3.2. Elevation View of the Residential Nautical College in the Long Direction.

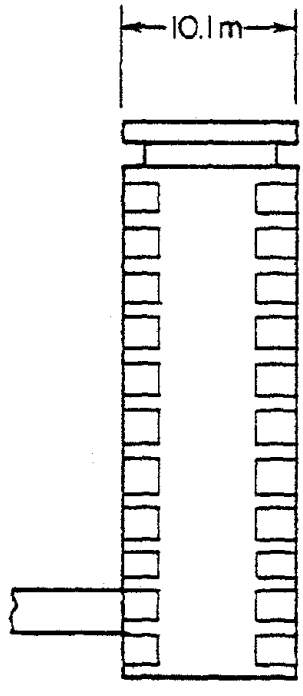

Figure 3.3. Elevation View of the Residential Nautical College in the Short Direction.

3.2 Partitions and cladding

The R. N. C. structure has many internal partitions. Its light outside cladding is connected to the floor slabs. This is indicated in Figure 3.2 and 3.3.

Figure 3.4 shows the location of the infill walls contained in row B, and the transverse partition walls. All partitions have a thickness of 0.2 m.

3.3 Experimental Procedure

For the R. N. C. building, a small contra-rotating mass vibrator was used for test purposes. The technique described in section 2.2 was applied to obtain the dynamic characteristics of the structure. The position of the vibrator on the building was determined by an available open space on the top floor near the center of the building. This central location coupled with wind conditions existing at the time of the test prevented excitation in torsional modes. The details of this test and the experimental results are given by Jeary and Sparks (16).

3.4 Structural Analysis of the R. N. C. Building

In this section some designer idealizations are postulated and the results of a TABS-77 analysis for each idealizations are presented. Then modifications to the input parameters are made in an attempt to match the predicted and observed natural frequencies and mode shapes. A parametric study is then made to give an indication of the importance of each parameter. Following that, some analyses are presented indicating the significance of variations from the correct model.

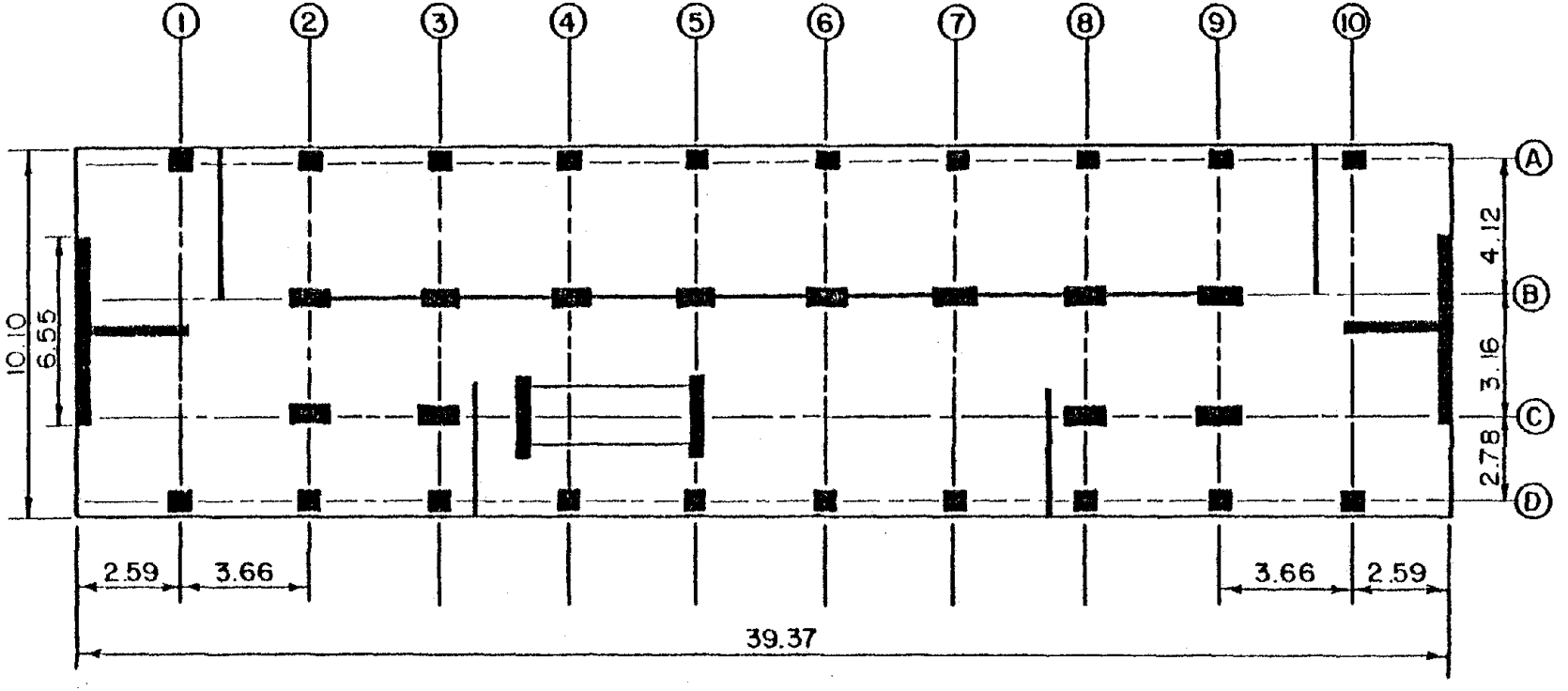

Figure 3.4. Locations of Internal Partitions in the Residential Nautical College.

3.4.1 Traditional Structural System Idealization

Traditionally the structural designer would idealize the structural system of the R. N. C. building as some variation of a 'bare frame' system. A bare frame structural idealization is defined as one that considers only those structural elements such as beams, columns, portions of slabs and shear walls which in this case are designed to resist lateral loads.

3.4.1.1 Designer Idealizations

Consideration will be given to the structural system in 1) the x (longintudinal) direction and 2) the y (transverse) direction. In the x direction one possible idealization is to consider the building to be a series of parallel frames along the column rows. Recommended values for an effective slab width to be included in each frame are given by Khan (9). This will be referred to idealization type AX. Type AX idealization is shown in Figure 3.5 indicating the effective slab widths used.

Another and perhaps better designer idealization would be to include the two end shear walls into frame line B rather than assuming the shear walls to be a separate and independent column row as was done in the type AX. This idealization is referred to as type BX and is shown in Figure 3.6.

In the y direction it is assumed that the traditional designer would idealize the system as a series of parallel frames acting independently of each other with the two end walls each assumed to be

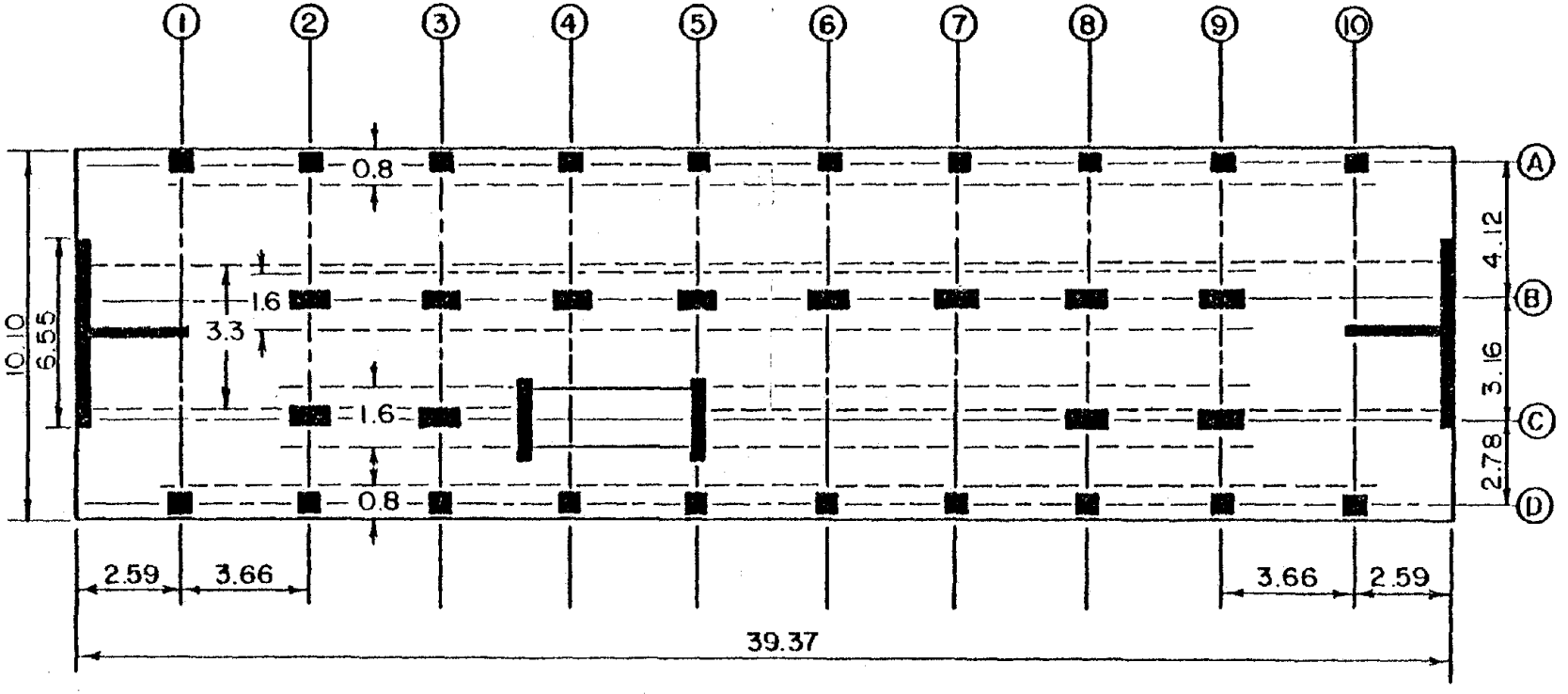

Figure 3.5. AX Structural Idealization for the Residential Nautical College.

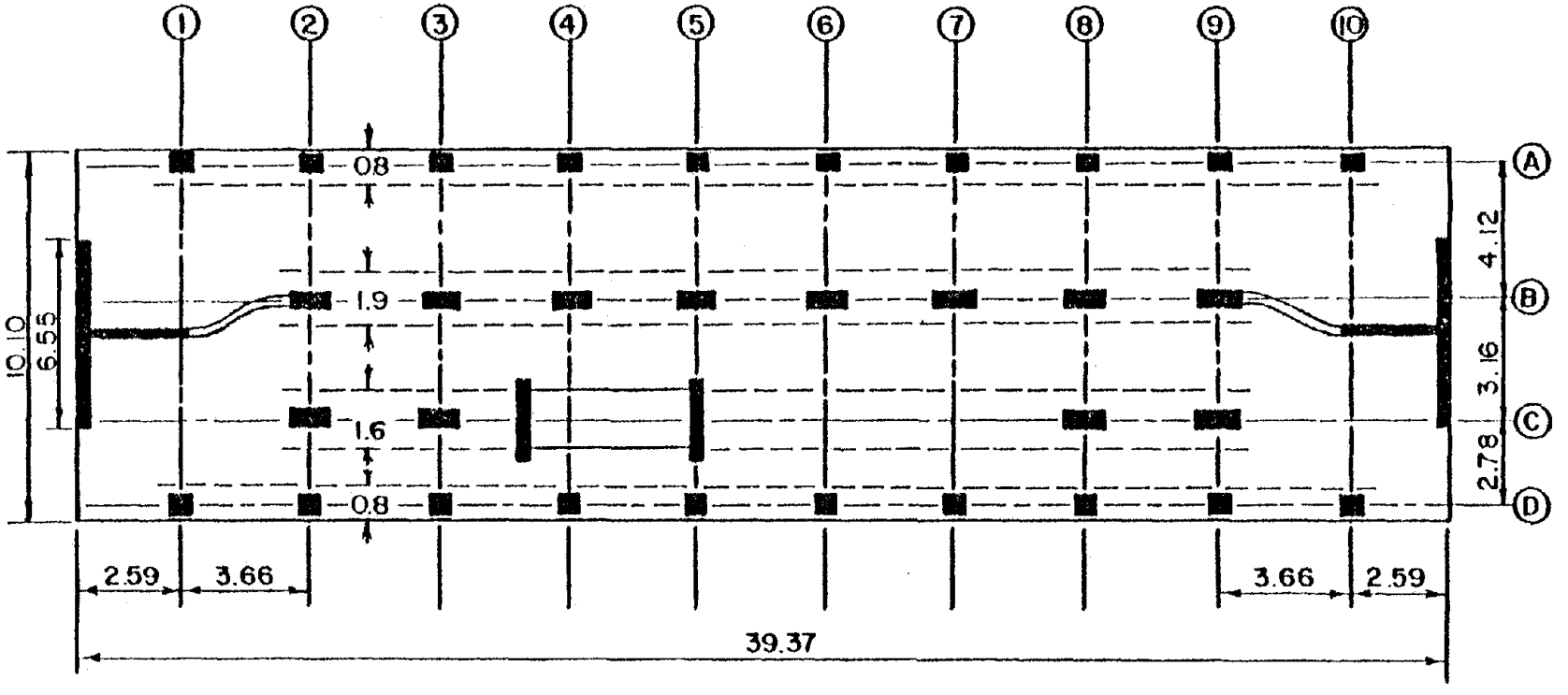

Figure 3.6. BX Structural Idealization for the Residential Nautical College.

single columns. Again, the effective slab widths were calculated in accordance with Kahn's recommendations (9). This idealization is shown in Figure 3.7.

3.4.1.2 Experimental Results vs. bare Frame Predictions

Table 3.1 shows the experimental values determined for the natural frequencies of the R. N. C. building along with the predicted values for the bare frame idealizations. The comparisons, which will be discussed later, are obvious.

TABLE 3.1 Measured and Predicted Fundamental Frequencies

Type of Analysis	Direction	Frequency Hz
experimental	x	1.97
	y	1.33
AX	x	0.9
BX	x	1.05
AY	y	1.04

Natural frequency comparisons are useful but this is not the only comparison that can be made. Enough measurements were made by Jeary and Sparks (16) and sufficient deflections were calculated using TABS-77 to determine the mode shapes. Deflection measurements and calculations were normalized so that comparisons between the various idealizations could be made. The deflection at any level, δ, was divided by the deflection at the top, δ_h. The building elevation is also normalized.

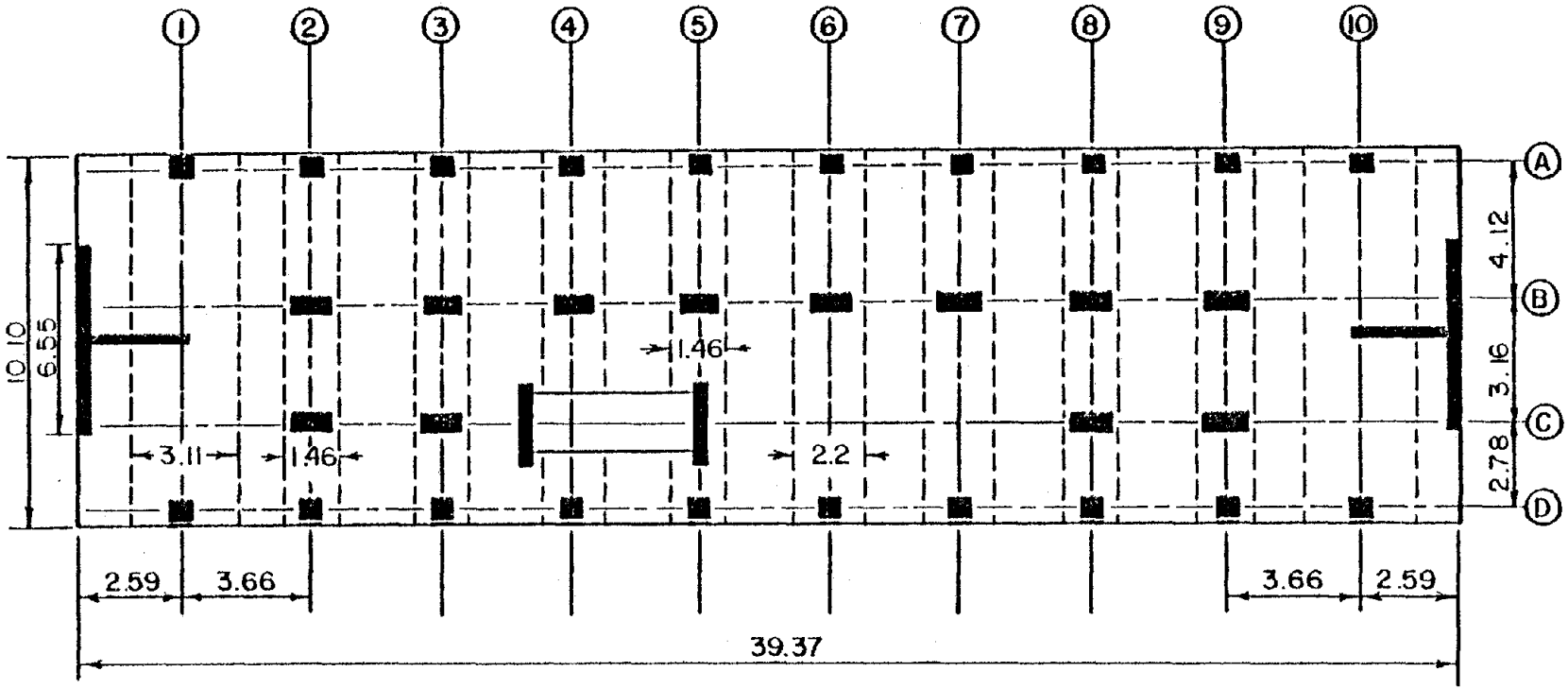

Figure 3.7. AY Structural Idealization for the Residential Nautical College.

If the elevation of each floor is z and the total height to the top of the structure is h, the normalized elevation is z/h.

The normalized plots in Figure 3.8 show the mode shape obtained from experimental measurements and those computed using the idealizations of type AX and BX. The measured mode shape indicates that shear deformation is dominant, and this is due to relative motion between the floors. This is typical of the way framing action affects mode shape. However, the mode shapes produced by TABS-77 for both AX and BX types of idealization are more or less straight lines. This is an indication of interaction of the shear walls with the frame. This results from the fact that the frame tends to reduce the lateral deflection of the shear wall at the top while the shear wall lends lateral support to the frame near the base.

In the x direction the agreement between actual and predicted mode shapes leaves something to be desired, but in the y direction there is reasonable agreement betweeen measured and predicted mode shapes. The normalized plots for the y direction are shown in Figure 3.9.

The agreement between experimental and predicted shapes is an indication that the idealizaiton in the y direction and the method of calculation is valid for this case.

Considering the measured experimental results and comparing them with the predictions based on the bare frame idealizations, the following comments can be made:

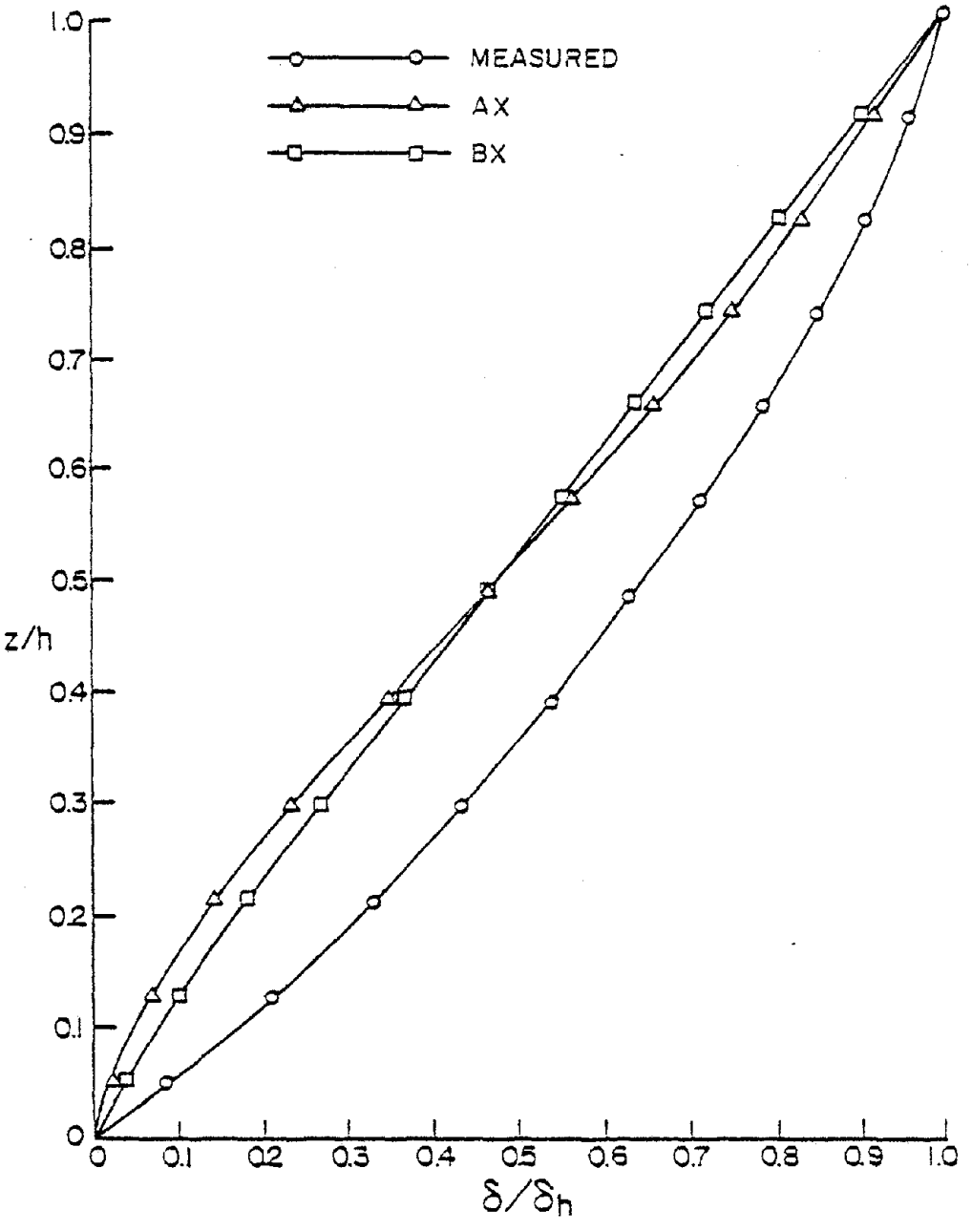

Figure 3.8. X Mode Shapes for the Residential Nautical College.

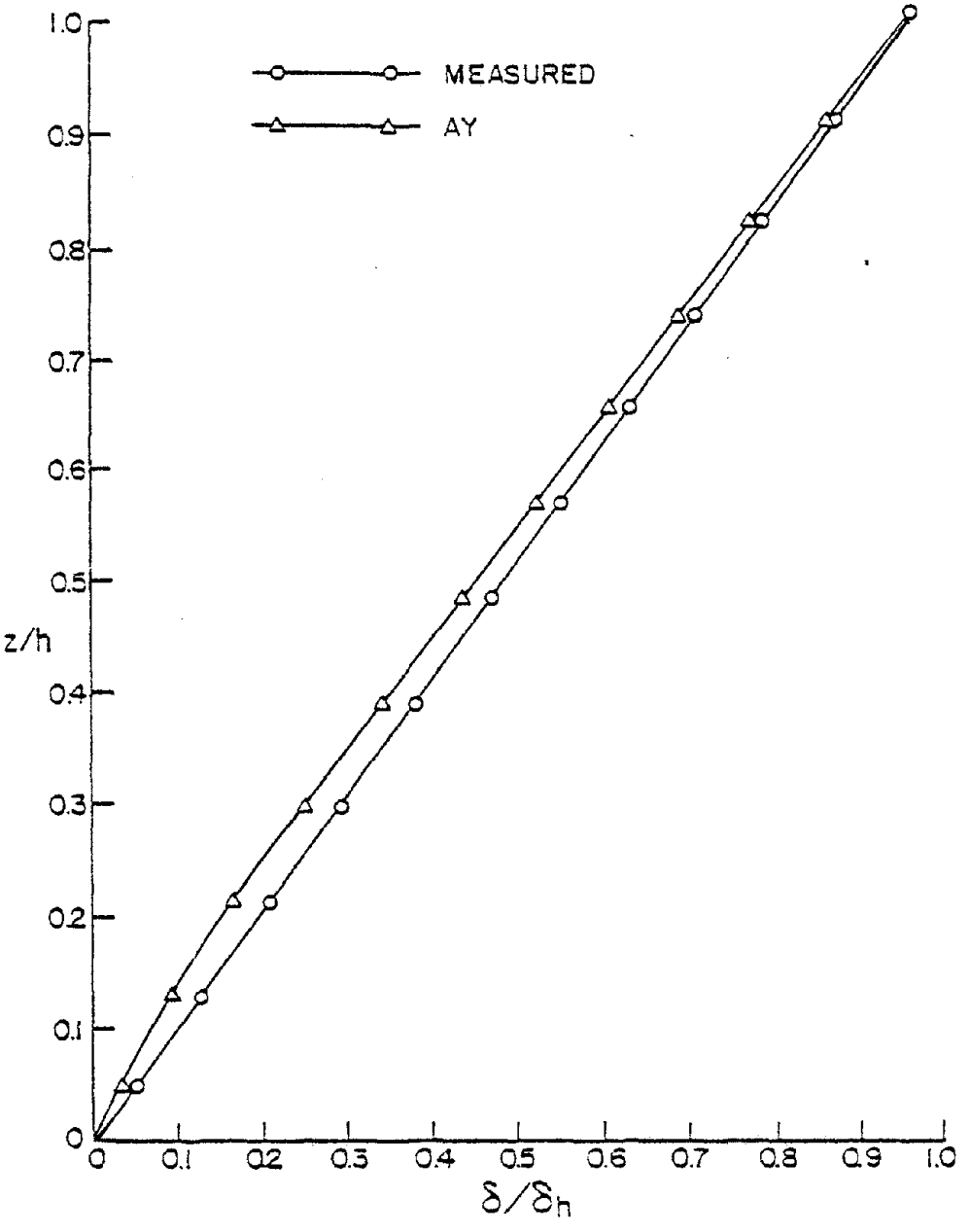

Figure 3.9. Y Mode Shapes for the Residential Nautical College.

1. The bare frame idealization badly underestimates the natural frequency of the R. N. C. building. The actual natural frequency in the x direction is twice the predicted value. Thus the actual stiffness is about four times the predicted stiffness in this direction. In the y direction the predictions are better but still not good for the actual frequency is 1.3 times the predicted value.
2. The predicted mode shape is equally important to the frequency prediction. In the x direction, very poor agreement with the measured values was obtained. In the y direction the agreement is considered to be reasonably good.

3.4.2 Modifications to the Bare Frame Models

The next obvious step was to try to add extra stiffness to the building in a reasonable way, since the stiffness was underestimated in all models and directions analysed. In addition, alterations had to be made in the x direction so that the mode shape prediction more closely match the actual mode shape. The literature search discussed in detail in Chapter I showed that there have been only two significant and comprehensive papers addressing this problem within the last decade. These papers are the one by Smith (2) and the one by Mallick (3). Other references exist but they are prior to these two papers and appropriate parts of the prior papers have been integrated into those by Smith and by Mallick.

Smith recommends that the effects of infill walls in a frame be approximated by adding to the frame idealization an equivalent strut wherever the infill wall appears. He also gives appropriate formulae so that the equivalent strut can be sized. This would add lateral stiffness to the frame. Thus, adding equivalent struts at infill wall sites was selected as the first modification to the bare frame model. The bare frame idealizations AX and BX were affected by this modification and these new idealizations are referred to as types AX1 and BX1.

Mallick recommends that openings in infill walls should affect the sizing of the equivalent struts determined in accordance with Smith's recommendations. Mallick presents charts which determine the reductions in sizing to account for the opening effects.

The results of the first modification using the full diagonal struts yielded an excellent match with the measured frequency in the x direction. If Mallick's recommendations were to be applied as he has made them, it would obviously lower the predicted frequency. Therefore, an examination of the real building with infill walls stacked continuously from the bottom floor to the roof suggested that the floor slabs under the infill walls were not free to bend and this should have some important influence on stiffness distribution and should increase the overall lateral stiffness. Accordingly, Mallick's recommendations were used with the added modification of taking the floor slab acting in frame line B as being effectively infinitely stiff. Thus, the second modification is a refinement of the first modification so that openings

in infill walls can be accomodated along with the increased stiffness in the slab resulting from the influence of the infill walls. These new idealiations are referred to as types AX2 and BX2.

3.4.2.1 Experimental Results vs. Modified Frames AX1 and AX2

Figures 3.10 shows the idealization for type AX1, and Figure 3.11 shows the idealization for type AX2. The first modification sized the equivalent struts in acordance with Smith's recommendation, and the second modification reduced the equivalent strut width in accordance with Mallick's recommendations, in this case to 30% of the original value. The slab along frame B was assumed to be infinitely stiff.

Table 3.2 shows the results of TABS-77 predictions with these idealizations. A glance at Table 3.2 shows that both modifications for types AX1 and AX2 resulted in excellent predictions for the frequency for they are identical to the measured values. As far as frequencies are concerned, both modifications are vast improvements over the bare frame or AX idealization.

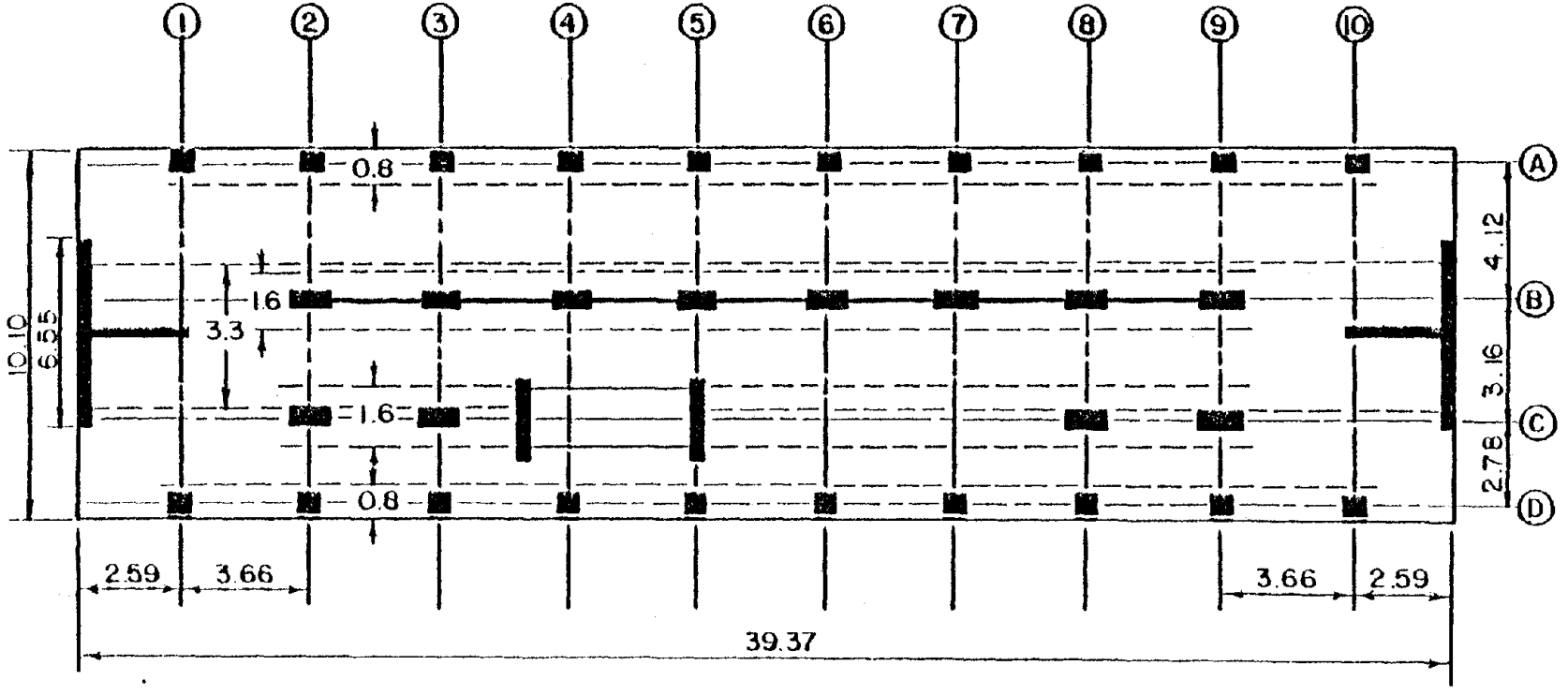

Figure 3.10. AX1 Structural Idealization for the Residential Nautical College.

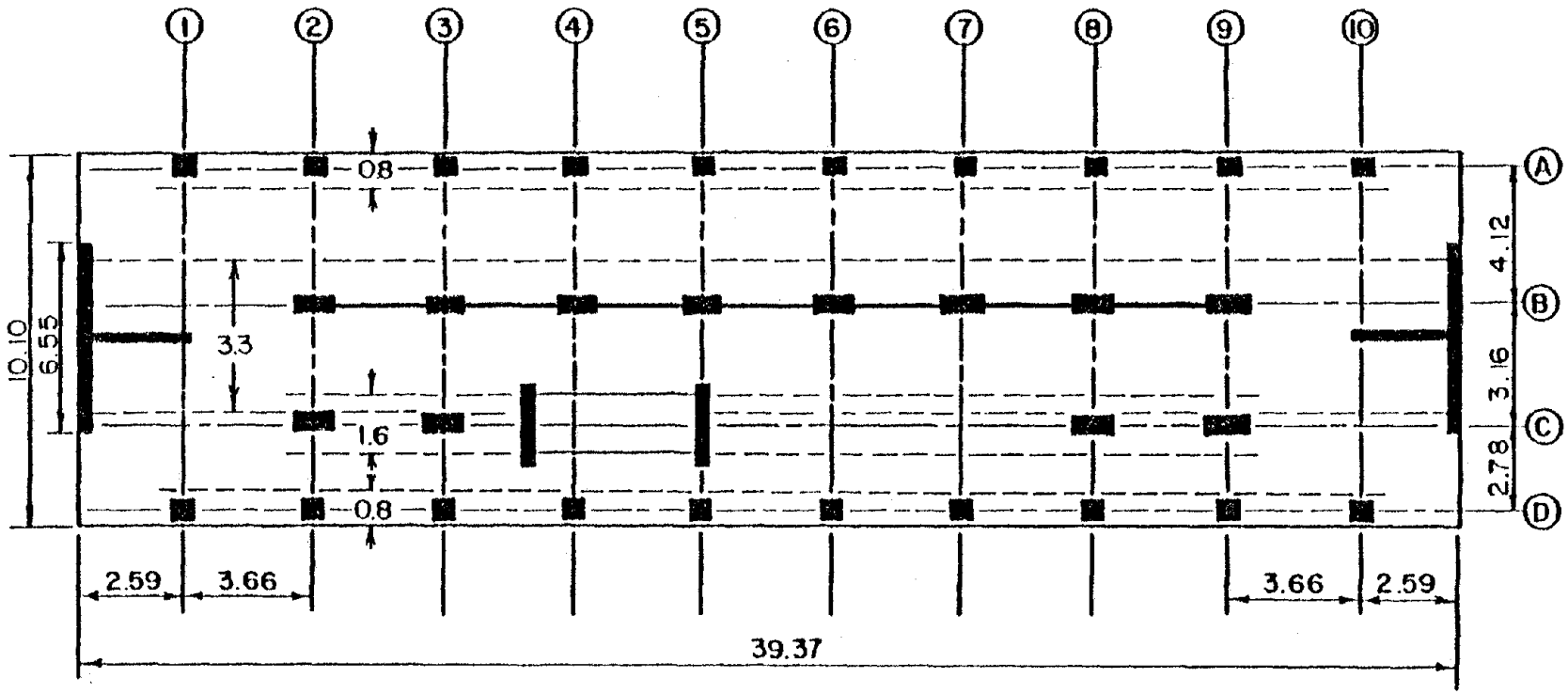

Figure 3.11. AX2 Structural Idealization for the Residential Nautical College.

TABLE 3.2 Measured and Predicted Fundamental Natural Frequencies

Type of Analysis	Direction	Frequency Hz
experiment	x	1.97
AX	x	0.9
AX1	x	1.97
AX2	x	1.97

Figure 3.12 compares the actual measured mode shape with the mode shapes predicted by TABS-77 for frames AX1 and AX2. It can be seen that the second modification, AX2, yields a better mode shape than does AX1 but neither matches the observed shape well. The mode shapes is an indication of the distribution of the lateral stiffness over the height of the building, which affects the distribution of internal forces resulting from lateral loads. Thus it is most important to predict mode shape as closely as possible. Prediction of frequency alone is not an adequate test of an analytical model.

3.4.2.2 Experimental Results vs. Modified Frames BX1 and BX2

Figure 3.13 shows the idealization for type BX1, and Figure 3.14 shows the idealization for type BX2. Modifications were made in exactly the same way as with AX1 and AX2.

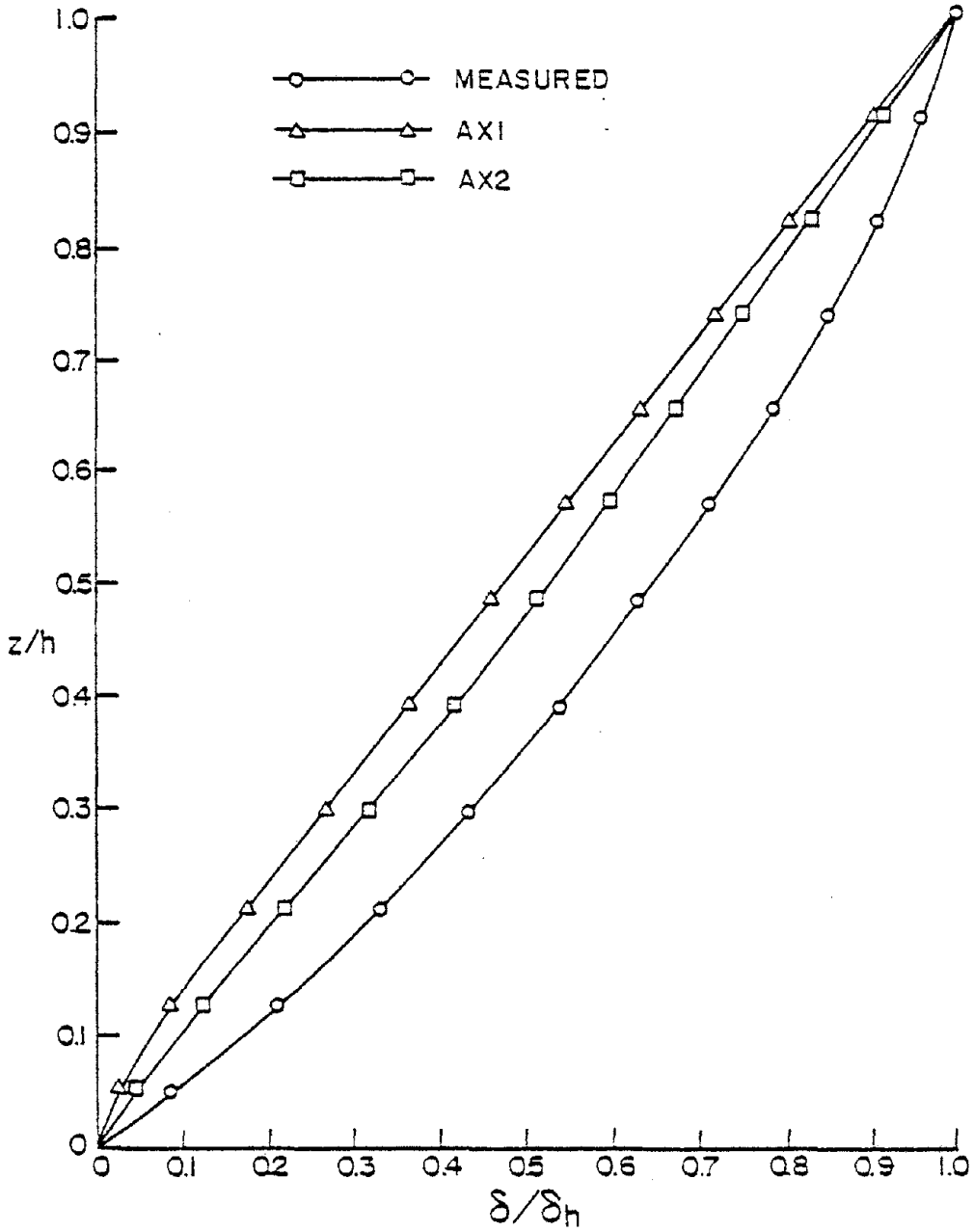

Figure 3.12. X Mode Shapes for the Residential Nautical College.

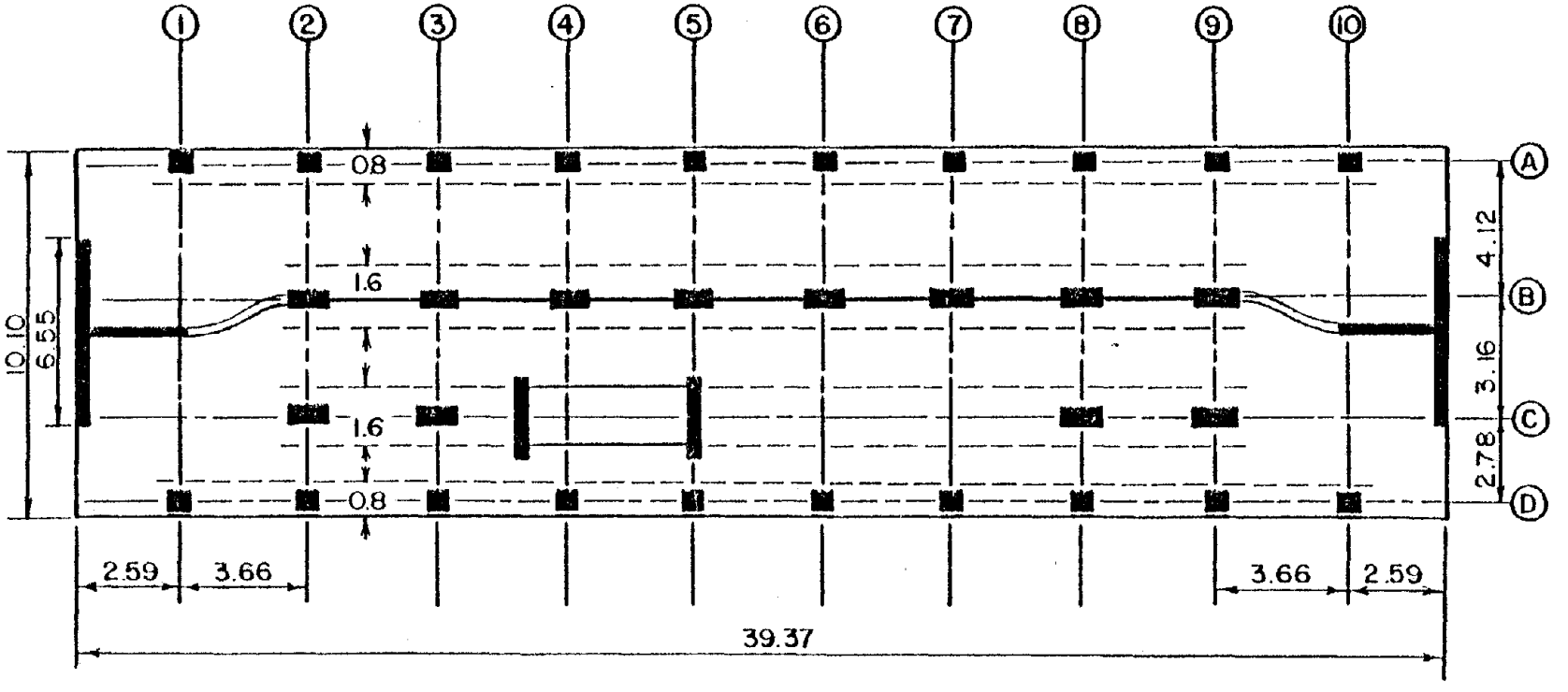

Figure 3.13. BX1 Structural Idealization for the Residential Nautical College.

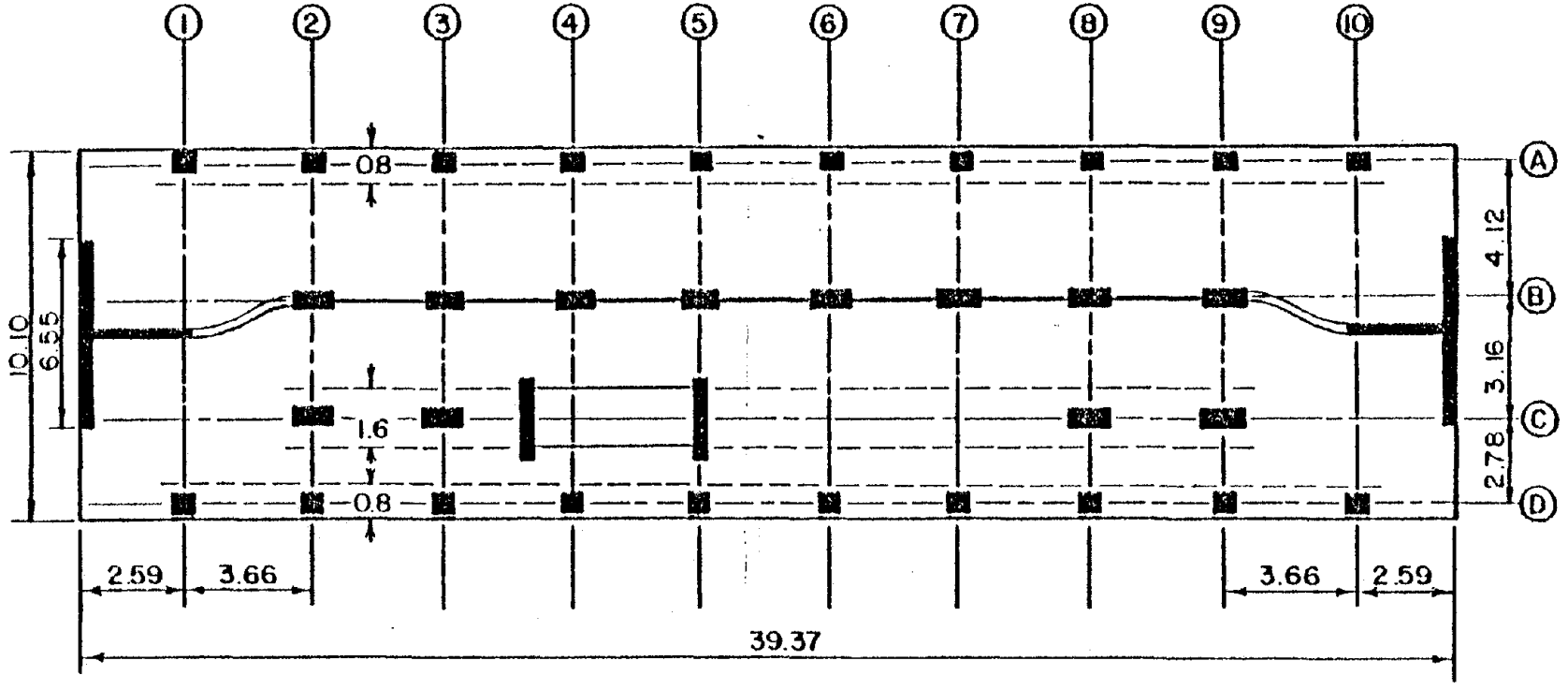

Figure 3.14. BX2 Structural Idealization for the Residential Nautical College.

Table 3.3 shows the results of the TABS-77 frequency predictions for types BX1 and BX2 along with the bare frame prediction for BX and the measured value. Both modifications produced excellent predictions for the frequency when compared to the measured value, and both are vast improvements over the BX idealization.

TABLE 3.3 Measured and Predicted Fundamental Frequencies

Type of Analysis	Direction	Frequency Hz
experiment	x	1.97
BX	x	1.05
BX1	x	2.08
BX2	x	1.97

Figure 3.15 presents a comparison of the predicted mode shapes for BX1 and BX2 along with the measured mode shape. The BX1 mode shape is not a close fit for the measured mode shape while the BX2 curve approaches the actual curve very closely.

If an idealization predicts both frequency and mode shape very closely, then this is a strong indication that the idealizatio is a proper one. It can reasonably be assumed that the idealizations resulting in type BX2 are very close to being correct, especially since only modifications that any engineer might reasonably elect have been made.

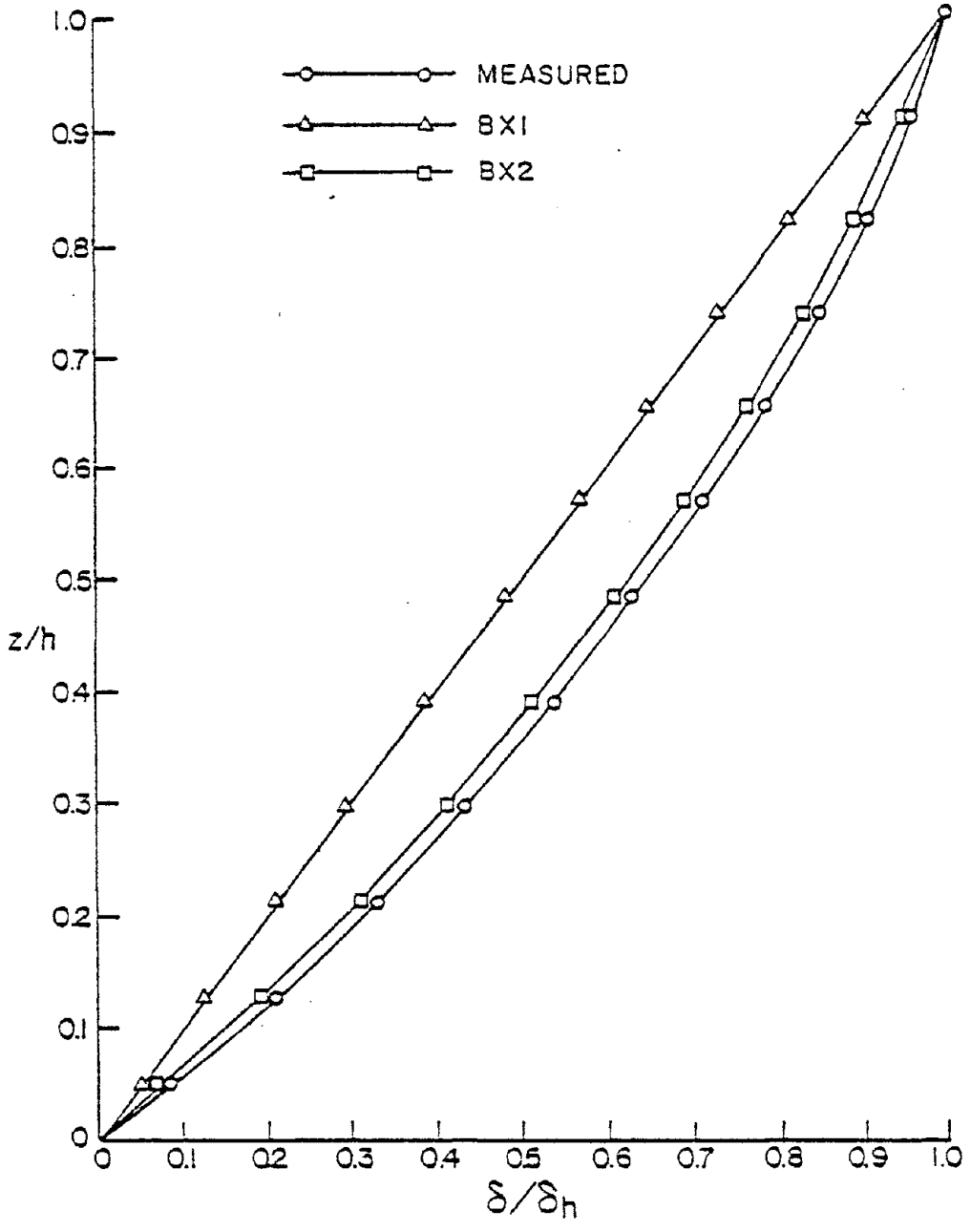

Figure 3.15. X Mode Shapes for the Residential Nautical College.

It is interesting to note that for this building four different idealizations have accurately predicted the fundamental longitudinal frequency but only one has also matched the actual mode shape.

3.4.2.3 Experimental Results vs. Modified Transverse Frames

The bare frame idealization in the transverse or y direction underestimated the natural frequency in that direction by 30 per cent but predicted the mode shape closely. Therefore it was decided to add extra stiffness by taking into account the effect of the partition walls shown in Figure 3.4. These partition walls were added to the bare frame idealization by modelling them each as a single column in its appropriate position. This was the only modification made in the y direction. This yielded a perfect match for the frequency prediction, and a slight improvement in the mode shape prediction. The mode shape curves are shown in Figure 3.16.

3.4.3 Parametric Studies

The BX2 idealization appears to predict the characteristics of the building well. However it is interesting to see how sensitive the R. N. C. building is to the various parameters involved in evaluating the BX2 idealization. Accordingly, several parametric studies were performed and the results are included in this section. The parameters studied were floor stiffness and equivalent strut size. Each was changed through a reasonable range on each side of the value used in BX2 while the other parameter was kept constant at the BX2 value.

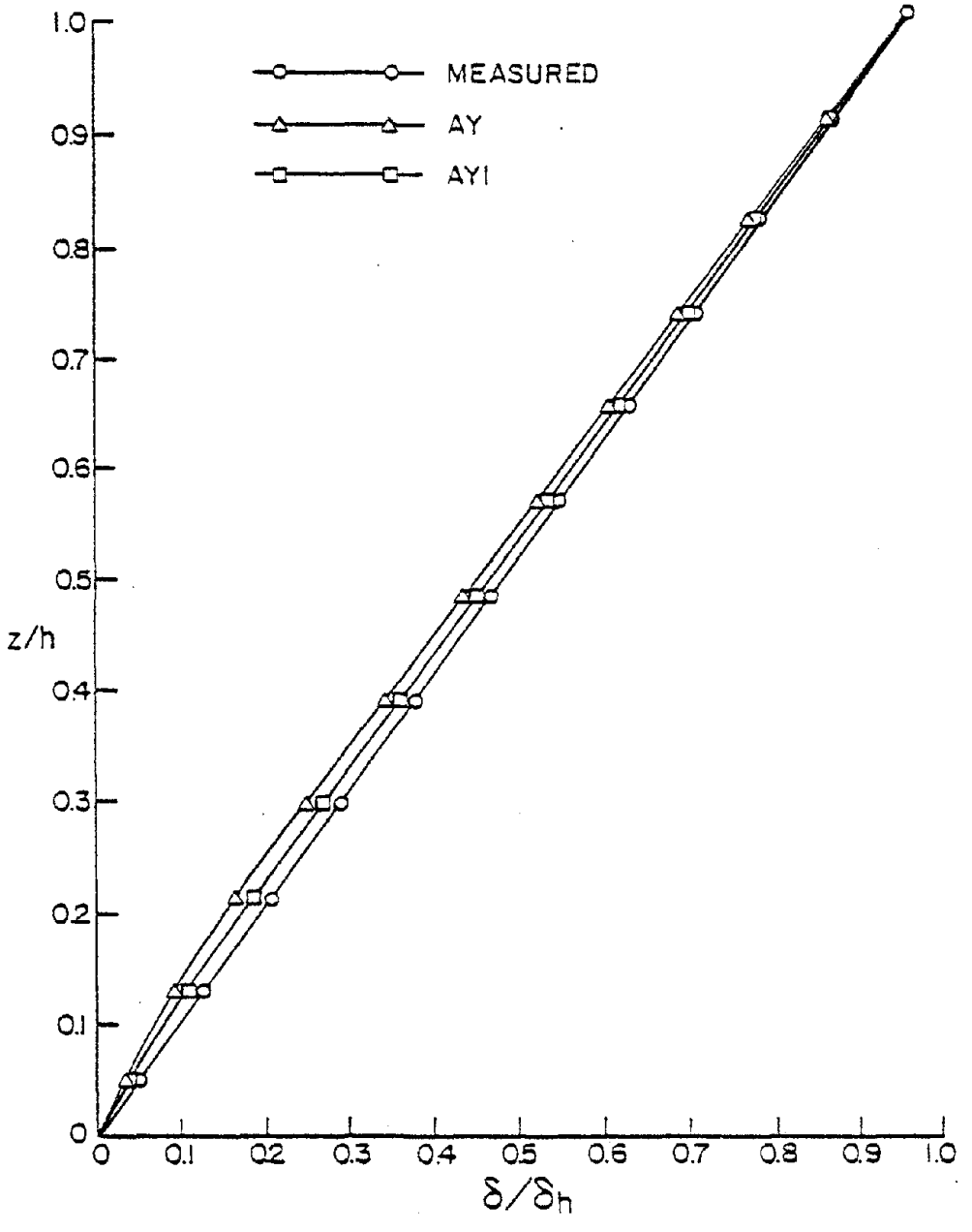

Figure 3.16. Y Mode Shapes for the Residential Nautical College.

First, the floor stiffness along frame lines A, D, and C was changed by varying the effective floor widths while keeping the equivalent strut size, constant at the BX2 idealization value. The results for this study are shown in Table 3.4 and Figure 3.17. In the table and graph S is the varying stiffness and S_0 is the value of the stiffness used in the BX2 idealization. In Table 3.4 and in tables in the parametric study sections throughout this and subsequent chapters, experimental values of frequency are shown enclosed in a box for ease of comparison.

Both the table and the graph show that the R. N. C. building is not sensitive to changes in the stiffness parameter used in frame lines A, D, and C. Natural frequency and modal mass change hardly at all as the stiffness is varied. Since modal mass does not vary much it is reasonable to conclude that mode shape does not vary appreciably. The graph of normalized frequency vs. normalized stiffness is a very flat curve indeed. It appears that any reasonable value for the widths in frame lines A, D, and C would be adequate for structural design.

Secondly, all parameters except the depth of the diagonal elements approximating the effects of the infill walls were kept constant at the BX2 idealization and the diagonal depths were varied over a reasonable range. The results of this study are shown in Table 3.5 and Figure 3.18. The table and the figure both indicate that the R. N. C. building natural frequency computations are quite sensitive to the selection of effective strut depth. The curve of Figure 3.18 shows that the change in frequency is rapid with small changes in size of the diagonal element

Table 3.4. Parametric Study of Effective Floor Slab Widths in the Residential Nautical College, X Direction

S/S_o	Frequency (Hz)	Modal Mass (Kg)
0.46	1.96	1469237
0.61	1.97	1469237
0.94	1.98	1472806
1.00	2.00	1472806
1.30	2.02	1472806
1.53	2.03	1472806
2.30	2.04	1472806

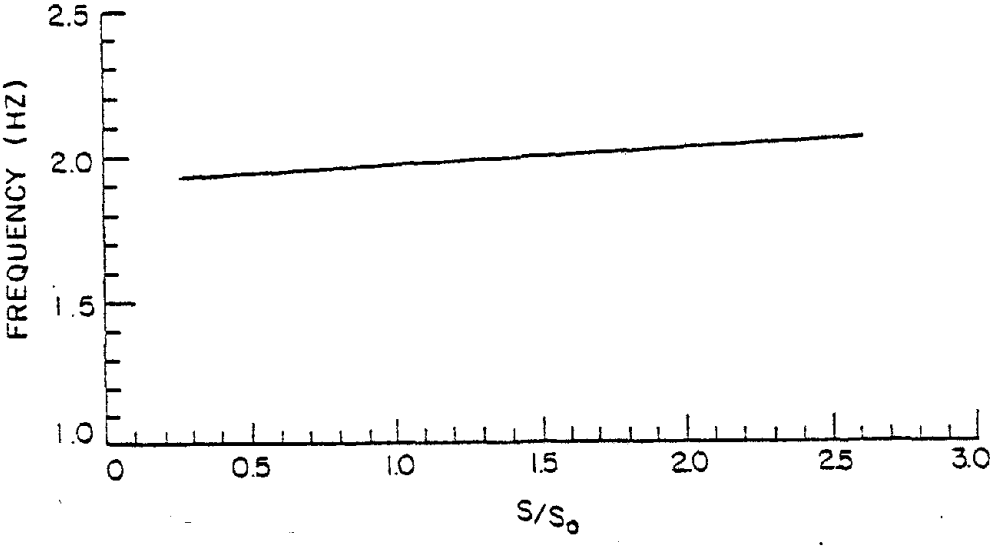

Figure 3.17. Frequency vs. Normalized Stiffness for Parametric Study of Effective Floor Slab Widths in the Residential Nautical College, X Direction.

Table 3.5. Parametric Study of Equivalent Diagonal Elements in the Residential Nautical College, X Direction

S/S_o	Frequency (Hz)	Modal Mass (Kg)
0.00	1.53	1600000
0.05	1.74	1480000
0.17	1.83	1476387
0.40	1.91	1476387
1.00	2.00	1472806
2.40	2.14	1465682
5.18	2.26	1462140
9.2	2.36	1455093
15	2.45	1444619
32	2.62	1430828
38	2.66	1424000

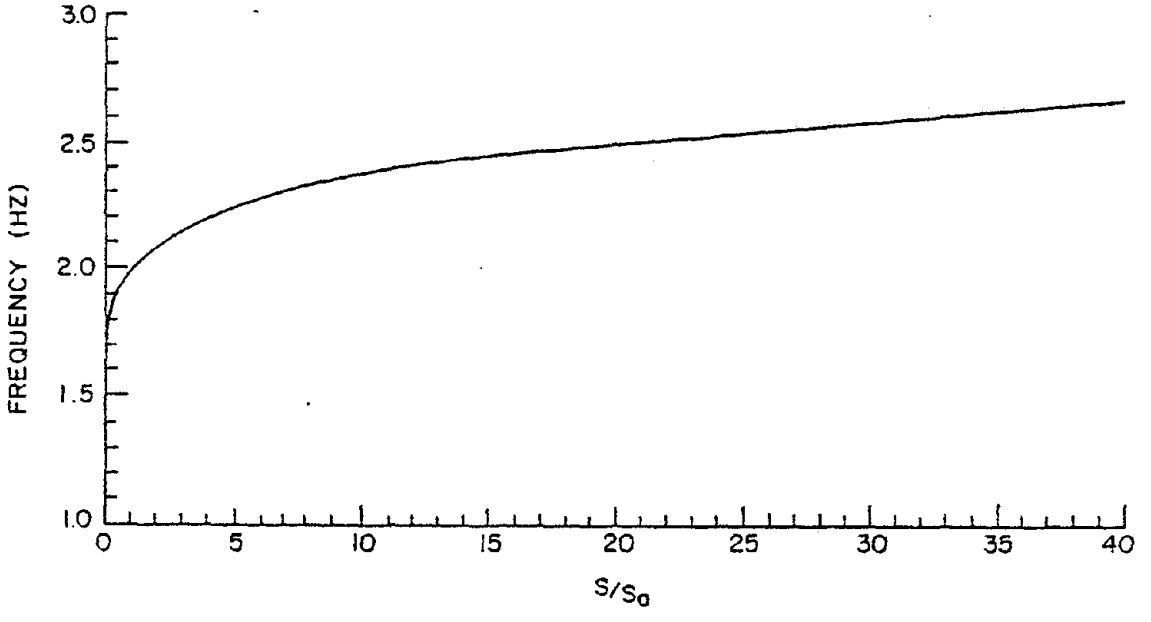

Figure 3.18, Frequency vs. Normalized Stiffness for Parametric Study of Equivalent Diagonal Elements in the Residential Nautical College, X Direction.

in the neighborhood of the BX2 idealization. When the strut size becomes very much larger, then its relative stiffness effect is diminished and the curve tends to flatten out somewhat. Again, it is noted that the logical modifications contained in type BX2 appears to be the correct approach for it predicts the experimental measurements for this building.

Table 3.5 shows that the modal mass is also quite sensitive to changes in effective strut depth. This sensitivity is not obvious for all of the values are large. One must look at the differences in values rather than ratios of values. To emphasize the effects of these seemingly meager differences Figure 3.19 is presented. This figure contains plots of each mode shape corresponding to each value of the diagonal depth used to compute these modal mass values. The significance of the mode shape has already been presented; thus Figure 3.19 emphasizes the significance of small changes in modal mass values.

Thirdly, the BX2 idealization was maintained everywhere in the structure except the stiffness of the floor along frame line B was varied from a lower limit that was taken as one-half the equivalent width recommended by Khan (9) to infinity as was assumed for the BX2 idealization. The results are shown in Table 3.6 and Figure 3.20. Table 3.6 shows that small values of equivalent floor width along frame line B can have a significant effect on the predicted natural frequency of the R. N. C. building when compared to the measured value. However, the predicted frequency slowly increases with rather rapid increases in stiffness. When the stiffness becomes a large value the frequency

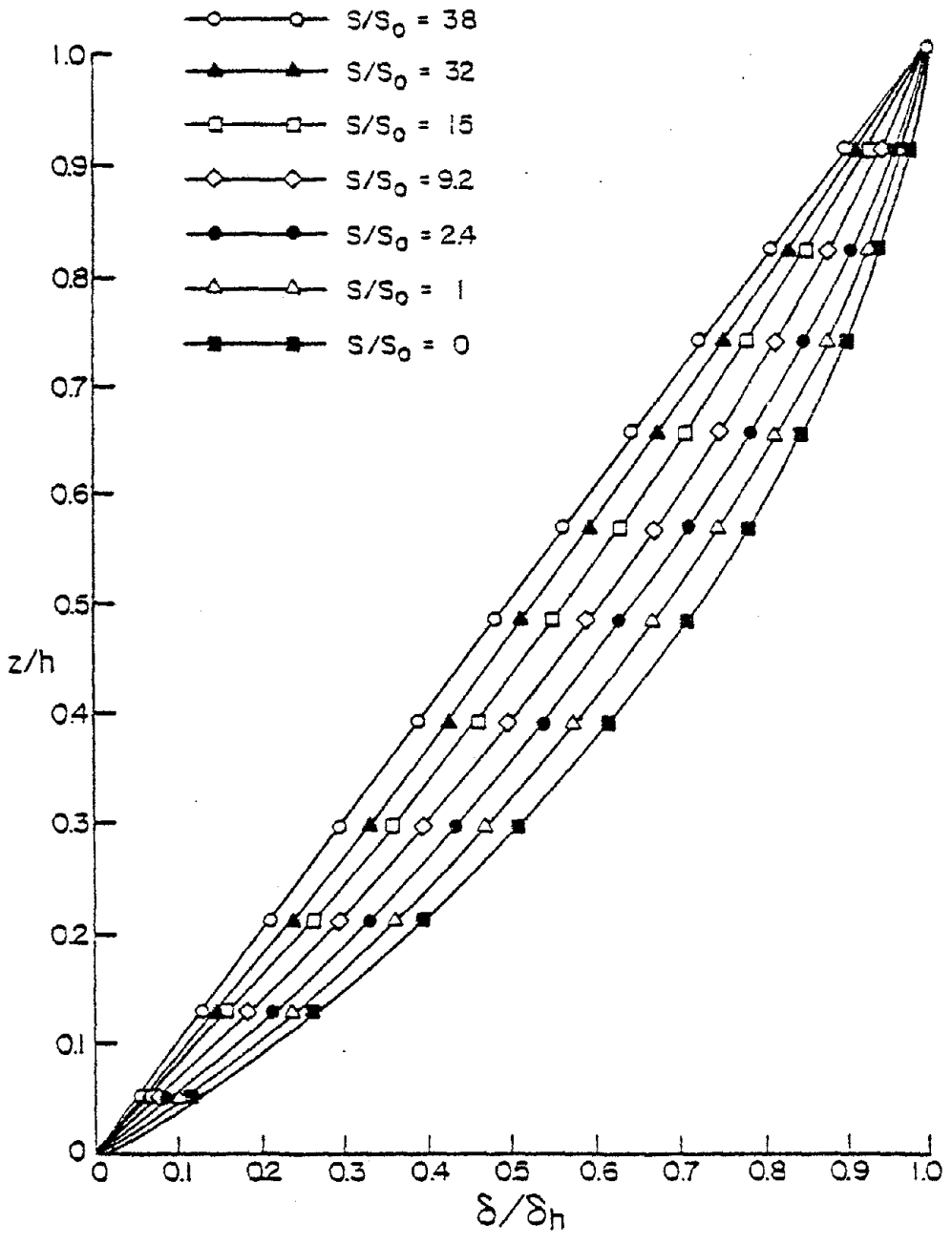

Figure 3.19. X Mode Shapes for the Residential Nautical College.

Table 3.6. Parametric Study of Effective Floor Slab Width Along Frame B in the Residential Nautical College, X Direction

S/S_o	Frequency (Hz)	Modal Mass (Kg)
0.50	1.58	1312113
0.76	1.60	1318146
1.00	1.62	1324220
1.25	1.64	1333411
2.70	1.71	1371147
69.4	1.86	1451589
125	1.95	1483589
1250	2.00	1479981
12500	2.00	1472806

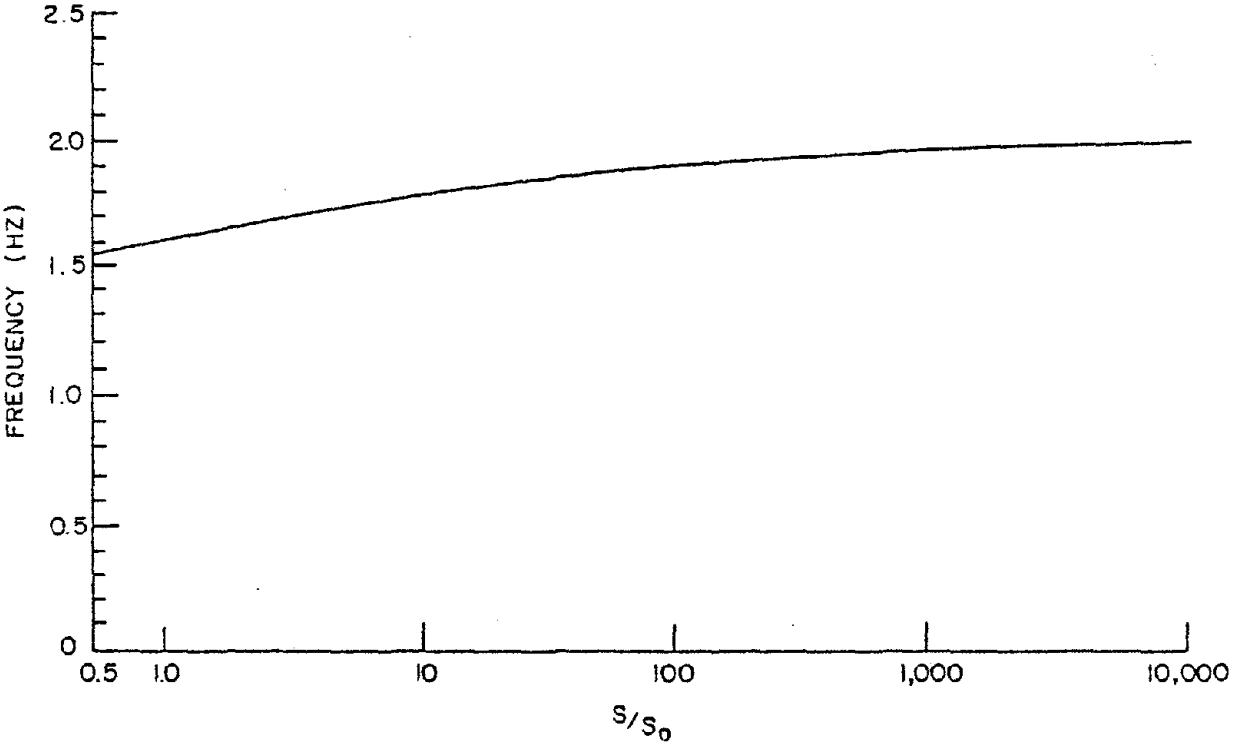

Figure 3.20. Frequency vs. Normalized Stiffness for Parametric Study of Effective Floor Slab Width Along Frame B in the Residential Nautical College, X Direction.

approaches the measured value. Figure 3.20 shows the relationship between floor stiffness and frequency.

Table 3.6 also shows that modal mass is sensitive to this parameter; as the floor along frame line B gets stiffer, the modal mass increases so that ultimately the mode shape becomes typical of frame action.

There is only one parameter that may be varied in the y direction for the R. N. C. building. This is the effective slab width in that direction. In setting up the parametric study in the y direction the effective slab widths were each determined in accordance with Khan's (9) recommendations. Then each of the effective slab widths in frame lines 1 through 10 were varied by the same percentage and an analysis was made for each of these different sets of slab widths. The results of this study are shown in Table 3.7 and Figure 3.21. Both the table and the figure show that both natural frequency in this direction and modal mass are almost totally insensitive to this parameter.

3.4.4 Significance of Proper Modelling

The structural analysis that has been presented so far for the R. N. C. building has shown that there are several models or idealizations which will result in an adequate calculation of the natural frequency for this building. As stated in chapter I, one must be careful not to infer that simply because the correct frequency of a structure has been determined, then the correct stiffness distribution is known since the simple relationship between frequency and stiffness

Table 3.7. Parametric Study of Effectice Floor Slab Widths in the Residential Nautical College, Y Direction

S/S_o	Frequency (Hz)	Modal Mass (Kg)
0.44	1.27	1174498
0.59	1.28	1180296
0.74	1.30	1182240
1.00	1.32	1181070
1.16	1.35	1100740
1.38	1.36	1120470
2.13	1.40	1198002

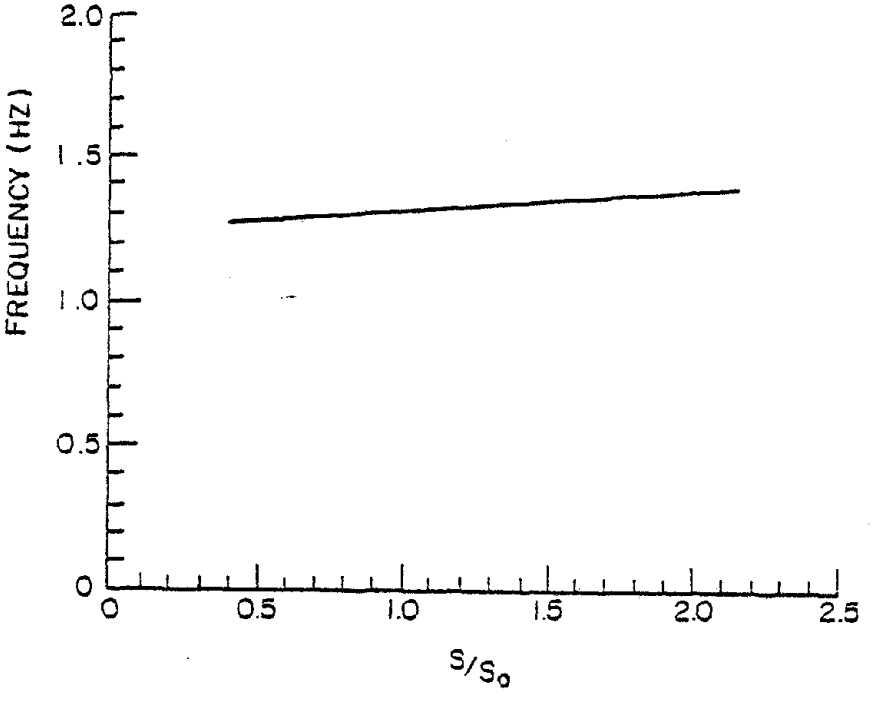

Figure 3.21. Frequency vs. Normalized Stiffness for Parametric Study of Effective Floor Slab Widths in the Residential Nautical College, Y Direction.

determines only the overall stiffness. The designer must know the stiffness distribution before he can make an adequate analysis of a trial design. The stiffness distribution is manifest in the mode shape. Each of the models postulated in this analysis yielded different mode shapes with type BX2 most nearly predicting the actual mode shape. In order to evaluate the significance of mode shapes (and at the same time frequency predictions) and thus the significance of proper modelling for the designer, a study was made of the response of the building to both lateral static and dynamic loadings for each model.

For the static loading a typical distribution of wind load as indicated in Table 3.8 was applied in the x and y directions. In Table 3.8 the column headed "Normalized Wind Load" expresses each of these values as a proportion of the largest value. The distribution was in accordance with reference (17).

For the dynamic load a low intensity earthquake which is assumed would not exceed the elastic limit of the structure was applied in turn along the x and y axes. For this purpose the ground accelerations proportional to those associated with the 1940 El Centro earthquake were used in conjunction with the measured values of damping.

For this portion of the study of the R. N. C. building only a few structural elements were chosen for analysis. Other elements could have been chosen but it is believed that the three chosen are reasonably typical for this building and should therefore yield representative results.

TABLE 3.8 NORMALIZED WIND LOAD FOR THE RESIDENTIAL NAUTICAL COLLEGE

Level	Load Ratio
12	0.51
11	1.00
10	0.95
9	0.90
8	0.87
7	0.81
6	0.76
5	0.69
4	0.63
3	0.58
2	0.49
1	0.71

For loadings in the x direction, columns B3 and along with the shear wall at one end were chosen. These elements are encircled on Figure 3.22. For the y direction loadings, only column B3 was analysed.

The results of the analysis of the three elements in the x direction and the one element in the y direction are shown in the remaining tables in this chapter. These tables illustrate the discrepancies brought about by choosing models that neglect the effects of the partitions, and show the effects on these members of choosing models on the basis of frequency matching only. Considered together they are an indication of the errors introduced by improper modelling.

Each of the tables show the results in dimensionless form with the results for the most accurate BX2 model compared to the results calculated by other models. As stated previously, the AX and BX models are referred to as bare frames, and the AX1 and BX1 models are called modified frames.

3.4.4.1 Lateral Static Loading

Tables 3.9 through 3.11 compare the BX2 model to the bare frame models for static lateral loading in the x direction. Table 3.9 shows that column D3 is unaffected by the type of assumption made about the interaction between column line B and the shear walls. When line B is stiffened by the partitions it absorbs load from line D so that the forces are reduced by as much as 10 times.

Table 3.10 shows that for column line B connection to the shear walls greatly increases the loads and the moments due to interaction.

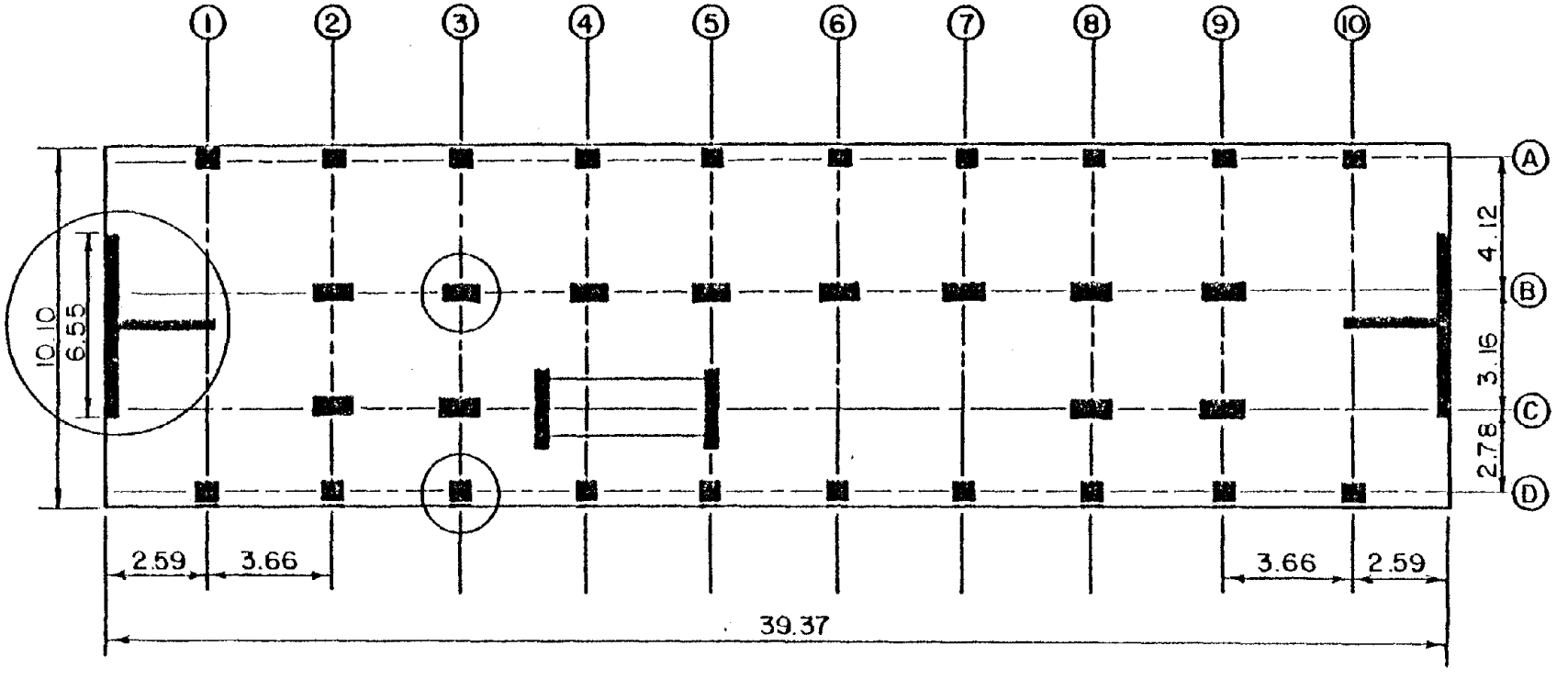

Figure 3.22. Elements Chosen for the Analysis of the Residential Nautical College.

TABLE 3.9 RESULTS OF ANALYSES IN DIMENSIONLESS FORM FOR

BUILDING: R. N. C.
ELEMENT: COLUMN D3
LOADING: WIND
DIRECTION: X

LEVEL	BOTTOM MOMENT		TOP MOMENT		AXIAL FORCE		SHEAR FORCE	
	$\frac{BX2}{AX}$	$\frac{BX2}{BX}$	$\frac{BX2}{AX}$	$\frac{BX2}{BX}$	$\frac{BX2}{AX}$	$\frac{BX2}{BX}$	$\frac{BX2}{AX}$	$\frac{BX2}{BX}$
12	0.12	0.11	0.1	0.10	0.14	0.22	0.07	0.07
11	0.13	0.13	0.12	0.13	0.20	0.28	0.09	0.09
10	0.12	0.11	0.10	0.11	0.10	0.20	0.14	0.15
9	0.15	0.16	0.14	0.16	0.14	0.33	0.12	0.14
8	0.13	0.16	0.12	0.15	0.25	0.33	0.10	0.14
7	0.16	0.21	0.15	0.21	0.77	0.70	0.15	0.20
6	0.15	0.21	0.15	0.21	0.33	0.18	0.14	0.21
5	0.17	0.27	0.18	0.27	0.14	0.12	0.14	0.21
4	0.18	0.29	0.19	0.29	0.08	0.12	0.19	0.30
3	0.20	0.31	0.21	0.33	0.10	0.20	0.22	0.33
2	0.24	0.38	0.29	0.45	0.16	0.07	0.26	0.44
1	0.36	0.47	0.50	0.60	0.25	0.40	0.32	0.50

Although some of the load is carried by the diagonal bracing of the partitions, the extra load attracted to that column line exceeds the relief provided by the partitions, and there are very high increases in the forces and moments as compared to the design assumption BX. The maximum ratio for this comparison is 29. However, the loads actually drop in comparison to design assumption AX because in this assumption the column line stood alone and would have carried more load than in BX where the shear walls provided some relief.

Table 3.11 shows that the BX2 model, which is the best model analysed and takes into account the effect of the partitions, yielded lower moments and shear forces in the shear wall than did the bare frame models. The tabulation shows that the axial force is very small when the shear wall is assumed to act independently of column line B, and there was little change in axial force in that shear wall when the shear walls were assumed to act with frame line B (type BX model).

Tables 3.12 through 3.15 are also concerned with lateral static loading in the x direction, and these tables compare the best model BX2 with the modified frame models AX1 and BX1. These modified frames matched the observed frequency but not the mode shape.

Table 3.12 shows that the moments and forces calculated by the modified frame models for column D3 are not very different from those predicted by the better BX2 model. Further, study will show that each of the models is equally good.

Table 3.13 shows that for column B3 the moments and shear forces predicted by the BX model are higher than those calculated using AX1 and

TABLE 3.10 RESULTS OF ANALYSES IN DIMENSIONLESS FORM FOR

BUILDING: R. N. C.
ELEMENT: COLUMN B3
LOADING: WIND
DIRECTION: X

LEVEL	BOTTOM MOMENT		TOP MOMENT		AXIAL FORCE		SHEAR FORCE	
	$\frac{BX2}{AX}$	$\frac{BX2}{BX}$	$\frac{BX2}{AX}$	$\frac{BX2}{BX}$	$\frac{BX2}{AX}$	$\frac{BX2}{BX}$	$\frac{BX2}{AX}$	$\frac{BX2}{BX}$
12	0.62	2.23	0.44	1.20	0.12	0.20	0.51	1.53
11	0.79	3.50	0.70	2.70	0.04	0.07	0.74	3.25
10	0.76	3.72	0.62	2.41	1.32	2.17	0.68	2.90
9	0.78	4.16	0.65	3.12	1.18	2.00	0.72	3.54
8	0.80	4.61	0.69	3.75	1.06	1.75	0.74	4.27
7	0.81	5.00	0.74	4.67	0.92	1.51	0.77	4.90
6	0.83	5.26	0.79	6.00	0.71	1.24	0.80	5.54
5	0.85	5.37	0.86	7.81	0.53	0.88	0.85	6.70
4	0.88	5.75	0.96	11.5	0.26	0.43	0.92	7.88
3	0.92	4.90	1.14	23.5	0.06	0.09	1.01	8.00
2	0.93	4.52	1.50	28.6	0.48	0.77	1.15	11.0
1	0.67	1.14	3.50	6.12	1.02	1.67	1.13	3.60

TABLE 3.11 RESULTS OF ANALYSES IN DIMENSIONLESS FORM FOR

BUILDING: R. N. C.
ELEMENT: END SHEAR WALL
LOADING: WIND
DIRECTION: X

LEVEL	BOTTOM MOMENT		TOP MOMENT		AXIAL FORCE		SHEAR FORCE	
	$\frac{BX2}{AX}$	$\frac{BX2}{BX}$	$\frac{BX2}{AX}$	$\frac{BX2}{BX}$	$\frac{BX2}{AX}$	$\frac{BX2}{BX}$	$\frac{BX2}{AX}$	$\frac{BX2}{BX}$
12	0.19	-0.43	2.64	-12.30	2.16	1.33	0.10	0.20
11	0.04	0.15	0.33	0.69	4.20	16.0	0.92	0.25
10	0.10	0.57	0.22	0.48	62.0	1.60	0.87	0.40
9	0.09	0.78	0.32	0.67	82.5	1.03	0.83	0.50
8	0.06	0.32	0.37	0.79	95.9	0.84	2.18	0.50
7	-0.003	0.004	0.47	0.96	111.0	0.76	1.51	0.50
6	-0.40	0.10	0.72	1.28	128.0	0.71	1.21	0.50
5	0.38	0.15	0.76	2.37	141.0	0.68	1.01	0.50
4	0.23	-0.20	0.89	-0.94	154.0	0.67	0.87	0.50
3	0.21	-0.25	0.26	-0.86	170.0	0.66	0.77	0.52
2	0.24	-0.34	0.06	-0.14	188.0	0.66	0.73	0.58
1	0.38	0.54	0.11	-0.21	213.0	0.67	0.82	0.79

TABLE 3.12 RESULTS OF ANALYSES IN DIMENSIONLESS FORM FOR

BUILDING: R. N. C.
ELEMENT: COLUMN D3
LOADING: WIND
DIRECTION: X

LEVEL	BOTTOM MOMENT		TOP MOMENT		AXIAL FORCE		SHEAR FORCE	
	$\frac{BX2}{AX1}$	$\frac{BX2}{BX1}$	$\frac{BX2}{AX1}$	$\frac{BX2}{BX1}$	$\frac{BX2}{AX1}$	$\frac{BX2}{BX1}$	$\frac{BX2}{AX1}$	$\frac{BX2}{BX1}$
12	0.50	0.77	0.40	0.65	1.00	1.00	0.34	0.45
11	0.67	0.72	0.67	0.72	1.00	1.00	0.50	0.50
10	0.50	0.70	0.50	0.70	1.00	1.00	0.67	0.89
9	0.75	0.95	0.75	0.95	1.00	1.00	0.67	0.80
8	0.75	0.84	0.75	0.84	1.00	1.00	0.67	0.73
7	1.00	1.00	1.00	1.00	1.00	1.00	1.00	1.00
6	1.00	1.00	1.00	1.00	1.00	1.00	1.00	1.00
5	1.25	1.21	1.25	1.21	1.00	1.00	1.00	1.00
4	1.25	1.20	1.25	1.20	0.50	1.00	1.33	1.23
3	1.25	1.21	1.25	1.25	0.67	1.00	1.33	1.33
2	1.67	1.30	1.67	1.40	1.00	1.00	2.00	1.37
1	1.53	1.17	3.00	1.34	1.60	1.00	1.42	1.10

TABLE 3.13 RESULTS OF ANALYSES IN DIMENSIONLESS FORM FOR

BUILDING: R. N. C.
ELEMENT: COLUMN B3
LOADING: WIND
DIRECTION: X

LEVEL	BOTTOM MOMENT		TOP MOMENT		AXIAL FORCE		SHEAR FORCE	
	$\frac{BX2}{AX1}$	$\frac{BX2}{BX1}$	$\frac{BX2}{AX1}$	$\frac{BX2}{BX1}$	$\frac{BX2}{AX1}$	$\frac{BX2}{BX1}$	$\frac{BX2}{AX1}$	$\frac{BX2}{BX1}$
12	1.07	17.0	1.86	120.0	0.098	5.20	1.20	42.0
11	1.75	51.0	1.75	14.0	0.022	2.0	1.73	24.0
10	1.86	66.0	1.87	102.0	0.41	1.16	1.77	145.0
9	2.17	192.0	2.09	30.0	0.30	3.14	2.17	73.0
8	2.60	200.0	2.50	38.0	0.23	8.30	2.61	77.0
7	2.91	25.0	2.91	41.0	0.17	2.06	3.00	58.0
6	3.43	102.0	3.30	48.0	0.12	1.17	3.38	64.0
5	3.73	65.0	3.90	57.0	0.08	0.73	3.72	60.0
4	4.18	51.0	4.60	75.0	0.03	0.34	4.43	60.0
3	4.65	27.0	5.47	93.0	0.007	0.08	5.14	42.0
2	5.37	37.0	7.16	191.0	0.06	0.81	6.10	93.0
1	2.88	2.67	8.16	245.0	0.12	1.33	4.12	5.26

BX1. These models predict moments and shear forces that are very much less than they apparently should be. This underestimation is much more pronounced in type BX1. Also AX1 and BX1 do not vary from the more correct values by some common amount; they often yield considerably different values. The axial forces in column B3 are in general overestimated by models AX1 and BX1.

Table 3.14 shows that for the shear wall the modified frame predictions are erratic when compared to the more correct BX2 computation. Not only are there wide variations in numerical values but the signs or directions of the forces and moments change in an erratic fashion. Perhaps the complexity of the interactions between the various components of the structure can explain this type of discrepancy. No general pattern of variation can be easily identified.

Table 3.15 shows the result of the only column studied for lateral static loading in the y direction. Column B3 was chosen as a typical member for loading in the y direction. Study of Table 3.15 shows that when the partitions are added in the modified frame model, the moments and forces are carried somewhat by the partitions and thus the values for the column are reduced from those of the bare frame model by about 30 percent.

3.4.4.2 Dynamic Loading

For dynamic or earthquake loading, calculations were made using the TABS-77 program, and the results are shown in dimensionless form in Tables 3.16 through 3.22. The results are similar but not identical to those obtained for lateral static loading.

TABLE 3.14 RESULTS OF ANALYSES IN DIMENSIONLESS FORM FOR

BUILDING: R. N. C.
ELEMENT: END SHEAR WALL
LOADING: WIND
DIRECTION: X

LEVEL	BOTTOM MOMENT		TOP MOMENT		AXIAL FORCE		SHEAR FORCE	
	$\frac{BX2}{AX1}$	$\frac{BX2}{BX1}$	$\frac{BX2}{AX1}$	$\frac{BX2}{BX1}$	$\frac{BX2}{AX1}$	$\frac{BX2}{BX1}$	$\frac{BX2}{AX1}$	$\frac{BX2}{BX1}$
12	69.0	9.90	74.0	0.30	88.0	0.14	25.0	-0.27
11	0.60	-0.25	258.0	0.73	320.0	0.23	3.07	0.41
10	1.24	-1.00	2.94	0.91	370.0	0.30	8.60	0.31
9	1.28	-0.78	3.81	1.00	330.0	0.36	24.5	0.51
8	1.07	-0.33	5.10	1.06	422.0	0.41	14.1	0.62
7	1.40	0.009	8.30	1.09	518.0	0.47	11.1	0.70
6	1.80	0.28	36.2	1.14	620.0	0.53	10.1	0.78
5	1.50	0.50	10.63	1.22	721.0	0.58	8.90	0.87
4	1.41	0.73	3.65	1.34	822.0	0.63	7.70	1.00
3	1.50	1.04	1.60	1.52	923.0	0.70	7.73	1.17
2	1.70	1.30	0.36	2.30	1115.0	0.75	5.18	1.37
1	1.82	1.40	0.73	1.24	1066.0	0.80	2.63	1.43

TABLE 3.15 RESULTS OF ANALYSES IN DIMENSIONLESS FORM FOR

BUILDING: R. N. C.
ELEMENT: COLUMN B3
LOADING: WIND
DIRECTION: Y

LEVEL	BOTTOM MOMENT $\frac{AY1}{AY}$	TOP MOMENT $\frac{AY1}{AY}$	AXIAL FORCE $\frac{AY1}{AY}$	SHEAR FORCE $\frac{AY1}{AY}$
12	0.69	0.69	0.65	0.68
11	0.68	0.68	0.64	0.68
10	0.68	0.68	0.63	0.65
9	0.66	0.65	0.63	0.65
8	0.64	0.64	0.63	0.64
7	0.64	0.64	0.63	0.64
6	0.62	0.62	0.63	0.62
5	0.60	0.60	0.63	0.62
4	0.60	0.59	0.62	0.60
3	0.57	0.57	0.65	0.59
2	0.56	0.56	0.66	0.57
1	0.48	0.52	0.67	0.54

TABLE 3.16 RESULTS OF ANALYSES IN DIMENSIONLESS FORM FOR

BUILDING: R. N. C.
ELEMENT: COLUMN D3
LOADING: EARTHQUAKE
DIRECTION: X

LEVEL	BOTTOM MOMENT		TOP MOMENT		AXIAL FORCE		SHEAR FORCE	
	$\frac{BX2}{AX}$	$\frac{BX2}{BX}$	$\frac{BX2}{AX}$	$\frac{BX2}{BX}$	$\frac{BX2}{AX}$	$\frac{BX2}{BX}$	$\frac{BX2}{AX}$	$\frac{BX2}{BX}$
12	0.17	0.13	0.18	0.14	0.39	0.33	0.17	0.14
11	0.21	0.17	0.21	0.17	0.33	0.35	0.21	0.17
10	0.20	0.16	0.20	0.17	0.33	0.38	0.20	0.16
9	0.21	0.18	0.22	0.19	0.37	0.55	0.22	0.19
8	0.29	0.21	0.25	0.22	0.37	0.90	0.25	0.22
7	0.27	0.24	0.28	0.26	0.35	0.40	0.27	0.25
6	0.30	0.28	0.31	0.29	0.10	0.11	0.30	0.28
5	0.32	0.31	0.33	0.33	0.13	0.13	0.33	0.32
4	0.35	0.64	0.36	0.73	0.18	0.17	0.35	0.68
3	0.38	0.40	0.40	0.43	0.27	0.20	0.38	0.41
2	0.43	0.47	0.47	0.51	0.37	0.30	0.45	0.49
1	0.67	0.68	0.80	0.78	0.43	0.42	0.72	0.71

TABLE 3.17 RESULTS OF ANALYSES IN DIMENSIONLESS FORM FOR

BUILDING: R. N. C.
ELEMENT: COLUMN B3
LOADING: EARTHQUAKE
DIRECTION: X

LEVEL	BOTTOM MOMENT		TOP MOMENT		AXIAL FORCE		SHEAR FORCE	
	$\frac{BX2}{AX}$	$\frac{BX2}{BX}$	$\frac{BX2}{AX}$	$\frac{BX2}{BX}$	$\frac{BX2}{AX}$	$\frac{BX2}{BX}$	$\frac{BX2}{AX}$	$\frac{BX2}{BX}$
12	0.94	2.87	0.68	1.48	0.47	0.40	0.80	1.95
11	1.20	4.27	1.13	3.31	0.50	0.52	1.16	3.73
10	1.17	4.18	1.06	3.04	2.40	2.53	1.11	3.51
9	1.27	4.60	1.18	3.96	2.09	2.24	1.23	4.25
8	1.37	4.95	1.28	5.00	1.89	3.86	1.34	4.98
7	1.45	5.30	1.47	6.39	1.64	1.76	1.43	5.86
6	1.54	5.67	1.53	7.63	1.32	1.41	1.54	6.92
5	1.61	6.00	1.61	9.57	0.92	0.98	1.60	8.16
4	1.61	6.24	1.72	13.4	0.48	0.50	1.67	9.71
3	1.61	5.91	1.96	25.7	0.22	0.23	1.77	10.1
2	1.57	5.68	2.51	24.7	0.90	0.95	1.94	13.2
1	1.10	1.38	5.75	6.39	1.82	1.91	1.85	3.48

TABLE 3.18 RESULTS OF ANALYSES IN DIMENSIONLESS FORM FOR

BUILDING: R. N. C.
ELEMENT: END SHEAR WALL
LOADING: EARTHQUAKE
DIRECTION: X

LEVEL	BOTTOM MOMENT		TOP MOMENT		AXIAL FORCE		SHEAR FORCE	
	$\frac{BX2}{AX}$	$\frac{BX2}{BX}$	$\frac{BX2}{AX}$	$\frac{BX2}{BX}$	$\frac{BX2}{AX}$	$\frac{BX2}{BX}$	$\frac{BX2}{AX}$	$\frac{BX2}{BX}$
12	0.31	0.47	5.40	1.26	52.3	0.91	0.11	0.18
11	0.08	0.18	0.61	0.67	83.0	0.99	1.24	1.09
10	0.17	0.47	0.40	0.51	112.0	0.92	0.77	0.33
9	0.15	0.45	0.52	0.88	137.0	0.79	1.34	0.46
8	0.12	0.22	0.53	0.90	164.0	0.74	1.54	0.53
7	0.18	0.19	0.58	0.91	193.0	0.73	1.71	0.58
6	0.25	0.18	0.68	0.98	221.0	0.47	1.92	0.64
5	0.27	0.20	0.71	1.21	250.0	0.76	1.70	0.63
4	0.35	0.26	0.50	1.00	280.0	0.78	1.42	0.60
3	0.40	0.34	0.31	0.50	313.0	0.81	1.20	0.61
2	0.42	0.44	0.07	0.10	348.0	0.85	1.14	0.68
1	0.63	0.65	0.20	0.30	380.0	0.88	1.33	0.92

TABLE 3.19 RESULTS OF ANALYSES IN DIMENSIONLESS FORM FOR

BUILDING: R. N. C.
ELEMENT: COLUMN D3
LOADING: EARTHQUAKE
DIRECTION: X

LEVEL	BOTTOM MOMENT $\frac{BX2}{AX1}$	TOP MOMENT $\frac{BX2}{AX1}$	AXIAL FORCE $\frac{BX2}{AX1}$	SHEAR FORCE $\frac{BX2}{AX1}$
12	0.23	0.24	0.84	0.23
11	0.28	0.32	1.67	0.29
10	0.32	0.37	1.24	0.33
9	0.37	0.41	1.67	0.38
8	0.44	0.48	3.00	0.46
7	0.52	0.55	0.70	0.54
6	0.62	0.65	0.20	0.64
5	0.75	0.77	0.27	0.74
4	0.83	0.88	0.38	0.84
3	0.95	1.00	0.56	0.98
2	1.09	1.18	0.75	1.13
1	1.42	1.57	1.00	1.48

TABLE 3.20 RESULTS OF ANALYSES IN DIMENSIONLESS FORM FOR

BUILDING: R. N. C.
ELEMENT: COLUMN B3
LOADING: EARTHQUAKE
DIRECTION: X

LEVEL	BOTTOM MOMENT		TOP MOMENT		AXIAL FORCE		SHEAR FORCE	
	$\frac{BX2}{AX1}$	$\frac{BX2}{BX1}$	$\frac{BX2}{AX1}$	$\frac{BX2}{BX1}$	$\frac{BX2}{AX1}$	$\frac{BX2}{BX1}$	$\frac{BX2}{AX1}$	$\frac{BX2}{BX1}$
12	0.84	24.0	0.63	16.8	0.07	21.0	0.72	72.0
11	1.10	14.4	1.20	11.2	0.09	14.0	1.14	13.0
10	1.33	70.6	1.35	39.5	0.53	0.27	1.34	69.6
9	1.60	85.8	1.58	25.4	0.25	0.78	1.58	54.8
8	1.86	102.0	1.87	36.9	0.17	1.92	1.86	73.8
7	2.14	86.5	2.19	43.0	0.13	2.57	2.16	66.3
6	2.46	68.8	2.56	59.2	0.09	1.68	2.52	66.0
5	2.79	48.0	2.92	79.5	0.06	0.81	2.85	62.0
4	3.07	37.2	3.37	110.0	0.028	0.30	3.21	63.0
3	3.37	21.6	4.03	151.0	0.013	0.11	3.67	43.0
2	3.62	24.1	5.10	45.0	0.05	0.42	4.26	102.0
1	2.20	2.23	6.88	30.0	0.10	1.16	3.34	4.80

TABLE 3.21 RESULTS OF ANALYSES IN DIMENSIONLESS FORM FOR

BUILDING: R. N. C.
ELEMENT: END SHEAR WALL
LOADING: EARTHQUAKE
DIRECTION: X

LEVEL	BOTTOM MOMENT		TOP MOMENT		AXIAL FORCE		SHEAR FORCE	
	$\frac{BX2}{AX1}$	$\frac{BX2}{BX1}$	$\frac{BX2}{AX1}$	$\frac{BX2}{BX1}$	$\frac{BX2}{AX1}$	$\frac{BX2}{BX1}$	$\frac{BX2}{AX1}$	$\frac{BX2}{BX1}$
12	1.40	2.82	15.0	0.22	69.0	0.14	0.52	0.10
11	0.25	0.12	2.84	0.53	110.0	0.18	1.00	0.29
10	1.28	0.48	1.30	0.83	157.0	0.23	0.90	0.27
9	1.14	0.49	3.79	0.75	200.0	0.26	23.0	0.38
8	0.97	0.29	3.91	0.78	248.0	0.30	6.93	0.45
7	0.85	0.31	4.80	0.84	300.0	0.33	6.29	0.51
6	0.67	0.33	3.11	0.90	353.0	0.37	6.14	0.57
5	0.66	0.40	1.88	1.02	409.0	0.41	5.51	0.65
4	0.78	0.54	1.21	1.19	467.0	0.45	5.00	0.75
3	0.96	0.74	0.70	1.58	532.0	0.49	4.47	0.89
2	1.13	0.45	0.16	1.40	600.0	0.53	3.67	1.06
1	1.35	1.12	0.53	0.88	660.0	0.57	2.18	1.20

If the tabulations for each of the structural members are compared between static loading and dynamic loading in the x direction it can be noted that while the ratios are different, the trends are quite similar. Thus the general comments made for the static loading are applicable to the dynamic loading also. It is to be expected that the ratios for dynamic loading will be different from those for static loading for the nature of dynamic loading is different from the nature of static loading. Static wind loading is not dependent on the dynamic characteristics of the structure whereas dynamic earthquake loading is dependent on mode shape, frequency, and damping. In an earthquake the force generated at each floor level is proportional to the acceleration at each floor level, and this, in turn, is a function of the displacement of each floor and this is manifest in the mode shape. The influence of frequency and damping are shown in the frequency response spectrum for specified values of damping in a single degree of freedom system subjected to the earthquake.

If the initial design assumption underestimates the natural frequency and the spectrum increases with frequency then the design loads would underestimate the actual ones. If the spectrum decreases with frequency then the reverse would be true. Figure 3.23 shows the frequency response spectrum for the El Centro earthquake in the form of the peak acceleration for a single degree of freedom system with 1 per cent damping. The response at the design frequency, 1 Hz, as is computed by the bare frame model, is about 50 per cent less than at the measured frequency 1.99 Hz. Thus an underestimate of the natural

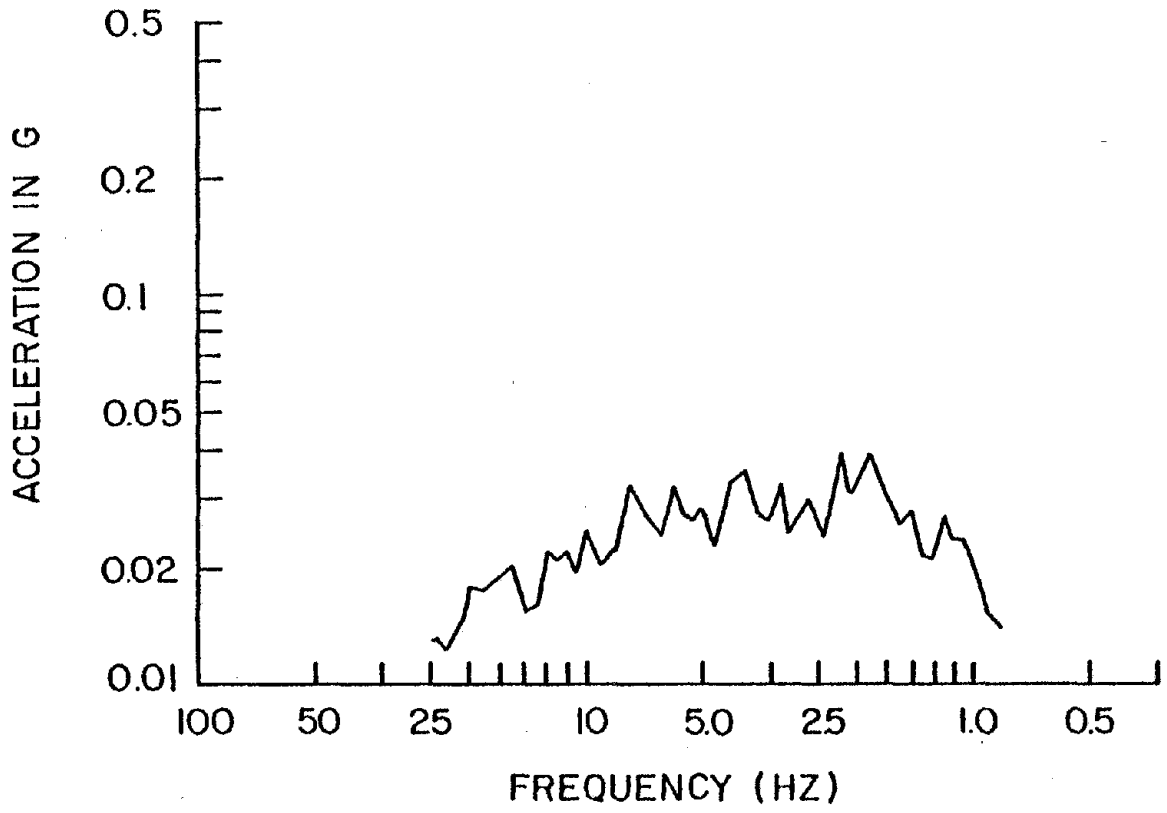

Figure 3.23. El centro Earthquake Peak Acceleration Response for 2 Percent Critical Damping.

frequency in this frequency region results in an underestimate of the peak earthquake load.

For the x direction each table shows the ratio of the BX2 model to some other postulated mode. The BX2 model produced more or less a straight line mode shape. Thus, in the x direction, close agreement in values of ratios between the static and dynamic results is not to be expected.

In the y direction the models produced mode shapes that agreed quite closely, and thus the static and dynamic loadings should produce reasonably close values. Study of Table 3.22 indicates that this is indeed the case.

3.5 Concluding Comments

An overview of the analysis of the Residential Nautical College building indicates that stiffening of one row of columns by adding infill partition walls attracts loading to that line of columns. This can increase the bending moment in the columns several times over that which is computed if the stiffening effect of the infill partitions is neglected. This could possibly seriously alter the factor of safety for this building.

It is disturbing to note that if an illogical design assumption is made, i.e. that the shear walls and column line B are independent (type AX) a simple bare frame analysis would yield much more accurate loads than would a more logical bare frame analysis (type BX).

TABLE 3.22 RESULTS OF ANALYSES IN DIMENSIONLESS FORM FOR

BUILDING: R. N. C.
ELEMENT: COLUMN B3
LOADING: EARTHQUAKE
DIRECTION: Y

LEVEL	BOTTOM MOMENT $\frac{AY1}{AY}$	TOP MOMENT $\frac{AY1}{AY}$	AXIAL FORCE $\frac{AY1}{AY}$	SHEAR FORCE $\frac{AY1}{AY}$
12	0.64	0.64	0.59	0.64
11	0.63	0.63	0.58	0.63
10	0.63	0.63	0.58	0.63
9	0.62	0.62	0.58	0.61
8	0.60	0.59	0.58	0.59
7	0.57	0.56	0.58	0.56
6	0.54	0.54	0.58	0.54
5	0.52	0.52	0.59	0.52
4	0.50	0.50	0.59	0.50
3	0.49	0.48	0.60	0.48
2	0.47	0.47	0.60	0.47
1	0.44	0.43	0.61	0.44

The results also indicate that a poorly conducted vibration test in which mode shapes were not obtained or used could result in highly erroneous assumptions of load distributions, sometimes far worse than would have been assumed had the test not been carried out.

It is noted that the models presented for the R. N. C. building represent different exampe of structural member interaction. For example, when end shear walls are included in frame line B, a different interaction from that obtained when they are omitted is observed. This means that the reversed moments put into the shear walls by the floors are intensified when end shear walls are integrated into frame line B. This changes the mode of deformation of the entire building. If, in addition, the effects of the partitions are included, then the mode shape for the structure changes further to the pronounced shear shape of the measured mode shape.

The ratios shown in the tables indicate that in some instances the more correct model will yield design values that are several orders of magnitude larger than the traditional model would provide. This does not necessarily mean that the structural member is underdesigned by this factor for different models could well provide a critical design value at some other level in the structure which would have a different ratio. This study deals only with estimation of lateral loads. Design is based upon a critical combination of vertical dead and live loads plus the effects of lateral loads. Therefore lateral loads that are orders of magnitude different from the design lateral loads affect the factor of safety by an amount depending upon the original design

assumptions of the contributions of lateral loads as compared to the remaining contributing loads. Since the exact design details are not known in this case no estimate of the safety of the structure can be based on this study alone.

CHAPTER IV. THE BRITISH RAIL BUILDING

4.1 Building Location and Geometry

The British Rail (B. R.) building in Plymouth, England, is sited in a small valley and is used as general office accomodation. The building is rectangular in section with a large raft type foundation. It is 42 m high and is comprised of eleven stories above ground. Figures 4.1, 4.2, and 4.3 show a typical floor plan and two elevations. Like the Residential Nautical College building studied in Chapter III, the B. R. building is a medium-rise concrete building. But while the R. N. C. building is a flat slab type of construction the B. R. building has ribbed floors and beams.

The plan view shown in Figure 4.1 portrays three elevator cores and three pairs of shear walls. One pair of elevator cores is near one end of the rectangle and the remaining core is close to the other end of the building. Two pairs of shear walls are external, and the remaining pair is near the single elevator core. The shear walls are 0.3 m thick. The columns in rows A and B are each 0.6 m by 0.3 m. Beams connect the columns in the x direction. The floor ribs run in the y direction. The floors in each end section are solid slabs, not ribbed, 0.15 m thick.

4.2 Partitions and Cladding

The B. R. building has a few internal partitions but none of these are infill partitions. Those partitions that do exist are located near the ends of each floor. Cladding on the longitudinal faces consists of

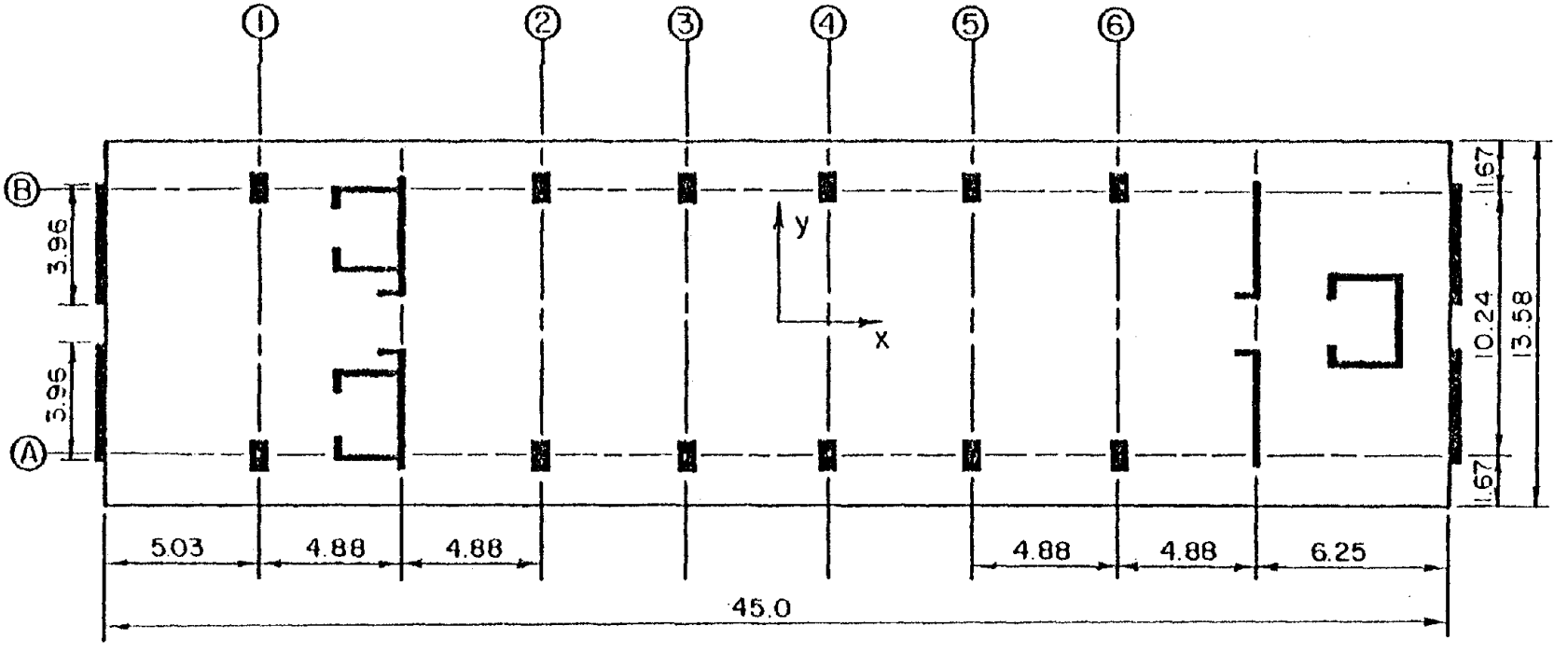

Figure 4.1. Typical Plan View of the British Rail Building (All Dimensions in Meters).

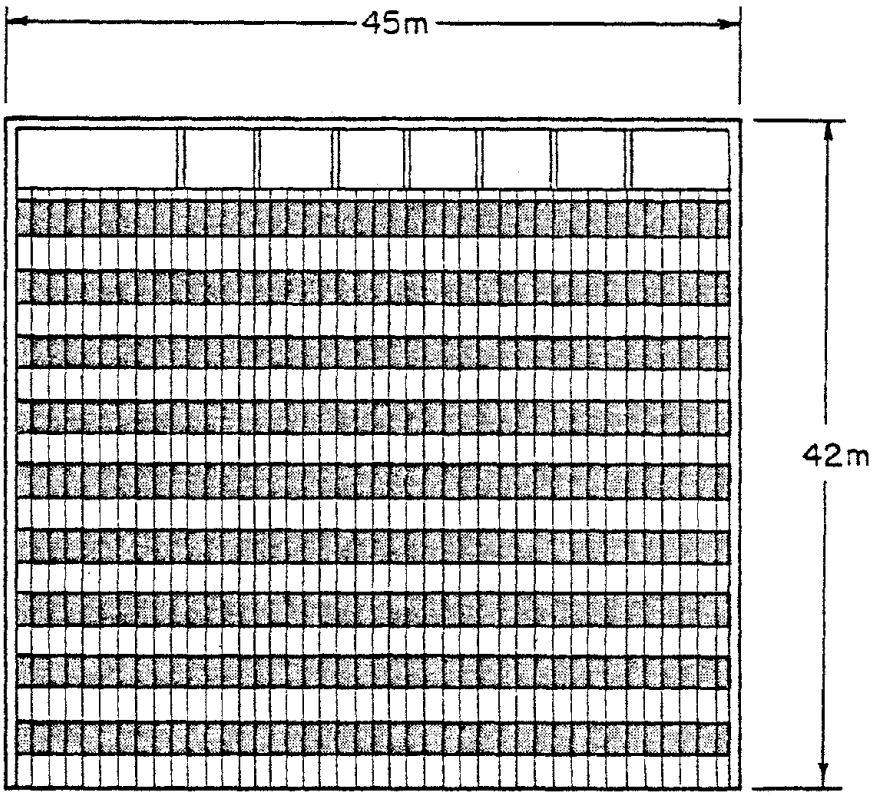

Figure 4.2. Elevation View of the British Rail Building in the Long Direction.

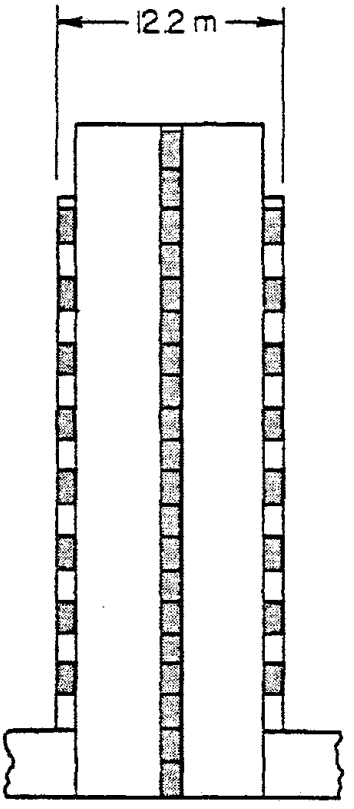

Figure 4.3. Elevation View of the British Rail Building in the Short Direction.

upstands joined to the floor at each floor level along with glass. The external shear walls provide most of the cladding in the transverse direction.

4.3 Experimental Procedure

The same vibrator was used for the B. R. building as was used for the R. N. C. building. The vibrator was placed in the elevator room at the right hand end of the building. This should have permitted torsional frequencies to be excited but it was not possible to detect a torsional mode, possibly due to the masking of that mode due to transverse wind excitation. The details of this test and the experimental results were given by Jeary and Sparks (16).

4.4 Structural Analysis of the B. R. Building

Roughly the same sequence of analysis was made for the B. R. building as was made for the R. N. C. building, but the modelling variations were not as extensive because the B. R. building is a much simpler structure.

4.4.1 Structural Idealizations

A preliminary analysis of the British Rail building was done assuming four frames for this might be the first idealization a designer would consider. These frame lines in the x direction were comprised of frame line A, frame line B, and two mirror image frames containing the shear walls and elevator cores on each side of the building. The

geometry of the two sets of frames (the interior set and the exterior set) are considerably different. It is noted that the TABS-77 program assumes that each frame acts inependently when, in fact, in this case it would be difficult for them to do so. Good results from this preliminary analysis were not expected nor were good results obtained. It is believed that since the exterior frames would try to deform in one way and the interior frames in quite a different manner, then there would be considerable interference between adjacent frame lines. It is believed that these overlapping effects probably account for the unsatisfactory results obtained for this preliminary model. Further, the experience gained from the study of the Residential Nautical College building indicates that this model for the British Rail building is not a logical idealization. Therefore, this model was not pursued and the results are not reported.

The experience gained from the study of the R. N. C. building strongly indicated that a more logical idealization would be to consider the shear walls, elevator cores, and the columns lumped together in two frame lines for the x direction. Thus each frame line would contain the exterior columns on one side along with the three shear walls for its side and one and one-half elevator cores. This model is referred to as CX for the B. R. building. Figure 4.4 shows the CX idealization in more detail.

An analysis was made for this idealization and the results are shown below in Table 4.1. This model underestimates the natural frequency.

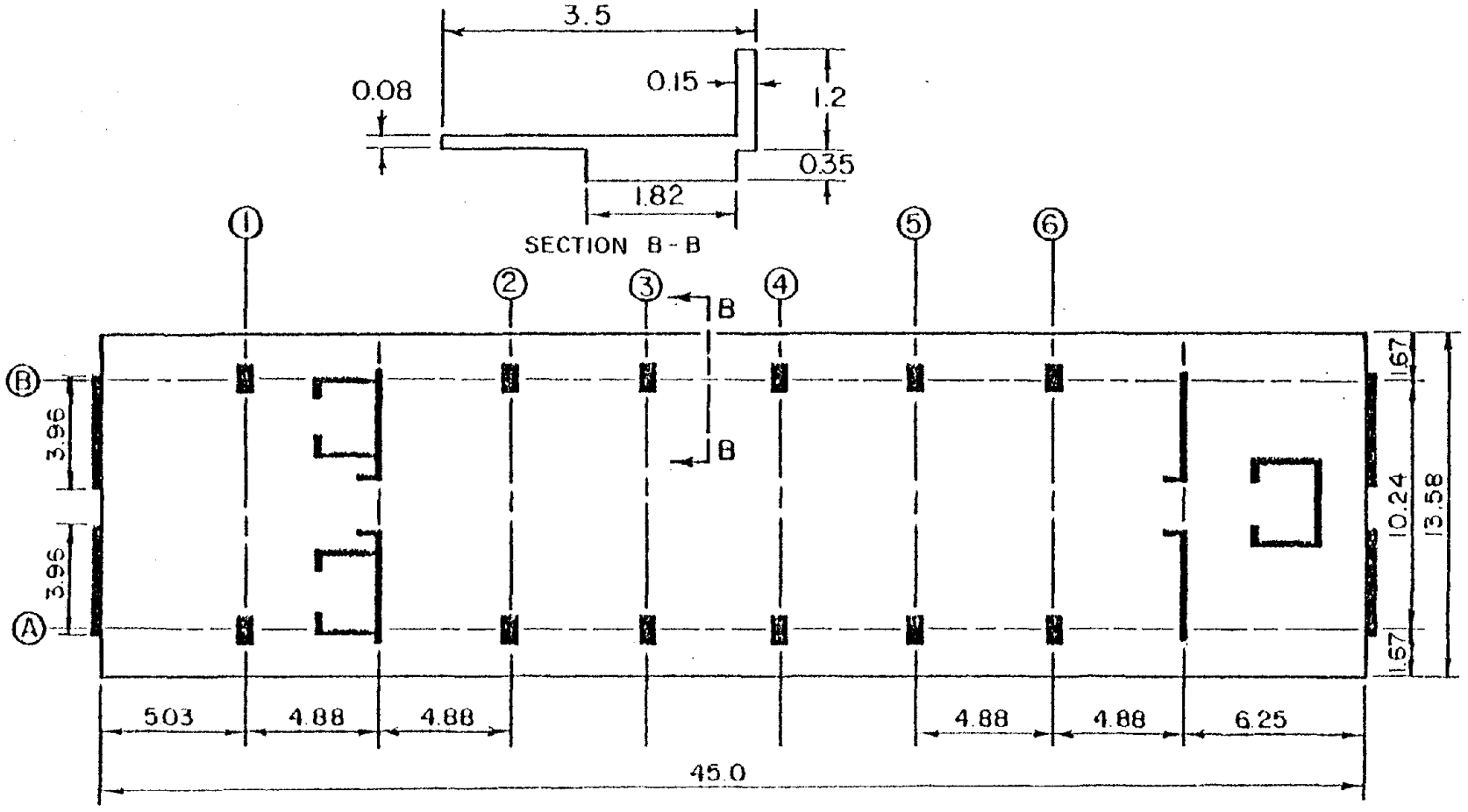

Figure 4.4. CX, CX1, CX2 Structural Idealization for the British Rail Building.

Table 4.1 Measured and Predicted Fundamental Frequencies

Type of Analysis	Direction	Frequency Hz
experimental	x	1.25
CX	x	1.0

by 25 per cent for the x direction. Figure 4.5 shows the comparison between the measured mode shape and the computed mode shape. The agreement is very poor. Such divergence from measured values indicates that either the idealization is not correct, or the theoretical treatment accorded the model by TABS-77 is inadequate, or both.

The R. N. C. analysis has shown that workable models and adequate theoretical treatments do exist. Based on the R. N. C. experience the TABS-77 program ought to have been able to provide satisfactory results provided suitable input parameters were available.

After some thought it was decided that the most logical modification for improving the frequency match would be to stiffen the end floor slabs. It is known that partitions exist over the end floor slabs but their distribution and structural details are not known. Further, there is no published information that can be used for guidance in modifying the stiffness of slabs to account for non-infill partitions. Under these circumstances it was decided to arbitrarily increase the end slab stiffness until a frequency match was obtained. The model that produced this match was termed CX1.

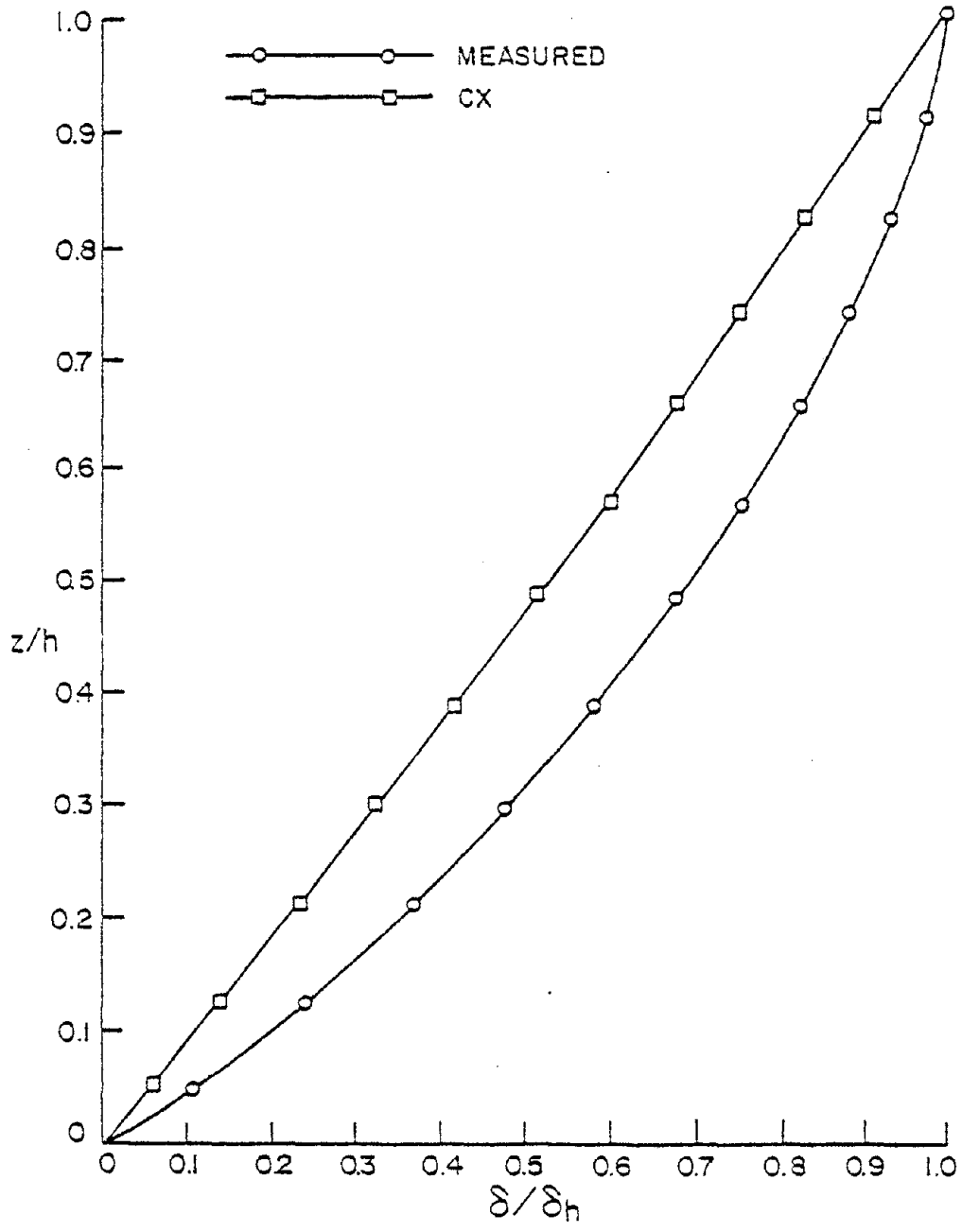

Figure 4.5. X Mode Shapes for the British Rail Building.

The mode shape type CX1 produced is shown in Figure 4.6 along with the measured shape and that produced by the CX model. It can be seen that the CX1 is a small improvement over CX. The next step was a logical modification that might improve the mode shape without affecting the frequency significantly.

The elevator cores are many orders of magnitude stiffer than the columns in the frame lines. Experience gained from the R. N. C. building suggested that a change in the stiffness of the elevator cores might have a significant effect on the mode shape. Also Clark (18) has indicated that significant changes can be made in the shear wall stiffnesses without significantly changing natural frequencies. Timoshenko (19) has given recommendations for effective flange width brought about by a consideration of shear lag. Khan (9) and other investigators (20) adapted Timoshenko's work so that effective floor slab widths could be calculated. This approach was used not only for the models dealt with so far for this structure but also for all the models used for the R. N. C. building. Although Khan's recommendations are widely used, no one seems to have recognized that these principles might well apply to such frame components as elevator cores which are considered to be thin walled members. It was decided that Timoshenko's principles could be applied to the elevator cores. When this was done it was observed that, for at least the cores at hand, the Timoshenko results could be approximated to within 10 per cent by simply neglecting the transverse flanges of the cores. In calculating the moment of inertia this approximation would be a convenience for the designer.

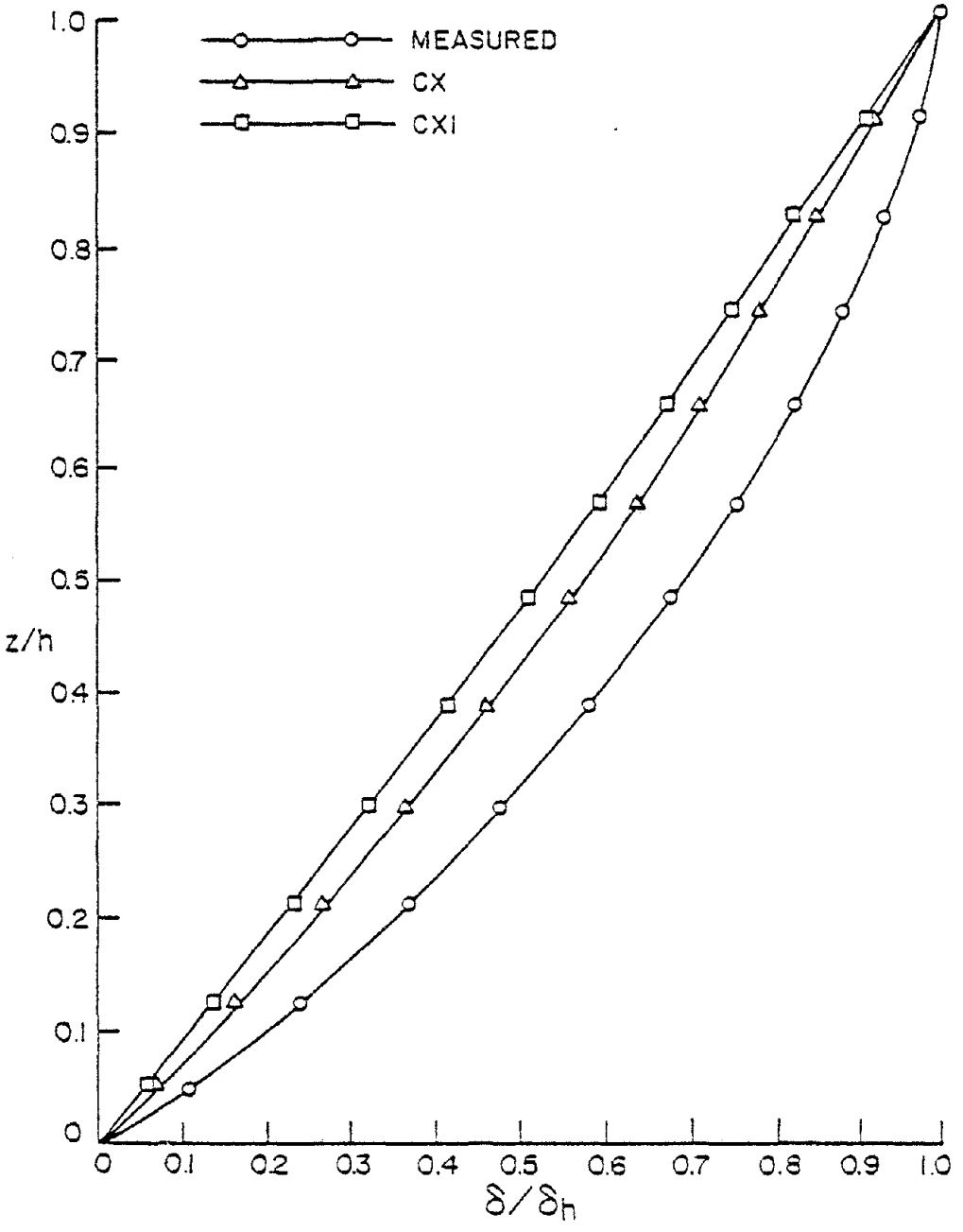

Figure 4.6. X Mode Shapes for the British Rail Building.

Using this approximation the next and last model for this building in the x direction, CX2, was developed. To achieve a match of both frequency and mode shape the end floors had to be stiffened further to account for the reduction in stiffness in the elevator cores. Figure 4.7 shows all of the mode shapes discussed for this building.

In the y direction it was assumed that the traditional designer would idealize this system as a series of parallel frames acting independently of each other. This is a good approach for the structure is simple and the frames are adequately separated. First a model was used which considered the moments of inertia of the entire elevator cores. The frequency computed (1.39 Hz) was slightly higher than the measured frequency (1.32 Hz) and the mode shape computed was in good agreement with the measured mode shape in this direction. Secondly, the elevator cores were modified as in the last x direction model, using the approximation rather than Timoshenko's exact recommendation, this caused the necessary small change in frequency and did not make a discernable change in the mode shape. This adds weight to the assumption made concerning shear lag effects. These models are indicated in Figure 4.8 and the mode shape comparison is shown in Figure 4.9

4.4.2 Parametric Studies

It has been shown that the CX2 idealization for the B. R. building is in full agreement with the experimental results. As in the R. N. C. building it is informative to examine the sensitivity of the building to the two parameters involved in establishing the CX2 model. Accordingly

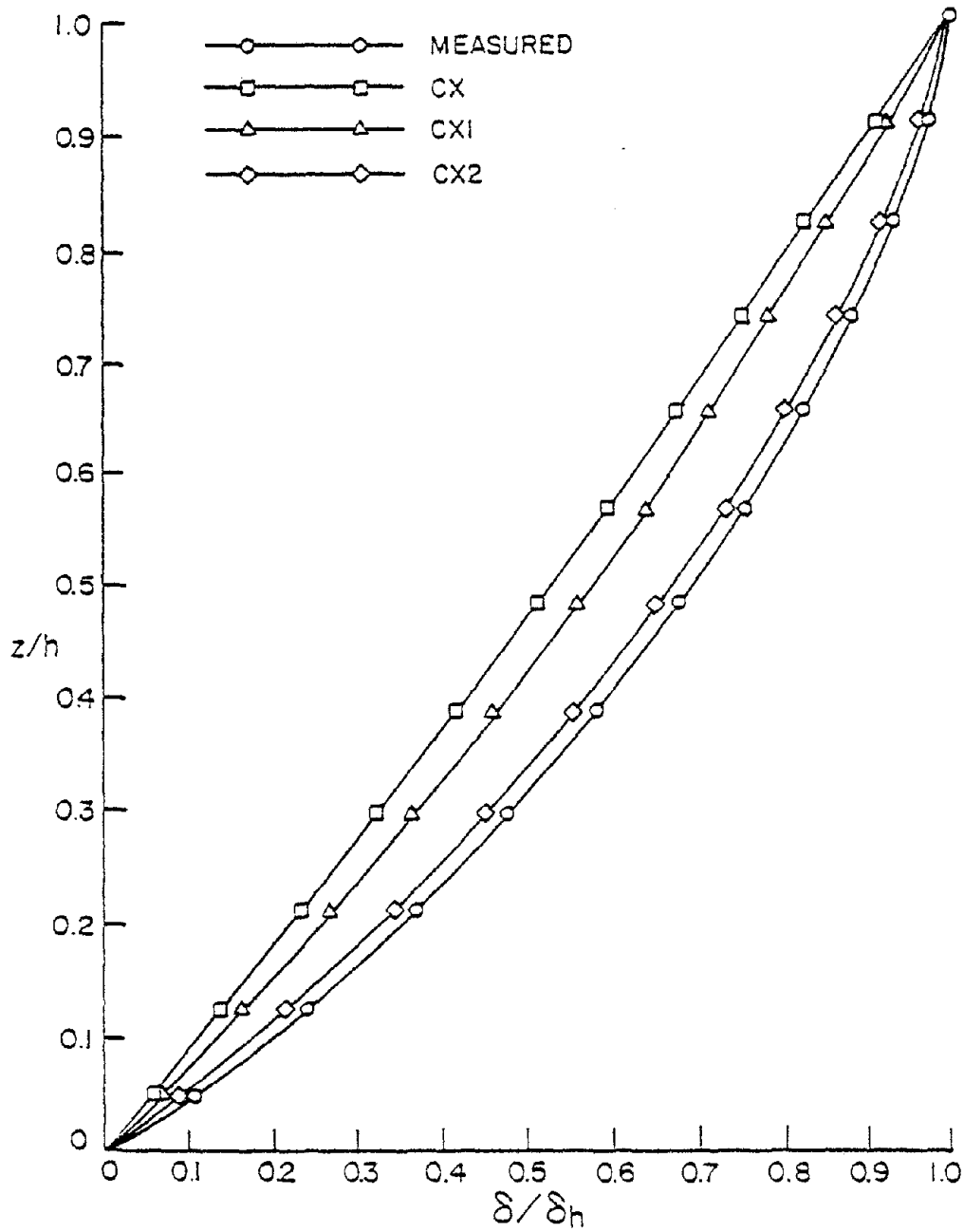

Figure 4.7. X Mode Shapes for the British Rail Building.

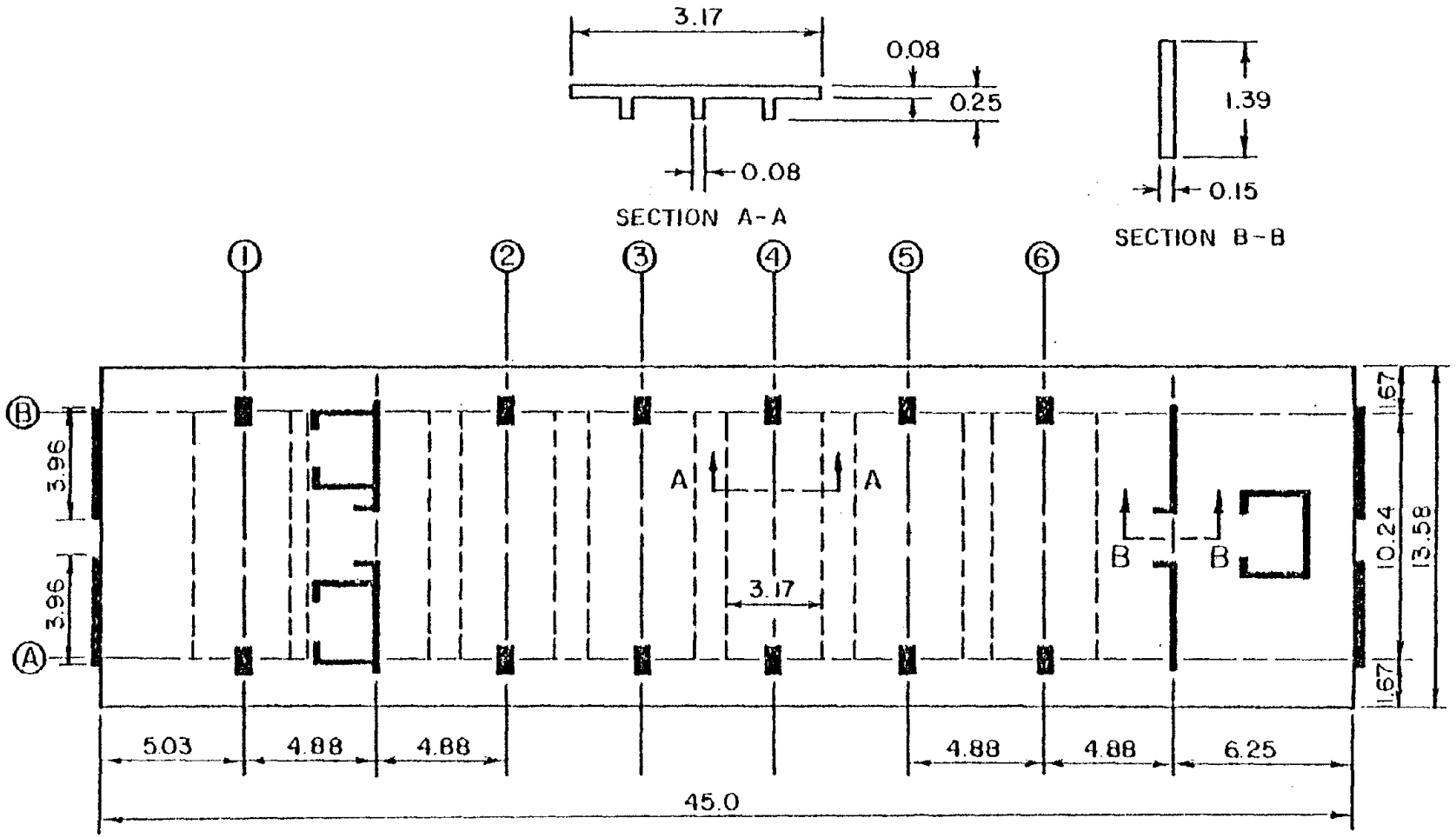

Figure 4.8. CY, CY1 Structural Idealization for the British Rail Building.

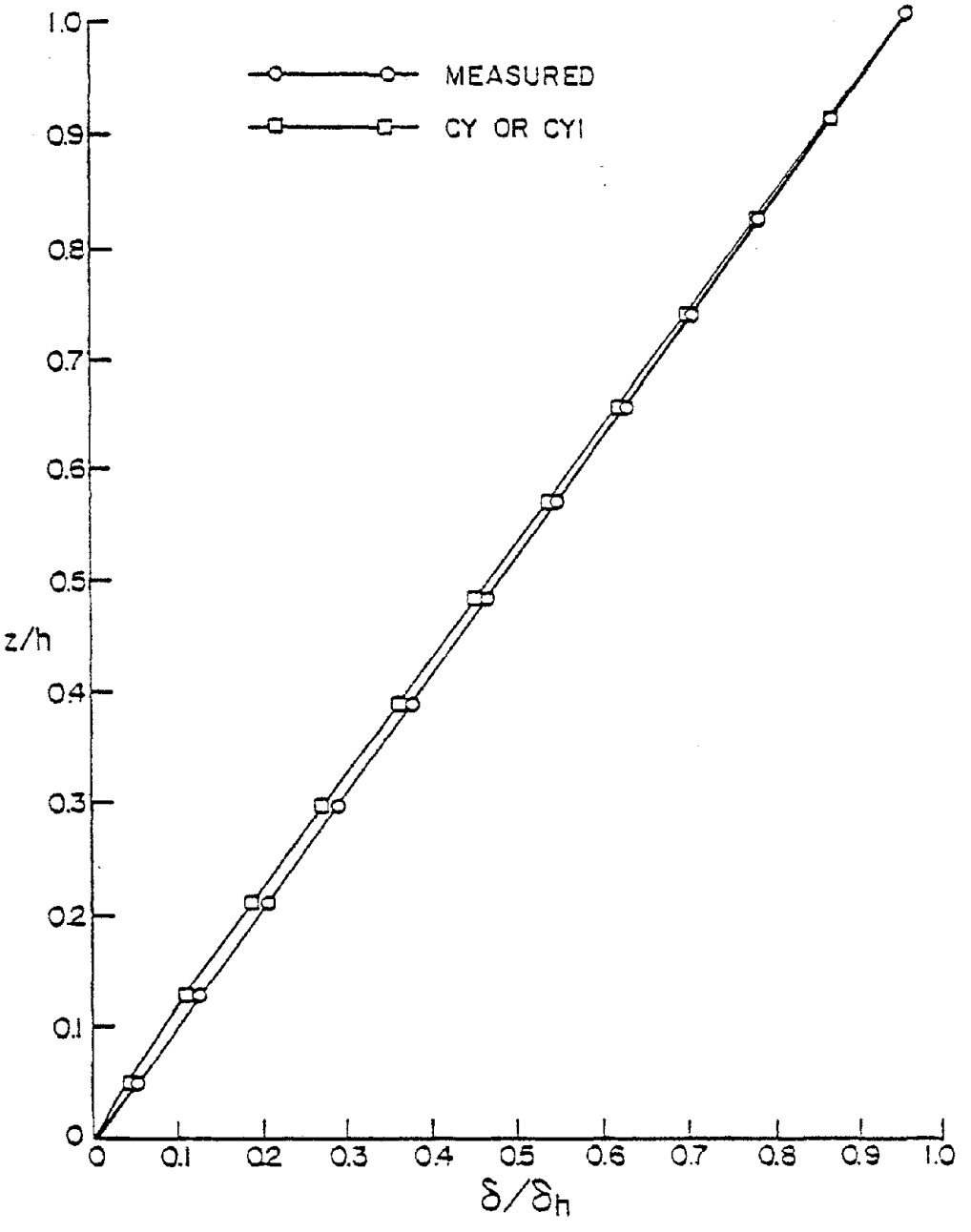

Figure 4.9. Y Mode Shapes for the British Rail Building.

two parametric studies were made and these results are indicated in this section.

One of the parameters was the stiffness of the end floor slabs. This parameter variation was logically called for by what is known about the structure but the magnitude of the variation had to be found by trial and error until the measured frequency was matched. A variation of the stiffness (thickness) of the floor is logically required by the known existence of partition walls; placement and details of the walls are unknown. In developing the CX2 model the stiffness was varied only in an upward direction until a frequency match occurred; in the parametric study the thickness of the end floor slabs was varied from a very small value, much less than the actual thickness, to a value that yielded for all practical purposes an infinite stiffness. For this study the second parameter, elevator core stiffness, was kept constant at the CX2 value. The results are shown in Table 4.2 and Figure 4.10.

A study of the results of this variation in end floor slab stiffness indicates that the natural frequency of this building is sensitive to changes in this stiffness. This sensitivity is more pronounced in the neighborhood of the value used for the CX2 idealization. When the stiffness becomes very much larger and the column stiffnesses are unchanged, then the relative stiffness effects diminish and the curve flattens out somewhat.

Table 4.2 shows that for this structure a variation of the end floor slab thickness from a very small value to almost infinite stiffness results in a doubling of the natural frequency. In terms of

Table 4.2. Parametric Study of Floor Slab Thickness in the British Rail Building, X Direction

S/S_0	Frequency (Hz)	Modal Mass (Kg)
0.015	0.79	1825320
0.06	0.89	1866284
0.1	0.96	1886849
0.375	1.11	1871394
0.625	1.17	1856127
0.875	1.21	1846053
1.00	1.25	1841047
1.5	1.28	1831096
2.75	1.35	1816319
6.5	1.44	1796893
12.5	1.50	1777777
62.5	1.60	1731301
125	1.62	1722225
625	1.64	1717714
1250	1.65	1704285
∞	1.65	1700000

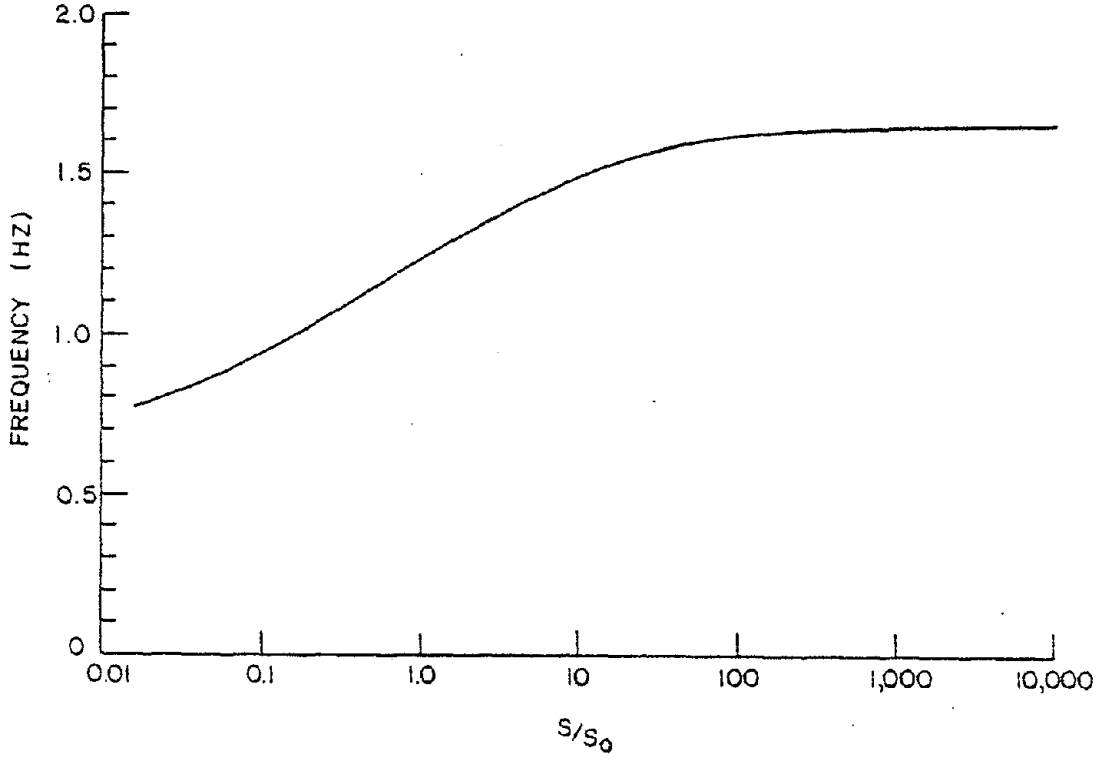

Figure 4.10. Frequency vs. Normalized Stiffness for Parametric Study of Floor Slab Thickness in the British Rail Building, X Direction.

stiffness of the structure as a whole this is a fourfold increase. If this is typical of buildings similar to the B. R. building this could be an important design consideration.

Further study of Table 4.2 indicates that the modal mass changes hardly at all, no matter what value of stiffness is used for the end floor slabs. Hence mode shape is insensitive to end floor slab stiffness.

The second parametric study kept the end floor slab constant at the CX2 value and a logical variation in the stiffness of the elevator core was made. This was accomplished by ignoring the flange of the cores at one end of the range to including the entire sections at the other end of the range. The results of this study are shown in Table 4.3 and Figure 4.11. Both the table and its accompanying plot strongly suggest that the natural frequency of the structure is not sensitive to changes in stiffness of the elevator cores. This indicates that these elevator cores are acting in much the same way as the plane shear walls reported by Clark (18).

Table 4.3 shows that the modal mass is quite sensitive to even small changes in stiffness of the elevator cores. Figure 4.12 shows the mode shape associated with each modal mass and indicates that the lowest modal mass associated with the full elevator core section is a more or less straight line. When the flanges are neglected to take into account the shear lag effects, then the largest modal mass is obtained and is associated with a mode shape that is very close to the measured mode shape.

Table 4.3. Parametric Study of Effectiveness of Flanges in Stiffening Cores in the British Rail Building, X Direction

S/S_o	Frequency (Hz)	Modal Mass (Kg)
1.00	1.25	1841047
1.26	1.26	1800000
1.50	1.29	1763640
2.00	1.31	1731301
2.47	1.34	1695421
3.00	1.37	1664932
3.42	1.38	1647878

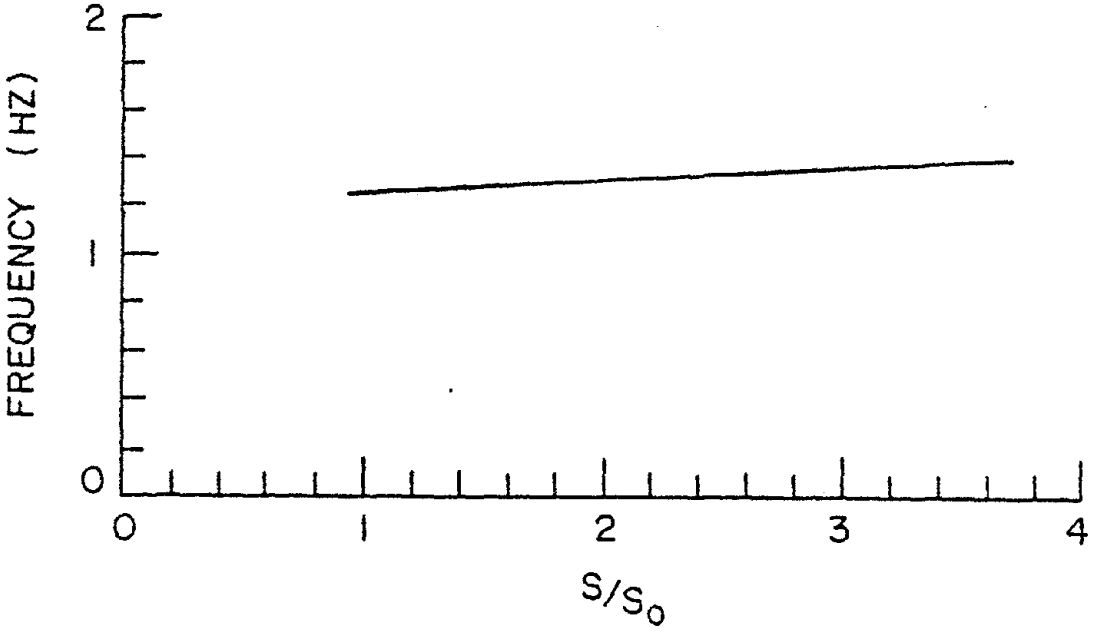

Figure 4.11. Frequency vs. Normalized Stiffness for Parametric Study of Effecticeness of Flanges in Stiffening Cores in the British Rail Building, X Direction.

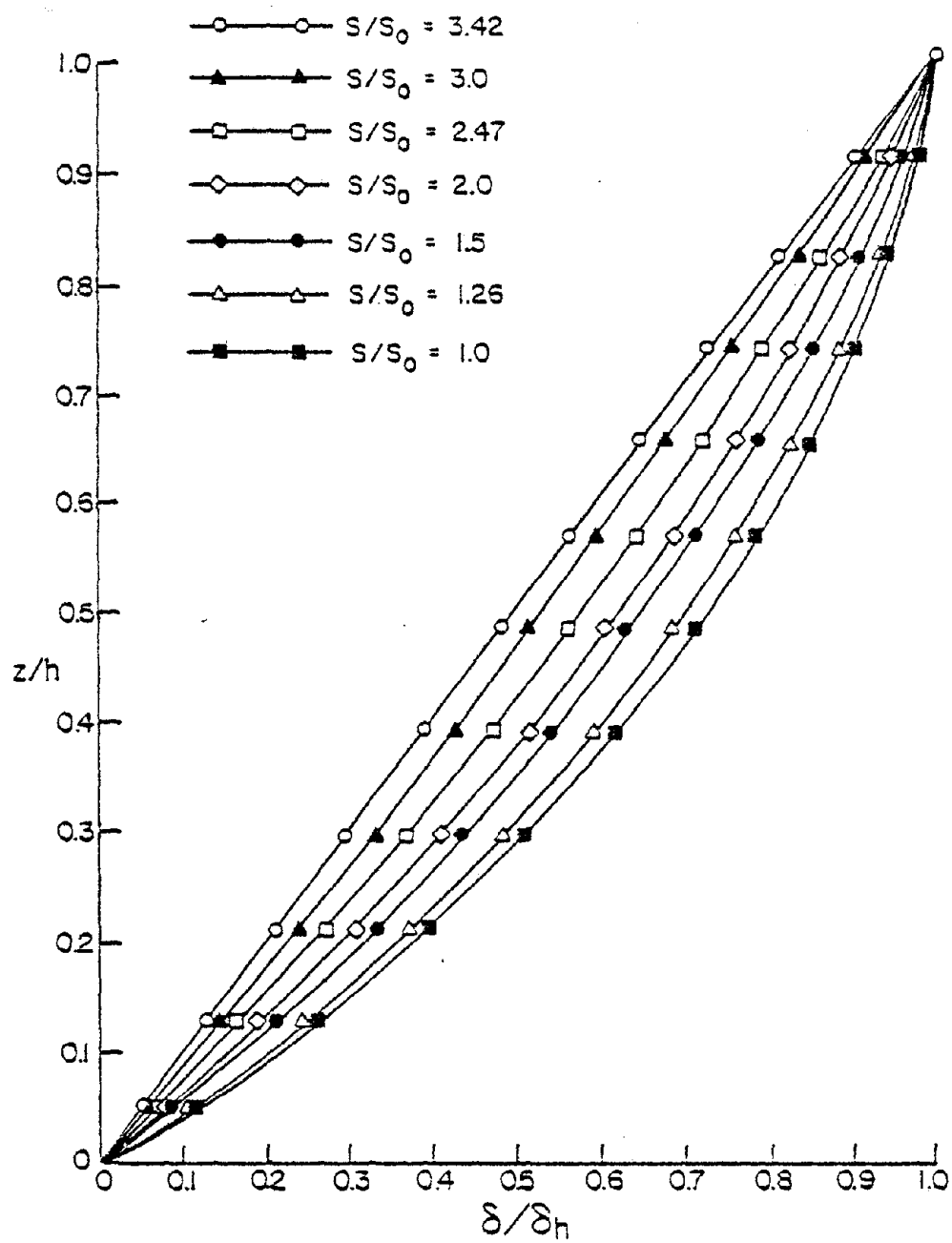

Figure 4.12. X Mode Shapes for the British Rail Building.

The second parametric study of this building emphasizes the fact that while neglecting the shear lag effects on elevator cores fails to produce significant inaccuracies in computing the natural frequency, it does produce a significant inaccuracy in computing mode shape. This inaccuracy will greatly affect the distribution of internal forces under any lateral loading and affect the distribution and magnitude of applied dynamic loads such as earthquake loading.

4.4.3 Significance of Choice of Models

As was done in section 3.4.4 for the Residential Nautical College building, the significance of the choice of analytical model for the British Rail building was tested by the application of static and dynamic lateral loads.

In the x direction, model AX was typical of an assumption made by a designer since it neglected both the effects of partitions on the end floor slab and shear lag effects within the elevator cores. The CX1 model was a modification of the CX model. The end floor slabs were stiffened by an amount that brought the model into agreement with the known natural frequency but did not match the mode shape. The CX2 model was a modification of the CX1 model which considered the effects of shear lag on the elevator cores. The CX2 model was the best predictor of the dynamic characteristics for this structure.

The loading on each of these models was as used for the R. N. C. building.

Column A2, one of the pair of elevator cores, and one of the exterior shear walls were chosen for analysis and these elements are encircled in Figure 4.13.

As was done for the R. N. C. building study, the results are shown in dimensionless form with the results for the most accurate CX2 model compared to the other results.

In the y direction the choice of models did not appear to be significant for both of the models yielded essentially the same results and so it was considered unnecessary to apply loadings in this direction.

4.4.3.1 Lateral Static Loading

Table 4.4 shows that if the CX model is used then the forces and moments in the outside shear walls are underestimated by as much as a factor of seven. This is of interest because Jeary and Sparks (16) report that close inspection of these outside shear walls reveal cracking that is indicative of overstressing from bending. If the designer had modified his analysis to take into account the interior partitions, in order to match an observed frequency, CX1, the underestimation would only be a factor of two.

Study of Table 4.5 indicates that both models CX and CX1 overestimate the loadings in the elevator cores. This is probably caused by the elevator cores being in actuality less stiff than the designer might have surmised.

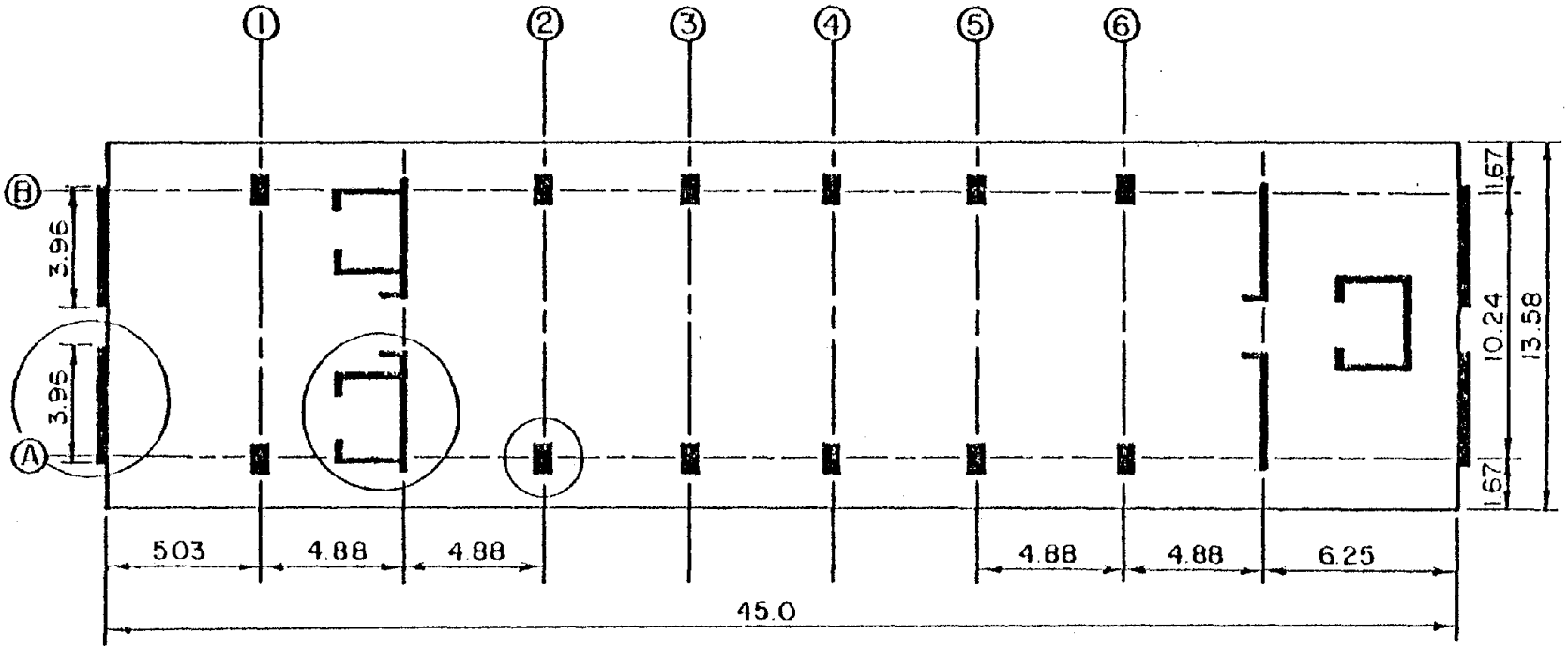

Figure 4.13. Elements Chosen for the Analysis of the British Rail Building.

TABLE 4.4 RESULTS OF ANALYSES IN DIMENSIONLESS FORM FOR

BUILDING: B. R.
ELEMENT: EXTERNAL SHEAR WALL
LOADING: WIND
DIRECTION: X

LEVEL	BOTTOM MOMENT		TOP MOMENT		AXIAL FORCE		SHEAR FORCE	
	$\frac{CX2}{CX}$	$\frac{CX2}{CX1}$	$\frac{CX2}{CX}$	$\frac{CX2}{CX1}$	$\frac{CX2}{CX}$	$\frac{CX2}{CX1}$	$\frac{CX2}{CX}$	$\frac{CX2}{CX1}$
11	2.79	0.89	1.80	0.80	1.67	0.72	2.10	0.82
10	4.03	1.05	3.08	1.05	2.00	0.78	3.40	1.02
9	4.15	1.12	2.80	1.10	2.18	0.83	3.25	1.08
8	4.46	1.19	3.17	1.15	2.31	0.86	3.59	1.15
7	4.56	1.24	3.40	1.23	2.43	0.89	3.78	1.20
6	4.66	1.28	3.71	1.28	2.53	0.92	4.00	1.25
5	4.68	1.35	4.04	1.34	2.64	0.94	4.22	1.31
4	4.68	1.41	4.51	1.41	2.74	0.96	4.47	1.37
3	4.40	1.50	5.21	1.51	2.84	0.99	4.62	1.47
2	4.53	1.61	7.52	1.68	2.94	1.02	5.50	1.60
1	1.73	1.59	6.54	2.00	3.00	1.04	2.78	1.74

TABLE 4.5 RESULTS OF ANALYSES IN DIMENSIONLESS FORM FOR

BUILDING: B. R.
ELEMENT: ELEVATOR CORE
LOADING: WIND
DIRECTION: X

LEVEL	BOTTOM MOMENT		TOP MOMENT		AXIAL FORCE		SHEAR FORCE	
	$\frac{CX2}{CX}$	$\frac{CX2}{CX1}$	$\frac{CX2}{CX}$	$\frac{CX2}{CX1}$	$\frac{CX2}{CX}$	$\frac{CX2}{CX1}$	$\frac{CX2}{CX}$	$\frac{CX2}{CX1}$
11	0.17	0.43	1.53	0.95	- 5.74	2.68	0.54	2.25
10	0.1	0.29	0.57	0.79	-13.35	2.09	2.94	1.05
9	-0.09	-0.09	0.53	0.80	- 5.75	1.34	1.44	1.00
8	-0.19	-4.45	0.52	0.82	- 3.37	1.04	1.14	1.00
7	-0.57	1.75	0.55	0.87	- 2.32	0.88	1.00	1.00
6	-3.78	1.11	0.59	0.93	- 1.78	0.78	0.93	1.00
5	1.55	0.90	0.67	1.01	- 1.45	0.70	0.86	1.00
4	0.70	0.79	0.86	1.16	- 1.22	0.64	0.78	0.97
3	0.44	0.69	1.76	1.45	- 1.05	0.58	0.70	0.93
2	0.30	0.60	-1.63	2.44	- 0.92	0.50	0.63	0.90
1	0.06	0.072	-0.3	3.84	- 0.80	0.44	0.78	0.82

The next table, Table 4.6, suggests in general the loadings in column A2 are not much affected by the model chosen.

4.4.3.2 Dynamic Loading

Tables 4.7 through 4.9 show the results of earthquake loading on the outside shear walls, the elevator cores, and column A2. A study of these tables shows the same trends as the wind load tables. While the trends are unchanged from the static loading, the magnitude and sign of the ratios change. The change in the value of the ratios is more pronounced at the lower levels. It is interesting to note that the largest discrepancy in mode shape also occurs at these levels. Again, this is probably indicative of the influence of mode shape on the distribution and magnitude of the applied dynamic loads, and this, in turn, changes the internal forces developed in the structure. Further, it should be noted that the discrepancy between the ratios of dynamic and static results are less for models CX1 than for model CX. It is noted that CX1 agreed better with the experimental mode shape than did CX.

4.5 Concluding Comments

Reviewing the analysis of the British Rail building indicates the elevator core sections are inefficient in their provision of stiffness and this is attributed to shear lag effects in thin walled members. Incorrectly assuming that box sections are fully effective not only changes the mode shape, and thus the distribution of stiffness over the

TABLE 4.6 RESULTS OF ANALYSES IN DIMENSIONLESS FORM FOR

BUILDING: B. R.
ELEMENT: COLUMN A2
LOADING: WIND
DIRECTION: X

LEVEL	BOTTOM MOMENT		TOP MOMENT		AXIAL FORCE		SHEAR FORCE	
	$\frac{CX2}{CX}$	$\frac{CX2}{CX1}$	$\frac{CX2}{CX}$	$\frac{CX2}{CX1}$	$\frac{CX2}{CX}$	$\frac{CX2}{CX1}$	$\frac{CX2}{CX}$	$\frac{CX2}{CX1}$
11	0.73	0.95	0.73	0.98	0.65	1.94	0.74	0.96
10	0.76	1.00	0.77	1.00	0.57	2.10	0.78	1.00
9	0.77	1.08	0.77	1.09	0.52	4.14	0.78	1.10
8	0.76	1.13	0.77	1.13	0.40	1.03	0.78	1.15
7	0.75	1.17	0.76	1.17	0.10	0.27	0.77	1.18
6	0.75	1.20	0.75	1.20	0.59	0.55	0.76	1.21
5	0.75	1.23	0.75	1.23	0.59	0.67	0.76	1.25
4	0.75	1.27	0.75	1.27	0.53	0.74	0.76	1.28
3	0.78	1.32	0.78	1.32	0.53	0.80	0.76	1.34
2	0.87	1.40	0.86	1.40	0.56	0.87	9,87	1.42
1	1.23	1.67	1.15	1.65	0.62	0.96	1.18	1.70

TABLE 4.7 RESULTS OF ANALYSES IN DIMENSIONLESS FORM FOR

BUILDING: B. R.
ELEMENT: EXTERNAL SHEAR WALL
LOADING: EARTHQUAKE
DIRECTION: X

LEVEL	BOTTOM MOMENT		TOP MOMENT		AXIAL FORCE		SHEAR FORCE	
	$\frac{CX2}{CX}$	$\frac{CX2}{CX1}$	$\frac{CX2}{CX}$	$\frac{CX2}{CX1}$	$\frac{CX2}{CX}$	$\frac{CX2}{CX1}$	$\frac{CX2}{CX}$	$\frac{CX2}{CX1}$
11	3.28	0.96	2.01	0.87	1.86	0.77	2.38	0.87
10	4.83	1.17	3.33	1.18	2.23	0.84	3.82	1.15
9	4.71	1.24	3.06	1.21	2.42	0.90	3.58	1.20
8	4.79	1.31	3.52	1.29	2.56	0.93	3.93	1.26
7	4.77	1.38	3.98	1.36	2.69	0.97	4.20	1.33
6	4.83	1.43	4.69	1.41	2.81	1.00	4.62	1.38
5	5.09	1.50	5.73	1.49	2.93	1.02	5.42	1.45
4	5.45	1.58	6.67	1.58	3.06	1.05	6.04	1.54
3	5.64	1.70	7.93	1.71	3.21	1.08	6.77	1.66
2	6.27	1.83	11.82	1.90	3.37	1.11	8.15	1.81
1	2.31	1.72	2.18	2.31	3.48	1.13	4.02	1.93

TABLE 4.8 RESULTS OF ANALYSES IN DIMENSIONLESS FORM FOR

BUILDING: B. R.
ELEMENT: ELEVATOR CORE
LOADING: EARTHQUAKE
DIRECTION: X

LEVEL	BOTTOM MOMENT		TOP MOMENT		AXIAL FORCE		SHEAR FORCE	
	$\frac{CX2}{CX}$	$\frac{CX2}{CX1}$	$\frac{CX2}{CX}$	$\frac{CX2}{CX1}$	$\frac{CX2}{CX}$	$\frac{CX2}{CX1}$	$\frac{CX2}{CX}$	$\frac{CX2}{CX1}$
11	0.19	0.46	1.27	1.05	3.10	4.00	0.49	4.81
10	0.16	0.45	0.54	0.83	2.97	2.70	1.38	1.19
9	0.23	0.63	0.51	0.83	2.55	1.55	1.07	1.09
8	0.32	0.97	0.57	0.85	1.92	1.14	0.90	1.03
7	0.48	0.98	0.67	0.91	1.53	0.95	0.85	1.04
6	0.78	0.86	0.69	1.00	1.25	0.84	0.86	1.05
5	0.56	0.83	0.76	1.05	1.10	0.77	0.96	1.05
4	0.49	0.80	0.81	1.09	1.00	0.71	1.07	1.04
3	0.44	0.73	1.03	1.29	0.94	0.65	0.97	1.00
2	0.40	0.63	0.74	1.98	0.88	0.56	0.86	1.00
1	0.74	0.76	0.34	1.51	0.83	0.56	1.08	0.90

TABLE 4.9 RESULTS OF ANALYSES IN DIMENSIONLESS FORM FOR

BUILDING: B. R.
ELEMENT: COLUMN A2
LOADING: EARTHQUAKE
DIRECTION: X

LEVEL	BOTTOM MOMENT		TOP MOMENT		AXIAL FORCE		SHEAR FORCE	
	$\frac{CX2}{CX}$	$\frac{CX2}{CX1}$	$\frac{CX2}{CX}$	$\frac{CX2}{CX1}$	$\frac{CX2}{CX}$	$\frac{CX2}{CX1}$	$\frac{CX2}{CX}$	$\frac{CX2}{CX1}$
11	0.70	1.00	0.70	1.00	0.66	1.76	0.70	1.00
10	0.74	1.08	0.74	1.08	0.70	1.75	0.74	1.09
9	0.74	1.13	0.74	1.13	0.58	1.74	0.75	1.14
8	0.74	1.16	0.74	1.17	0.50	1.13	0.75	1.18
7	0.75	1.21	0.75	1.21	0.67	0.76	0.76	1.22
6	0.79	1.23	0.79	1.23	0.53	0.75	0.80	1.24
5	0.86	1.27	0.86	1.27	0.50	0.75	0.87	1.28
4	0.96	1.31	0.96	1.31	0.51	0.80	0.97	1.33
3	1.06	1.37	1.05	1.37	0.55	0.84	1.06	1.39
2	1.18	1.47	1.16	1.47	0.63	0.88	1.19	1.48
1	1.70	1.84	1.57	1.73	0.76	0.98	1.63	1.80

height of the building, but also assigns more loads to these box elements and less to the remaining elements. In this building this has apparently overstressed the outside shear walls and has caused them to crack. In an attempt to account for the effect of the partitions over the end floor slabs these elements were stiffened. The parametric study of this variable indicates stiffening of the end floor slabs is an efficient way of stiffening the entire structure. This showed that if the effective stiffness of the end floor slabs were made large, and this might be easily and cheaply done by the addition of partitions then the overall stiffness of the structure would be double that of a building with unstiffened slabs.

CHAPTER V. THE CIVIC CENTER

5.1 Building Location and Geometry

The Civic Center for Plymouth, England, is a building fifteen stories high. From the ground level to the top of the elevator towers atop the roof deck is 57 meters. The structure is of conventional slab and column construction with shear walls. The slab is stiffened by being ribbed. Elevator cores are located near the ends of the structure and are of reasonably symmetric design. Each of the exterior columns along the sides are 0.4 m by 0.2 m. The larger exterior columns at each end are 0.45 m by 1.06 m. The four interior columns near the center are 0.76 m by 0.45 m.

At the third floor level there is a very strong and deep beam encircling the building. Below this level there is a reduction for one story in the floor area and this reduced cross-sectional area remains constant into the basement floor. At the levels below the third floor there is a gallery or mezzanine area, and the large interior columns are made even larger. There is, of course, a non-continuous floor slab for the mezzanine and this level is connected to a surrounding one story buildings which, when combined with the effects of the enlarged interior columns, appear to fix the Civic Center at the strong beam level. For all practical purposes the floor level above the strong beam is considered to be ground level, and thus there are twelve stories above this level, not including the elevator towers. Figures 5.1, 5.2, and 5.3 present a typical floor plan and two elevations.

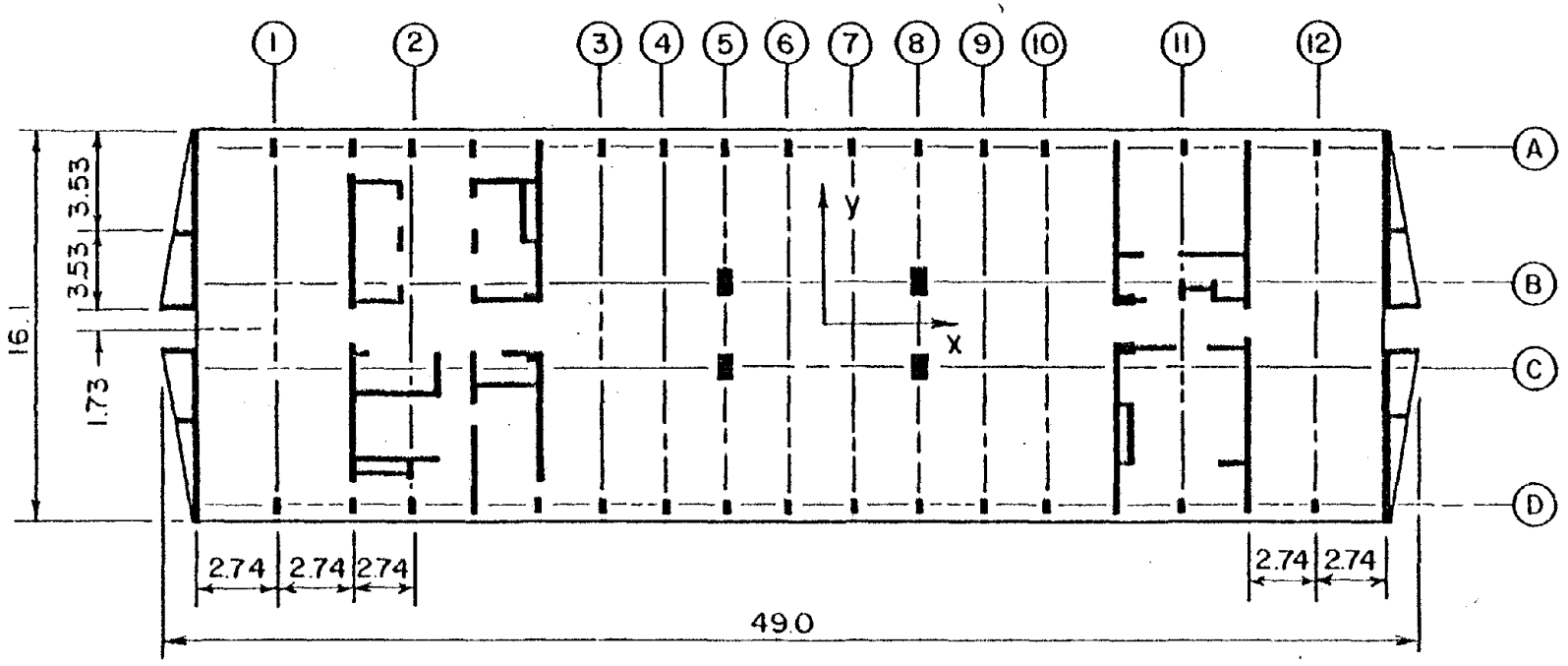

Figure 5.1. Typical Plan View of the Civic Center (All Dimensions in Meters).

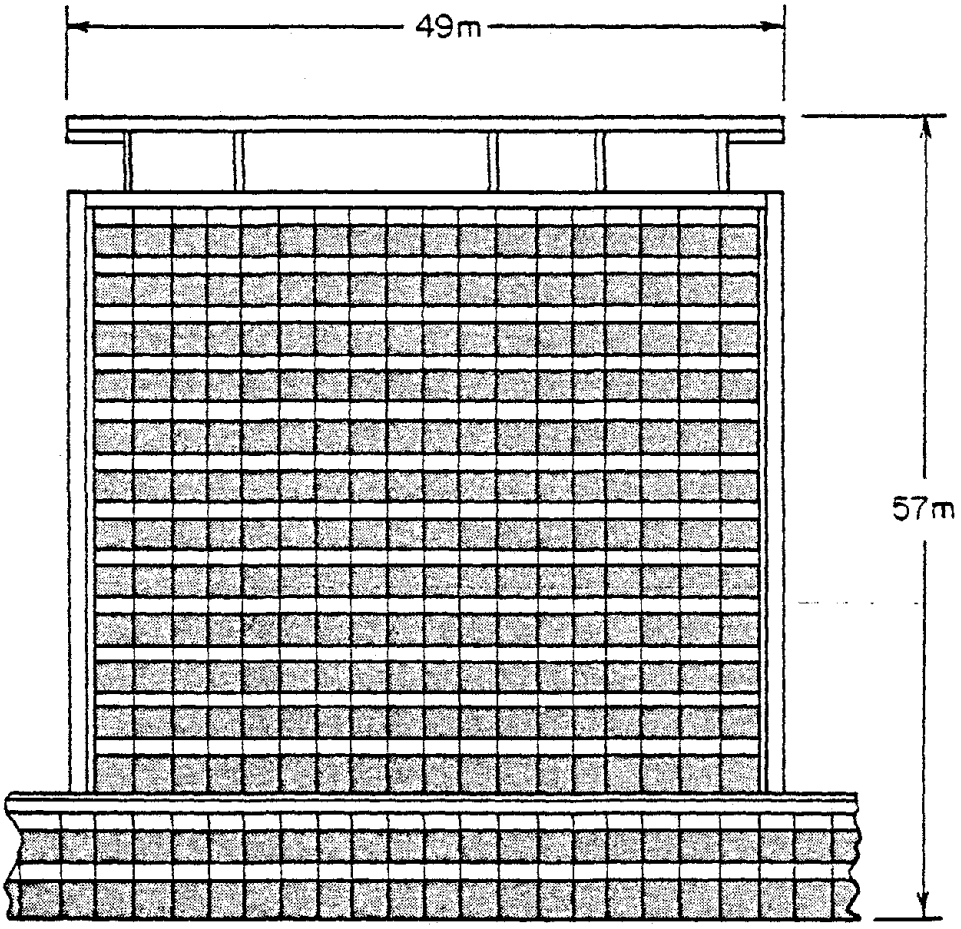

Figure 5.2. Elevation View of the Civic Center in the Long Direction.

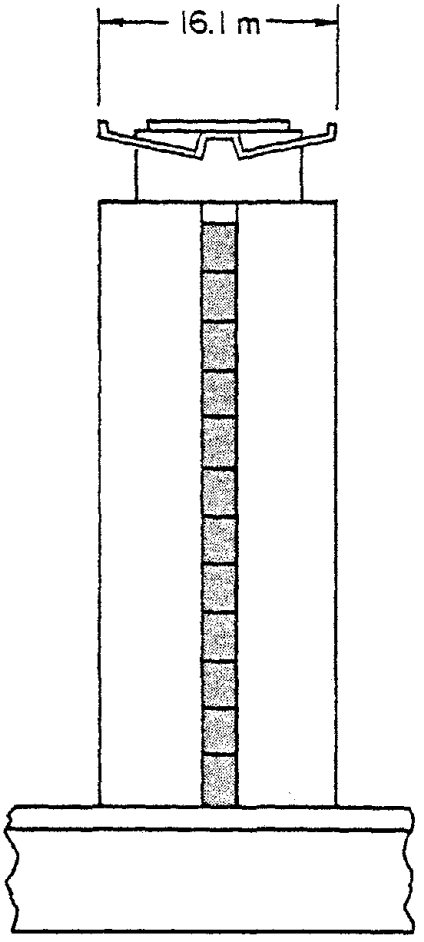

Figure 5.3. Elevation View of the Civic Center in the Short Direction.

As can be seen from the cross-section of Figure 5.1 the elevator cores are truly complex structural shapes.

No significant internal partitions are present in this building.

5.2 Experimental Procedure

The same type of vibrator was used to determine the dynamic characteristics of the Civic Center as was used for the two buildings reported in the previous two chapters. The vibrator was placed on the roof deck of the Civic Center in a positions near one end of the structure. Translational frequencies and mode shapes were determined along with both first and second torsional frequencies and mode shapes.

5.3 Structural Analysis of Civic Center Building

The experimental and analytical experience gained in the analysis of the buildings in the previous chapters pointed to using four distinct frame lines in the x direction, and these are shown in Figure 5.4. Column lines A and D contained the small outer columns and small portions of the end shear walls and cores. The lines B and C contained the interior columns and the majority of the shear walls and cores.

For the first analysis of the Civic Center building in the x direction the elevator cores were taken as fully effective sections with no reduction to account for shear lag effects in thin walled members. This idealization is referred to as type DX. The measured frequency for this building was given by Jeary and Sparks (16) as 1.13 Hz for the x direction. Model DX yielded 1.80 Hz. Thus the DX model produced a

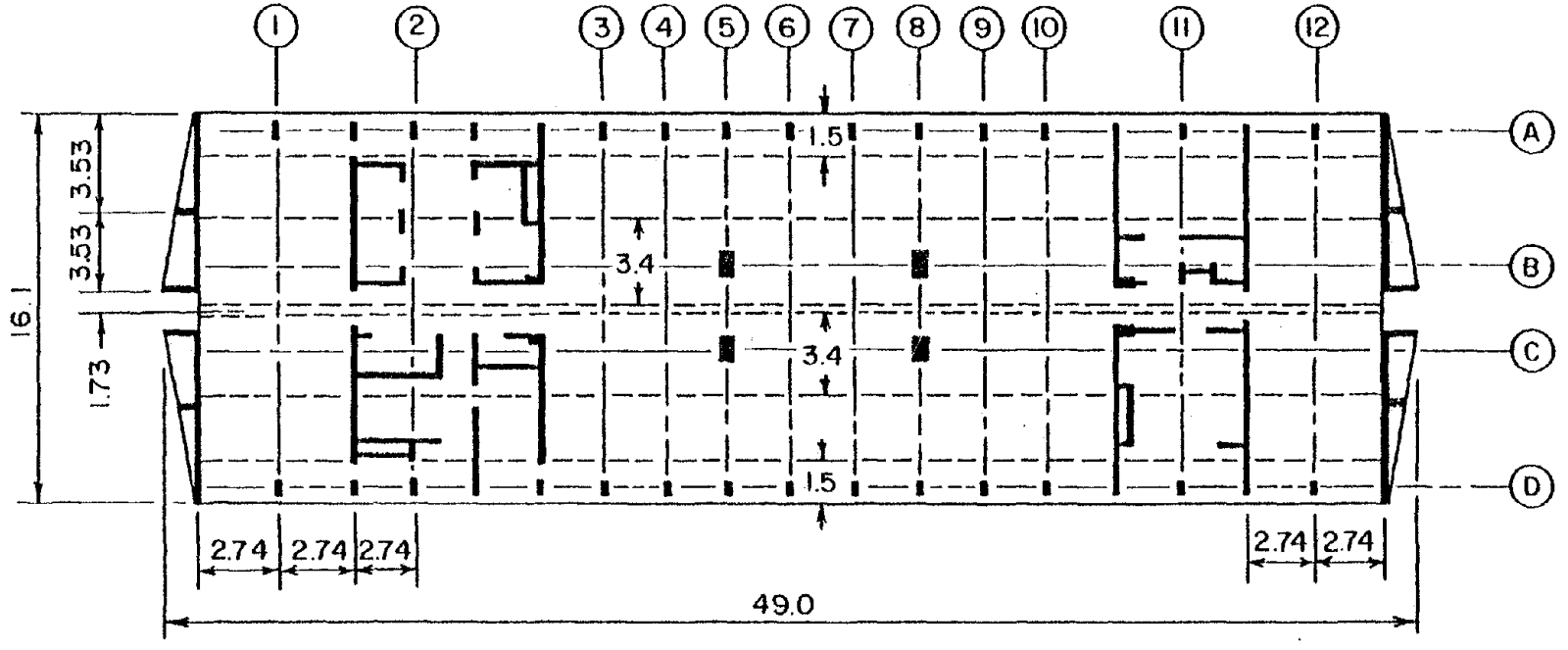

Figure 5.4. DX, DX1 Structural Idealization for the Civic Center.

natural frequency which was too high. Figure 5.5 presents a comparison between the measured mode shape and the one computed from the DX model, and the agreement is poor. This model does not appear to be adequate for predicting either the natural frequencies or the mode shape.

Apparently model DX should be modified to compensate for shear lag effects. Experience with the buildings previously analyzed showed that Timoshenko's modification of thin walled box members was likely to accomplish this, so the flanges were totally neglected as a practical application of his recommendation. This new configuration of cross-sections is referred to as model DX1. Model DX1 matched both natural frequency and mode shape. Figure 5.6 shows a comparison of the mode shapes in the x direction.

In the y direction a similar analysis yielded similar variations. The DY model, with full elevator core cross-sections, is shown in Figure 5.7. The DY model produced a natural frequency of 1.70 Hz while the measured frequency was 1.18 Hz, not a good match. However, there was a good match with the measured mode shape, and this is shown in Figure 5.8. When the DY1 model was formed by neglecting the flanges as was done for the DX1 model, both the natural frequency and the mode shape matched. The mode shape is so close to that shown for model DY in Figure 5.8 that it is not shown as a separate plot.

The TABS-77 program also computes torsional frequencies and mode shapes as well as those for translation in the x and y directions. Jeary and Sparks (16) reported measured torsional values for the Civic Center. The DX, DY model, without compensation for shear lag, computed

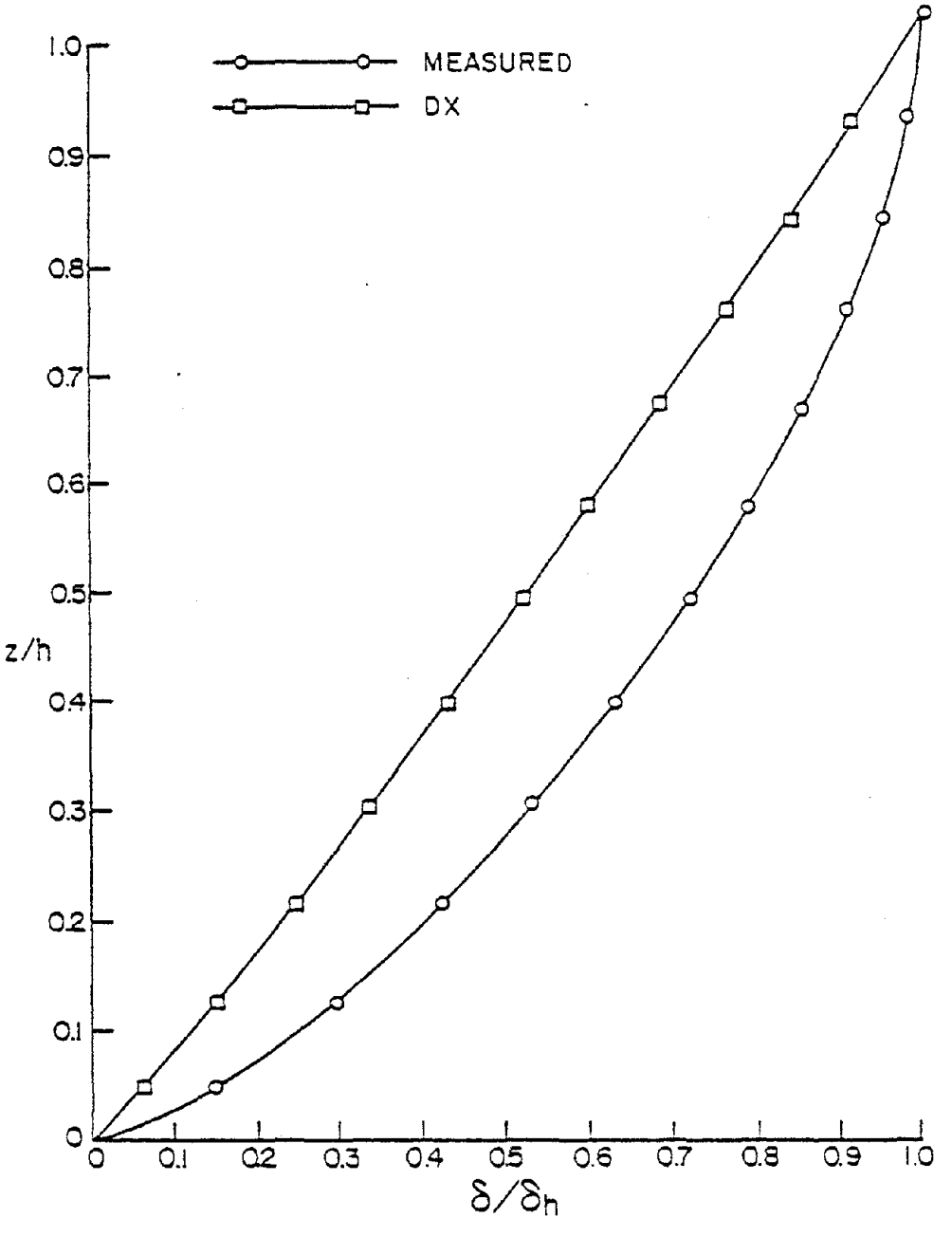

Figure 5.5. X Mode Shapes for the Civic Center.

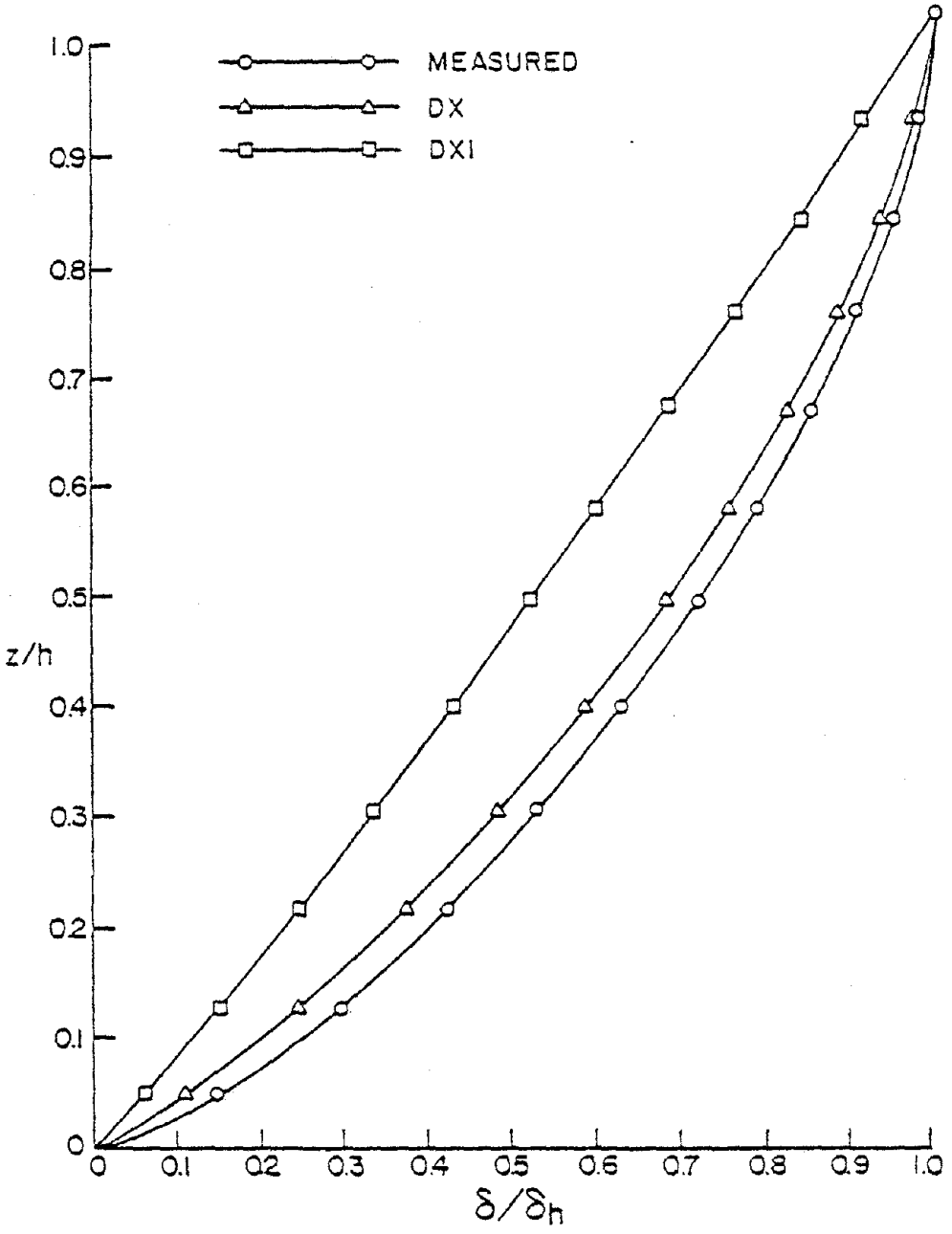

Figure 5.6. X Mode Shapes for the Civic Center.

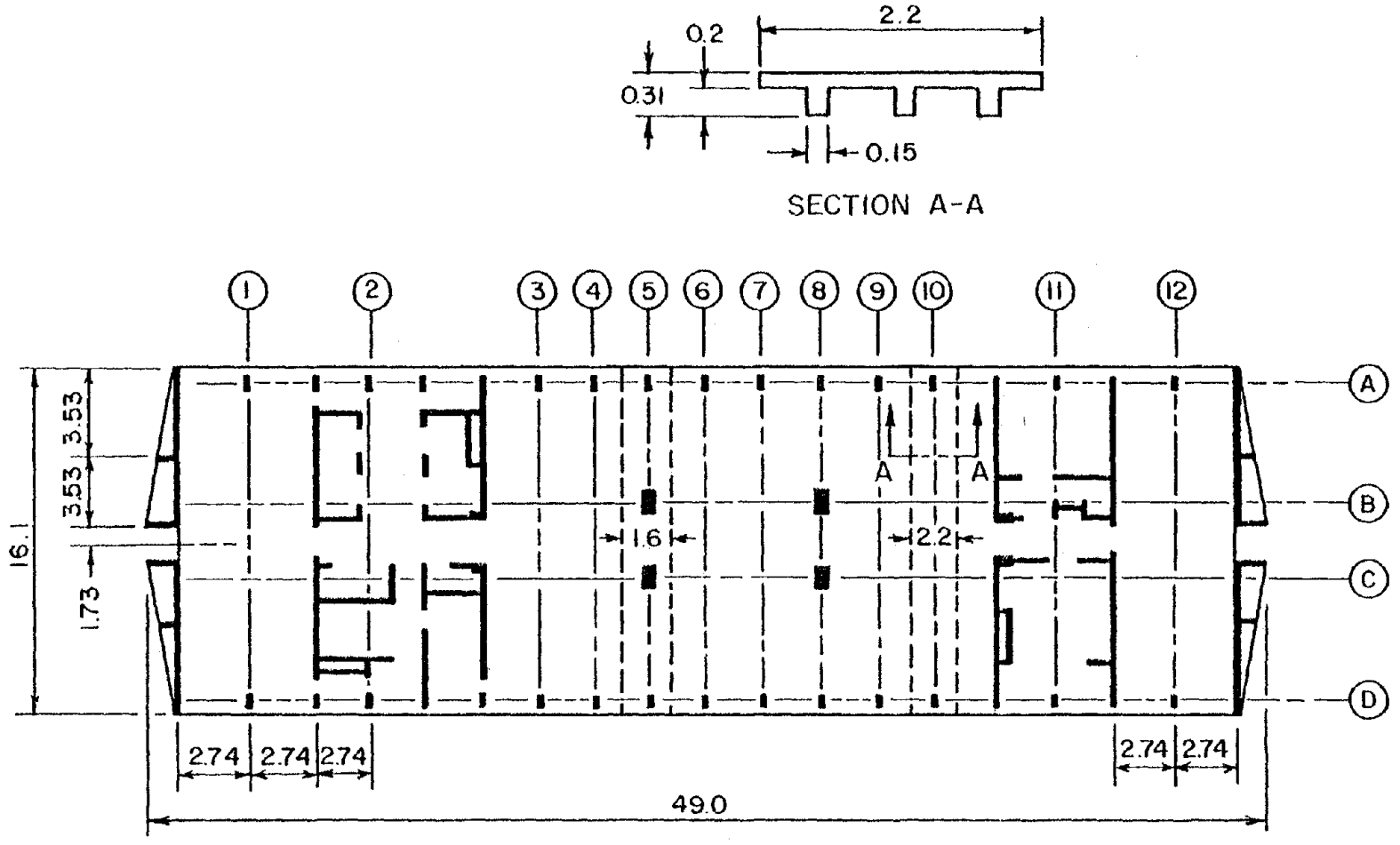

Figure 5.7. DY, DY1 Structural Idealization for the Civic Center.

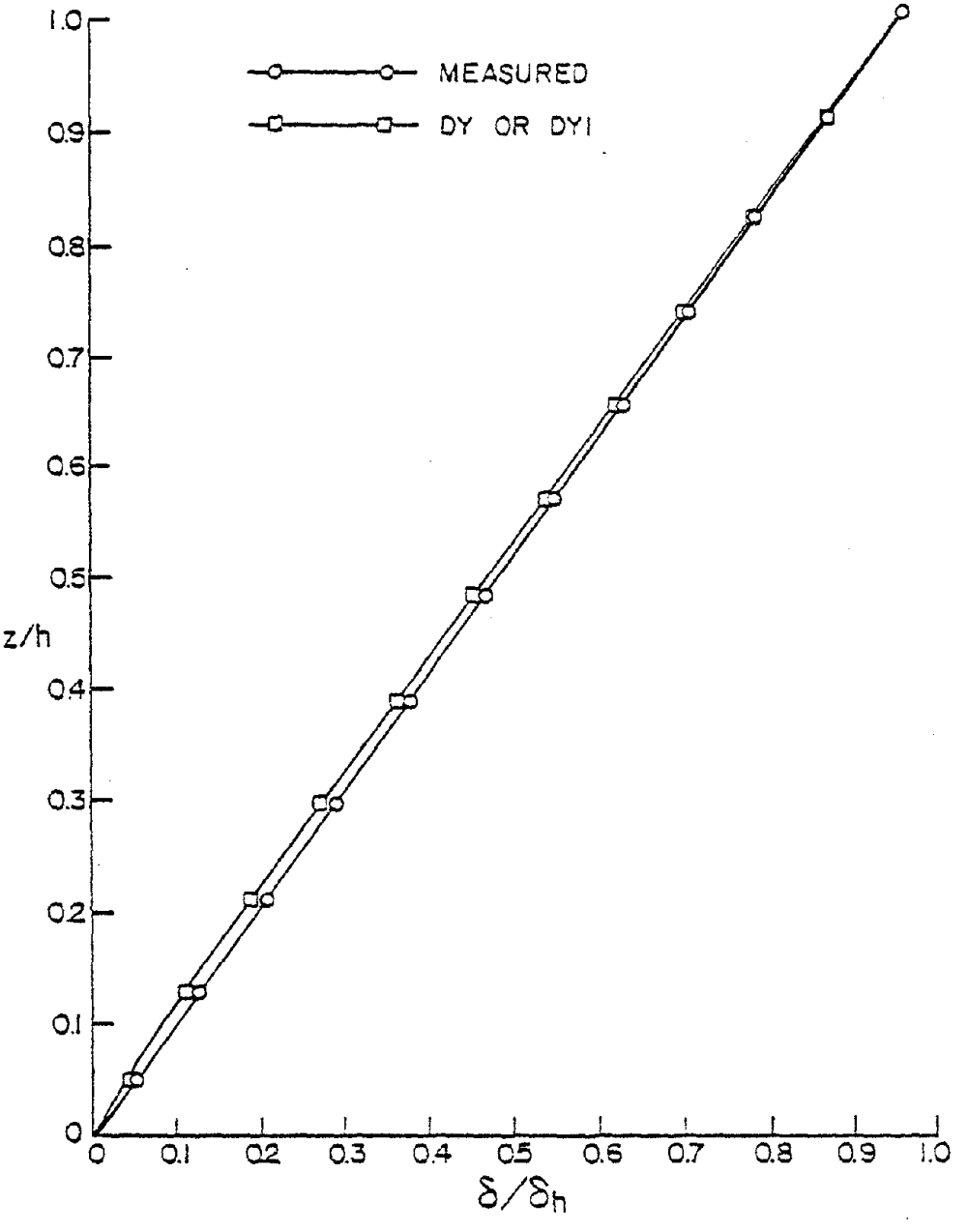

Figure 5.8. Y Mode Shapes for the Civic Center.

a natural frequency of 1.90 Hz as opposed to a measured torsional frequency of 1.47 Hz. However, the DX, DY model did produce a torsional mode shape that was in good agreement with the measured shape. When the DX1, DY1 model was used there was close agreement between not only the mode shape but also the measured natural frequency.

5.3.1 Parametric Studies

The first parametric study for this building addressed the effect of changing the stiffnesses of the elevator cores. They were changed, in steps, from an assumption of full effectiveness to fully neglecting the flanges. This is reported first for the x direction, and the results are shown in Table 5.1 and Figure 5.9. Both the table and the graph show that natural frequency values computed in this direction are only slightly affected by changes in stiffness of the cores. Changing the stiffness by a factor of 14 results in a change in the computed frequency by a factor of 2. Since the change in the computed natural frequency is indicative of the square of the change in the stiffness of the structure as a whole, then the total structure has been stiffened by only a factor of 4. This again confirms Clark's study (18).

Table 5.1 shows that modal mass is very sensitive to changes in stiffness in the elevator cores; proper choice of stiffness for these thin walled structural members is essential for adequate calculation of mode shape.

The second study investigated the effects of stiffness in the elevator cores on the dynamic characteristics of the structure in the y

Table 5.1. Parametric Study of Effectiveness of Flanges in Stiffening Cores in the Civic Center, X Direction

S/S_o	Frequency (Hz)	Modal Mass (Kg)
1.00	1.13	4216402
1.90	1.35	4000000
3.23	1.58	3859796
7.67	1.95	3628117
10	2.10	3480730
14	2.22	3280730

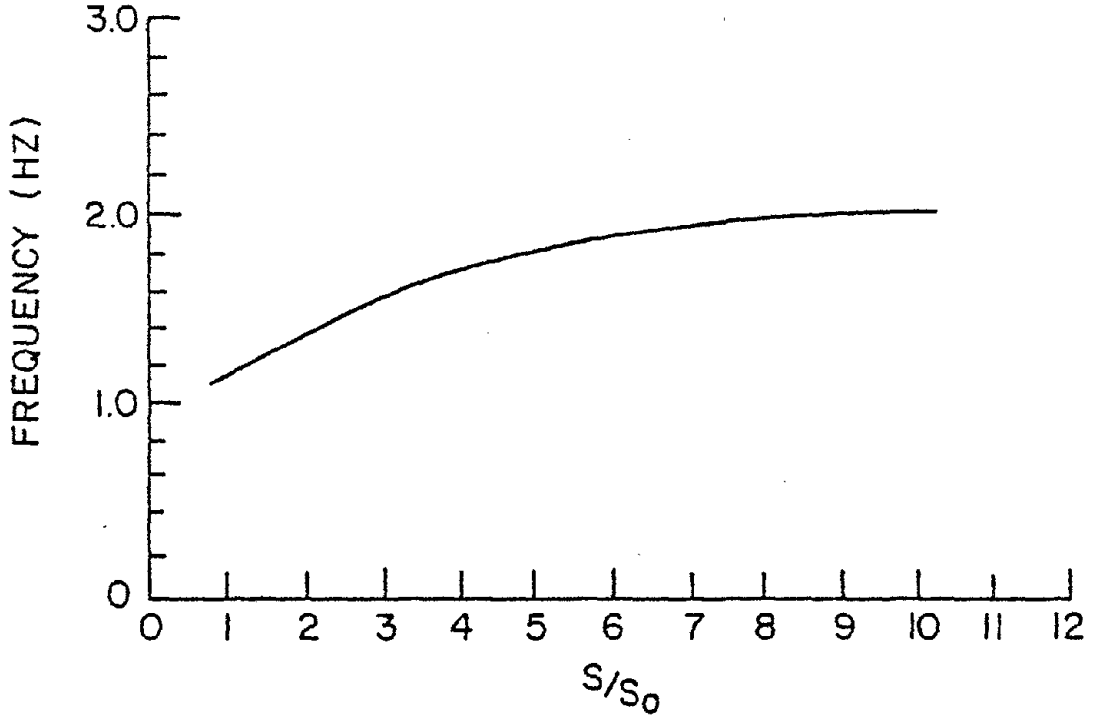

Figure 5.9. Frequency vs. Normalized Stiffness for Parametric Study of Effectiveness of Flanges in Stiffening Cores in the Civic Center, X Direction.

direction. The results are shown in Table 5.2 and Figure 5.10. Both the table and the graph show that the rate of change of the frequency for this direction is close to that obtained for the x direction. But it is important to note that in this direction the modal mass is virtually unchanged throughout the range of variation of the elevator core stiffnesses. The existence of two massive end shear walls at each end of the Civic Center probably accounts for this effect. These walls contribute greatly to the stiffness of the structure in the y direction, but their contribution in the x direction is much diminished.

5.3.2 Significance of Models

Models which take shear lag effects into account adequately predict the behavior of the Civic Center. These models are DX1 and DY1. In order to see if these models significantly affect the loadings of structural elements in this building both wind and earthquake loads were applied to this set of models as well as the DX and DY models which do not take shear lag into account.

Again, using the same procedure as was used for the R. N. C. building, the wind loads were computed. Since in this case the structure considered did not start at ground level a somewhat different distribution than for the other building was obtained. The normalized wind loading for this building is shown in Table 5.3.

The earthquake loading used is the same as was used for the previous reported buildings, and, as as done in every case, the measured value of damping for each mode was used.

Table 5.2. Parametric Study of Effectiveness of Flanges in Stiffening Cores in the Civic Center, Y Direction

S/S_o	Frequency (Hz)	Modal Mass (Kg)
1.00	1.18	3045725
1.31	1.26	3035122
1.62	1.33	3014081
2.65	1.51	3000000
4.46	1.75	2932069
6.25	1.88	3045725

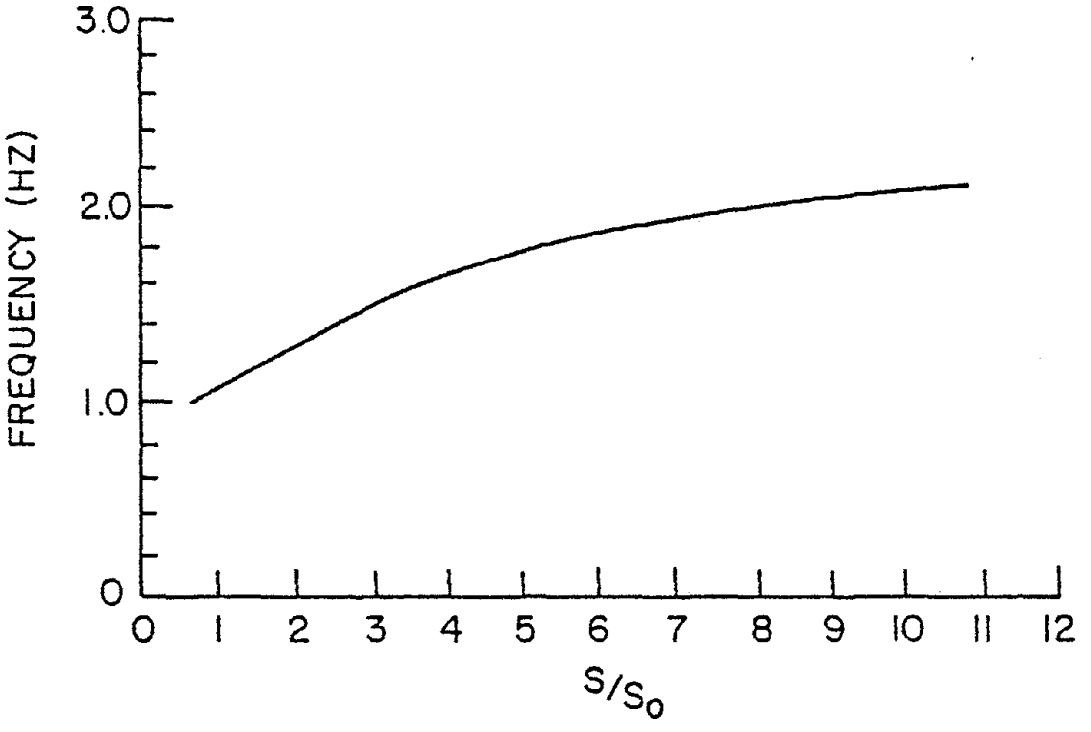

Figure 5.10. Frequency vs. Normalized Stiffness for the Parametric Study of Effectiveness of Flanges in Stiffening Cores in the Civic Center, Y Direction.

TABLE 5.3 NORMALIZED WIND LOAD FOR THE CIVIC CENTER

Level	Load Ratio
12	0.85
11	1.00
10	0.95
9	0.95
8	0.90
7	0.86
6	0.81
5	0.80
4	0.73
3	0.68
2	0.64
1	0.63

The elements chosen for analysis are encircled in Figure 5.11.

The results for static loading in both the x and y directions are shown in Tables 5.4 through 5.9. Considering all of these tables, it may be stated that neglecting shear lag effects overestimates the loading in the elevator cores and underestimates the loading in the adjacent columns. The underestimates are usually by a factor of about 2 but may be as high as 10.

Tables 5.10 through 5.12 present the results of earthquake loading in the x direction. The trend shown by these results is the same as that shown for wind loading on the Civic Center but the ratios are different. The difference in ratios are more pronounced in the lower stories since there is a greater discrepancy between the DX1 and DX mode shape predictions in the lower levels.

The results for the y direction are shown in Tables 5.13 through 5.15. For this direction not only is the trend similar for both static and earthquake loadings but also the ratios are close in value. This is because the mode shapes for the model are practically identical.

5.4 Concluding Comment

The Civic Center building analysis once again demonstrates that shear lag does indeed exist in structural shapes which are in fact thin walled sections, and shear lag effects should be accounted for in analysis and consequently in design.

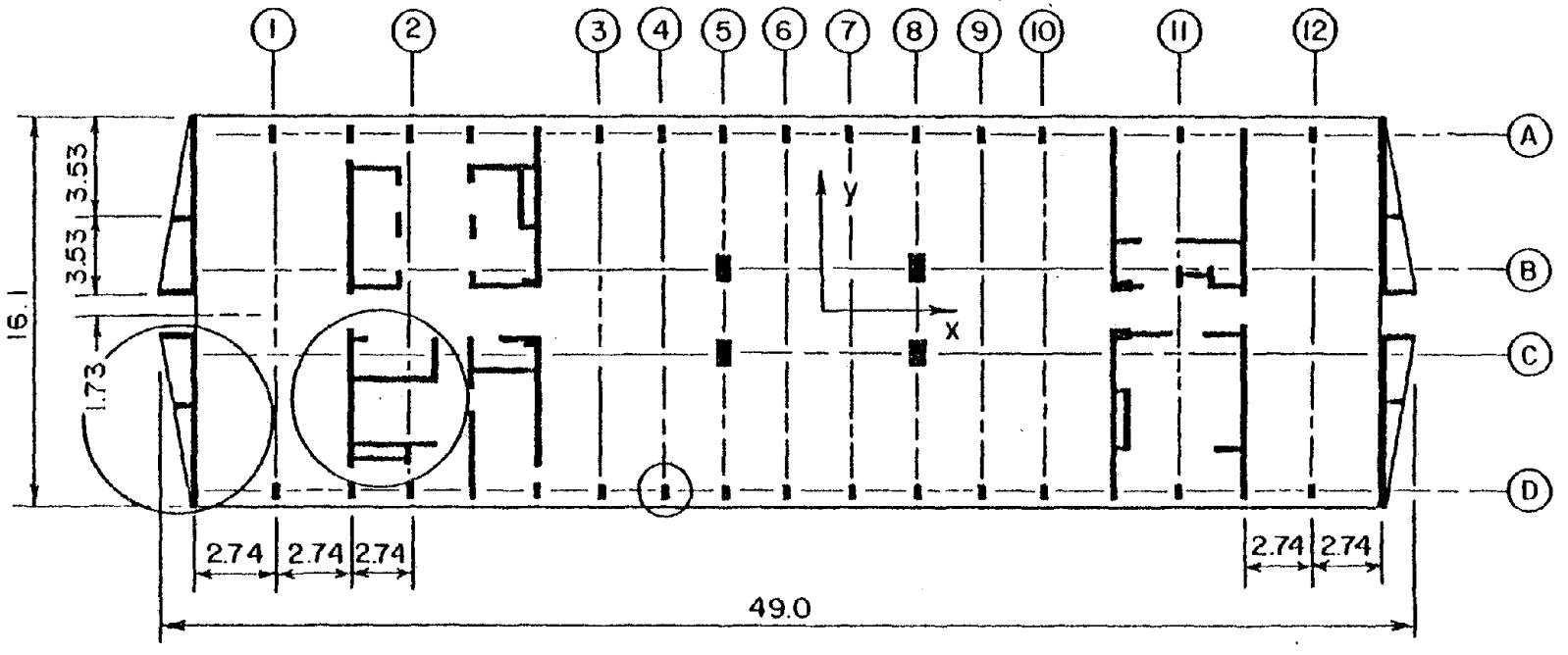

Figure 5.11. Elements Chosen for the Analysis of the Civic Center.

TABLE 5.4 RESULTS OF ANALYSES IN DIMENSIONLESS FORM FOR

BUILDING: CIVIC CENTER
ELEMENT: EXTERNAL SHEAR WALL
LOADING: WIND
DIRECTION: X

LEVEL	BOTTOM MOMENT $\frac{DX1}{DX}$	TOP MOMENT $\frac{DX1}{DX}$	AXIAL FORCE $\frac{DX1}{DX}$	SHEAR FORCE $\frac{DX1}{DX}$
12	1.20	1.25	0.80	1.20
11	1.70	1.66	0.88	1.52
10	1.70	1.73	0.95	1.75
9	1.80	1.82	1.01	1.94
8	2.10	2.18	1.08	2.09
7	2.23	2.27	1.13	2.23
6	2.35	2.42	1.18	2.35
5	2.50	2.57	1.23	2.49
4	2.65	2.73	1.27	2.65
3	2.90	2.96	1.32	2.85
2	3.11	3.17	1.37	3.05
1	4.42	4.6	1.42	4.30

TABLE 5.5 RESULTS OF ANALYSES IN DIMENSIONLESS FORM FOR

BUILDING: CIVIC CENTER
ELEMENT: ELEVATOR CORE
LOADING: WIND
DIRECTION: X

LEVEL	BOTTOM MOMENT $\frac{DX1}{DX}$	TOP MOMENT $\frac{DX1}{DX}$	AXIAL FORCE $\frac{DX1}{DX}$	SHEAR FORCE $\frac{DX1}{DX}$
12	0.67	0.61	1.32	0.64
11	0.73	0.74	25.32	0.74
10	0.75	0.74	-0.25	0.74
9	0.76	0.76	0.18	0.75
8	0.76	0.76	0.32	0.76
7	0.76	0.77	0.38	0.76
6	0.76	0.76	0.42	0.76
5	0.76	0.77	0.45	0.77
4	0.83	0.79	0.47	0.77
3	0.77	0.79	0.59	0.78
2	0.77	0.80	0.51	0.79
1	0.75	0.90	0.53	0.82

TABLE 5.6 RESULTS OF ANALYSES IN DIMENSIONLESS FORM FOR

BUILDING: CIVIC CENTER
ELEMENT: COLUMN D4
LOADING: WIND
DIRECTION: X

LEVEL	BOTTOM MOMENT $\frac{DX1}{DX}$	TOP MOMENT $\frac{DX1}{DX}$	AXIAL FORCE $\frac{DX1}{DX}$	SHEAR FORCE $\frac{DX1}{DX}$
12	1.57	1.56	2.62	1.56
11	1.90	1.89	2.71	1.92
10	2.17	2.16	2.80	2.17
9	2.36	2.35	2.64	2.37
8	2.54	2.54	2.58	2.54
7	2.70	2.70	2.55	2.70
6	2.85	2.84	2.54	2.85
5	3.01	3.00	2.60	3.00
4	3.20	3.21	2.46	3.20
3	3.39	3.40	2.53	3.39
2	3.74	3.74	2.51	3.65
1	4.67	4.65	2.55	4.67

TABLE 5.7 RESULTS OF ANALYSES IN DIMENSIONLESS FORM FOR

BUILDING: CIVIC CENTER
ELEMENT: END SHEAR WALL
LOADING: WIND
DIRECTION: Y

LEVEL	BOTTOM MOMENT $\frac{DY1}{DY}$	TOP MOMENT $\frac{DY1}{DY}$	AXIAL FORCE $\frac{DY1}{DY}$	SHEAR FORCE $\frac{DY1}{DY}$
12	3.40	1.57	1.51	1.15
11	4.18	2.18	1.52	1.19
10	9.92	2.50	1.53	1.38
9	-1.73	2.99	1.54	1.53
8	0.53	0.58	1.55	1.61
7	1.09	1.00	1.57	1.67
6	1.34	1.29	1.58	1.72
5	1.50	1.43	1.60	1.78
4	1.59	1.48	1.61	1.85
3	1.69	1.60	1.62	1.91
2	1.77	1.75	1.63	1.97
1	1.90	1.77	1.64	2.02

TABLE 5.8 RESULTS OF ANALYSES IN DIMENSIONLESS FORM FOR

BUILDING: CIVIC CENTER
ELEMENT: ELEVATOR CORE
LOADING: WIND
DIRECTION: Y

LEVEL	BOTTOM MOMENT	TOP MOMENT	AXIAL FORCE	SHEAR FORCE
	$\frac{DY1}{DY}$	$\frac{DY1}{DY}$	$\frac{DY1}{DY}$	$\frac{DY1}{DY}$
12	0.90	0.92	1.02	1.11
11	0.20	0.20	1.05	0.82
10	0.22	0.23	1.07	0.88
9	0.24	0.23	1.10	0.88
8	0.25	0.26	1.12	0.89
7	0.45	0.44	1.14	0.88
6	0.53	0.54	1.16	0.86
5	0.57	0.56	1.18	0.85
4	0.80	0.60	1.20	0.85
3	0.62	0.60	1.23	0.84
2	0.65	0.61	1.24	0.83
1	0.66	0.65	1.25	0.79

TABLE 5.9 RESULTS OF ANALYSES IN DIMENSIONLESS FORM FOR

BUILDING: CIVIC CENTER
ELEMENT: COLUMN D4
LOADING: WIND
DIRECTION: Y

LEVEL	BOTTOM MOMENT $\frac{DY1}{DY}$	TOP MOMENT $\frac{DY1}{DY}$	AXIAL FORCE $\frac{DY1}{DY}$	SHEAR FORCE $\frac{DY1}{DY}$
12	1.49	1.52	1.51	1.50
11	1.51	1.57	1.52	1.52
10	1.54	1.62	1.44	1.53
9	1.56	1.64	1.47	1.57
8	1.57	1.66	1.50	1.60
7	1.61	1.68	1.53	1.63
6	1.64	1.70	1.57	1.66
5	1.67	1.72	1.54	1.69
4	1.70	1.76	1.60	1.72
3	1.74	1.81	1.61	1.77
2	1.74	1.88	1.62	1.78
1	1.34	2.26	1.56	1.80

TABLE 5.10 RESULTS OF ANALYSES IN DIMENSIONLESS FORM FOR

BUILDING: CIVIC CENTER
ELEMENT: END SHEAR WALL
LOADING: EARTHQUAKE
DIRECTION: X

LEVEL	BOTTOM MOMENT $\frac{DX1}{DX}$	TOP MOMENT $\frac{DX1}{DX}$	AXIAL FORCE $\frac{DX1}{DX}$	SHEAR FORCE $\frac{DX1}{DX}$
12	1.32	1.33	0.87	1.35
11	1.71	1.72	0.93	1.66
10	1.80	1.83	0.99	1.87
9	1.90	1.92	1.09	2.09
8	2.14	2.19	1.16	2.22
7	2.31	2.37	1.20	2.36
6	2.42	2.49	1.29	2.46
5	2.65	2.58	1.33	2.63
4	2.75	2.78	1.40	2.83
3	3.12	3.15	1.57	2.97
2	4.62	4.63	1.72	3.29
1	5.12	5.27	1.83	4.50

TABLE 5.11 RESULTS OF ANALYSES IN DIMENSIONLESS FORM FOR

BUILDING: CIVIC CENTER
ELEMENT: ELEVATOR CORE
LOADING: EARTHQUAKE
DIRECTION: X

LEVEL	BOTTOM MOMENT $\frac{DX1}{DX}$	TOP MOMENT $\frac{DX1}{DX}$	AXIAL FORCE $\frac{DX1}{DX}$	SHEAR FORCE $\frac{DX1}{DX}$
12	0.69	0.72	1.57	0.73
11	0.78	0.80	28.23	0.79
10	0.79	0.81	-0.93	0.81
9	0.80	0.80	0.19	0.84
8	0.81	0.80	0.38	0.88
7	0.80	0.80	0.44	0.89
6	0.80	0.83	0.52	0.91
5	0.81	0.85	0.57	0.94
4	0.89	0.89	0.61	0.97
3	0.85	0.90	0.73	1.03
2	0.87	0.94	0.71	1.04
1	0.84	0.97	0.74	1.09

TABLE 5.12 RESULTS OF ANALYSES IN DIMENSIONLESS FORM FOR

BUILDING: CIVIC CENTER
ELEMENT: COLUMN D4
LOADING: EARTHQUAKE
DIRECTION: X

LEVEL	BOTTOM MOMENT $\frac{DX1}{DX}$	TOP MOMENT $\frac{DX1}{DX}$	AXIAL FORCE $\frac{DX1}{DX}$	SHEAR FORCE $\frac{DX1}{DX}$
12	1.61	1.60	2.73	1.61
11	1.96	1.96	2.80	1.98
10	2.23	2.23	2.91	2.24
9	2.41	2.42	2.73	2.41
8	2.60	3.61	2.70	2.61
7	2.77	3.78	2.66	2.79
6	2.92	3.92	2.65	2.93
5	3.17	3.17	2.67	3.18
4	3.29	3.30	2.59	3.29
3	3.51	3.52	2.69	3.51
2	3.93	3.93	2.74	3.83
1	4.96	4.98	2.89	4.94

TABLE 5.13 RESULTS OF ANALYSES IN DIMENSIONLESS FORM FOR

BUILDING: CIVIC CENTER
ELEMENT: END SHEAR WALL
LOADING: EARTHQUAKE
DIRECTION: Y

LEVEL	BOTTOM MOMENT $\frac{DY1}{DY}$	TOP MOMENT $\frac{DY1}{DY}$	AXIAL FORCE $\frac{DY1}{DY}$	SHEAR FORCE $\frac{DY1}{DY}$
12	3.42	1.59	1.53	1.20
11	4.20	2.24	1.56	1.27
10	9.93	2.56	1.56	1.32
9	-1.79	2.96	1.61	1.41
8	0.55	0.64	1.62	1.56
7	1.12	1.07	1.66	1.71
6	1.37	1.31	1.65	1.80
5	1.53	1.47	1.61	1.89
4	1.61	1.49	1.67	1.95
3	1.73	1.67	1.68	2.01
2	1.79	1.79	1.69	2.10
1	1.93	1.83	1.70	2.19

TABLE 5.14 RESULTS OF ANALYSES IN DIMENSIONLESS FORM FOR

BUILDING: CIVIC CENTER
ELEMENT: ELEVATOR CORE
LOADING: EARTHQUAKE
DIRECTION: Y

LEVEL	BOTTOM MOMENT $\frac{DY1}{DY}$	TOP MOMENT $\frac{DY1}{DY}$	AXIAL FORCE $\frac{DY1}{DY}$	SHEAR FORCE $\frac{DY1}{DY}$
12	0.92	0.93	1.04	1.17
11	0.23	0.23	1.08	0.84
10	0.25	0.26	1.10	0.92
9	0.25	0.26	1.13	0.91
8	0.26	0.27	1.15	0.90
7	0.46	0.47	1.18	0.91
6	0.57	0.58	1.20	0.91
5	0.58	0.59	1.22	0.89
4	0.63	0.63	1.24	0.88
3	0.66	0.66	1.27	0.87
2	0.68	0.68	1.30	0.87
1	0.69	0.69	1.31	0.84

TABLE 5.15 RESULTS OF ANALYSES IN DIMENSIONLESS FORM FOR

BUILDING: CIVIC CENTER
ELEMENT: COLUMN D4
LOADING: EARTHQUAKE
DIRECTION: Y

LEVEL	BOTTOM MOMENT $\frac{DY1}{DY}$	TOP MOMENT $\frac{DY1}{DY}$	AXIAL FORCE $\frac{DY1}{DY}$	SHEAR FORCE $\frac{DY1}{DY}$
12	1.53	1.59	1.57	1.53
11	1.50	1.63	1.58	1.51
10	1.57	1.60	1.50	1.57
9	1.57	1.63	1.51	1.57
8	1.59	1.65	1.53	1.61
7	1.62	1.69	1.56	1.61
6	1.63	1.69	1.60	1.63
5	1.65	1.71	1.61	1.66
4	1.71	1.74	1.63	1.73
3	1.73	1.83	1.67	1.74
2	1.77	1.85	1.66	1.79
1	1.42	2.33	1.60	1.83

CHAPTER VI. THE ARTS TOWER

6.1 Building Geometry and Location

The Arts Tower of the University of Sheffield is situated within the University site near the center of Sheffield, England. The Tower is exposed on the north and east sides but partially sheltered on the south and west by other low-rise University buildings. The building is a tube-in-tube structural design which is quite different from the structural arrangements of the buildings considered in the previous chapters. The Arts Tower is 20 stories or 80 m high, 36 m wide, and 20 m deep.

The structural elements of the Arts Tower consist of cast **in situ** reinforced concrete cores which are placed essentially symmetrically in the y direction as shown in Figure 6.1 but are somewhat asymmetrically located in the x direction. The floor slabs are 0.3 m thick and span from the cores to the external reinforced concrete columns. The external columns are connected with reinforced concrete spandrel beams which encircle the Tower at each floor level. Above the ground floor there are a total of 88 external columns evenly spaced around the perimeter, and each column is 0.2 m by 0.4 m. Between the ground floor level and the next level above the number of columns is reduced to 16 larger columns but these are considered to be the equivalent, for analysis, of the 88 used at higher levels.

The Arts Tower has a deep basement. It is founded on piles driven into shale.

Figures 6.1, 6.2, an 6.3 show a typical floor plan and two elevations of the Tower.

6.2 Partitions and Cladding

The Arts Tower contains extensive blockwork partitions whose distributions vary from floor to floor. In general these partitions connect the outside columns to the internal cores but this is not invariably true for every floor. However, it is true for such a large majority of the floors that this arrangement is certainly an adequate generalized model.

6.3 Experimental Procedures

The vibrator used for the Arts Tower was not the same as the one used for the three buildings in Plymouth. For the Tower a vibrator furnished by the Centre Experimental de Récherches et d'Etudes du Bâtiment et des Travaux Publics of Paris was used. This vibrator which is described by Jeary (21) is based on eccentric mass rotation in a plane parallel to the floor slab on which it is placed. This vibrator was mounted on the 20th floor, off center and near one corner. All other aspects of the test were the same as for the buildings previously discussed. Both translational and torsional modes were identified.

The vibration test indicated a pure fundamental mode in the y direction but in the x direction the fundamental mode was not pure for some torsion was detected in this direction. Likewise the torsional fundamental mode showed some translation. This coupling indicates that

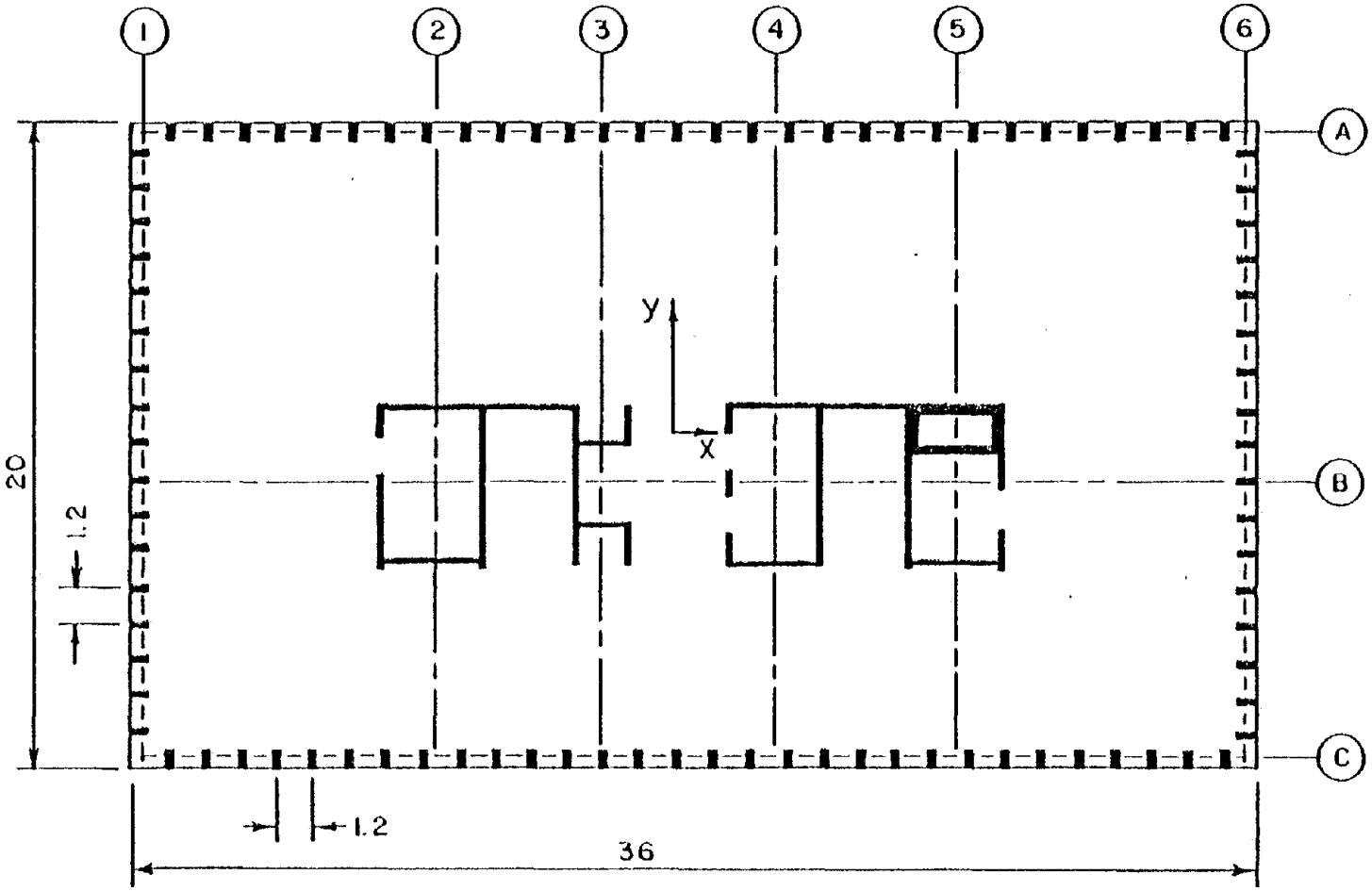

Figure 6.1. Typical Plan View of the Arts Tower (All Dimensions in Meters).

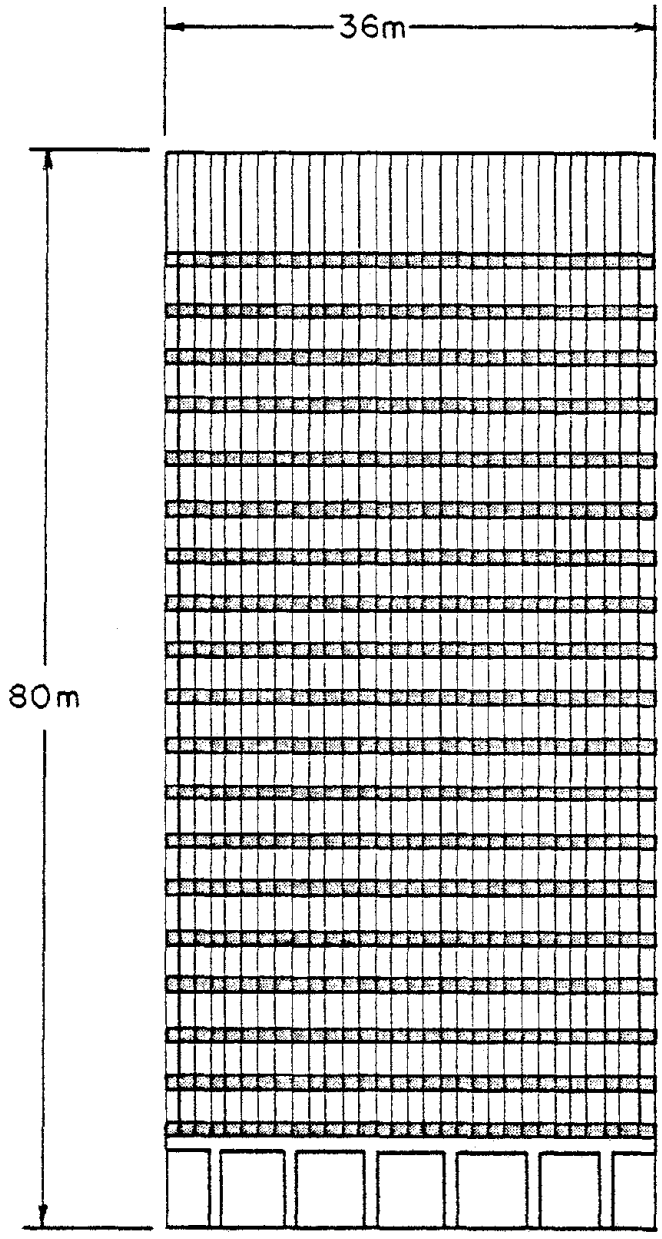

Figure 6.2. Elevation View of the Arts Tower in the Long Direction.

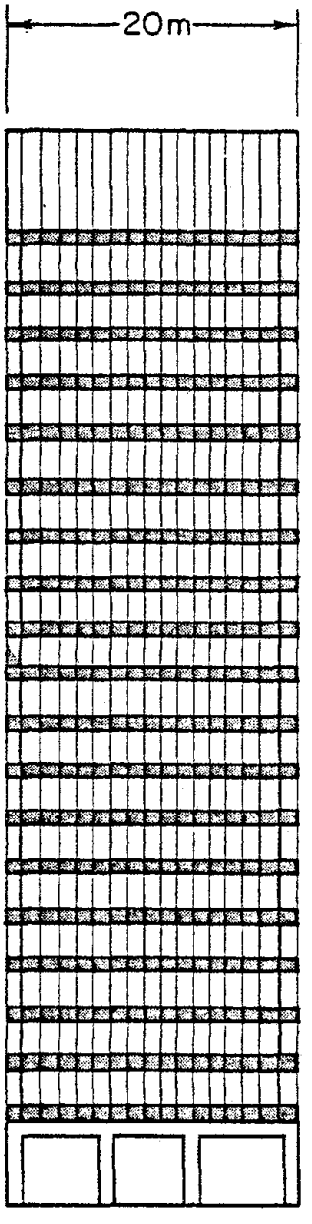

Figure 6.3. Elevation View of the Arts Tower in the Short Direction.

this building has a single eccentricity and the center of mass is displaced from the center of stiffness in the y direction.

6.4 Structural Analysis of the Arts Tower

A preliminary analysis of the Arts Tower was made to calculate the natural frequencies and the mode shapes. For this, three column lines were assumed in the x direction and six column lines in the y direction. The frame lines in the x direction were comprised of outside lines A and C as shown in Figure 6.1 and an internal frame line B which contained the elevator cores and two equivalent end columns, each of which comprised of the lumped value of all the 16 end exterior columns. The same simplification was used in the y direction with lumping of appropriate side exterior columns into the six frame lines. The two exterior frame lines 1 and 6 each contained the exterior columns at the ends of the building. Frame lines 2, 3, 4, and 5 each contained a core and one fourth of the external columns along each side at each end of each frame line. This idealization is called the bare frame idealization for this structure.

As this idealization was being formulated it was recognized as being rather contrived since Wilson, Dovey, and Habibullah (15) state that the TABS-77 program is "for buildings which can be approximated by independent frames and shear walls...," and the Arts Tower with its tube-in-tube design is far removed from the assumptions on which the TABS-77 program was based. Nevertheless, computations were made assuming TABS-77 was applicable. The results are shown in Table 6.1.

TABLE 6.1 Measured and Predicted Fundamental Frequencies

Direction	Frequency (Hz) Bare Frame	Frequency (Hz) Experimental
x	0.71	0.87
y	0.54	0.68
θ	0.47	0.79

The above table shows that the frequencies in all three directions were computed to be less than their experimental values. Note that no reduction in the effectiveness of the internal cores was assumed for the bare frame analysis.

Figures 6.4 and 6.5 show the measured mode shapes and the mode shapes computed using the bare frame models. For both directions the agreement between measured and computed shapes is good. It was noted above that some coupling exists between the x direction and the θ direction. Figure 6.6 shows both the measured and the computed plan mode shape for the x direction, and it can be seem that the measured mode shape indicates considerably more coupling for this direction than the computed plan mode shape.

Obviously a modification of the bare frame model should be made since an adequate model should not only match the observed frequencies and elevation mode shapes but also there must be a reasonable agreement between the measured and computed plan mode shape. Thus a modified model was attempted. Experience with the Plymouth buildings had indicated that partitions, cladding, and shear lag effects could each be

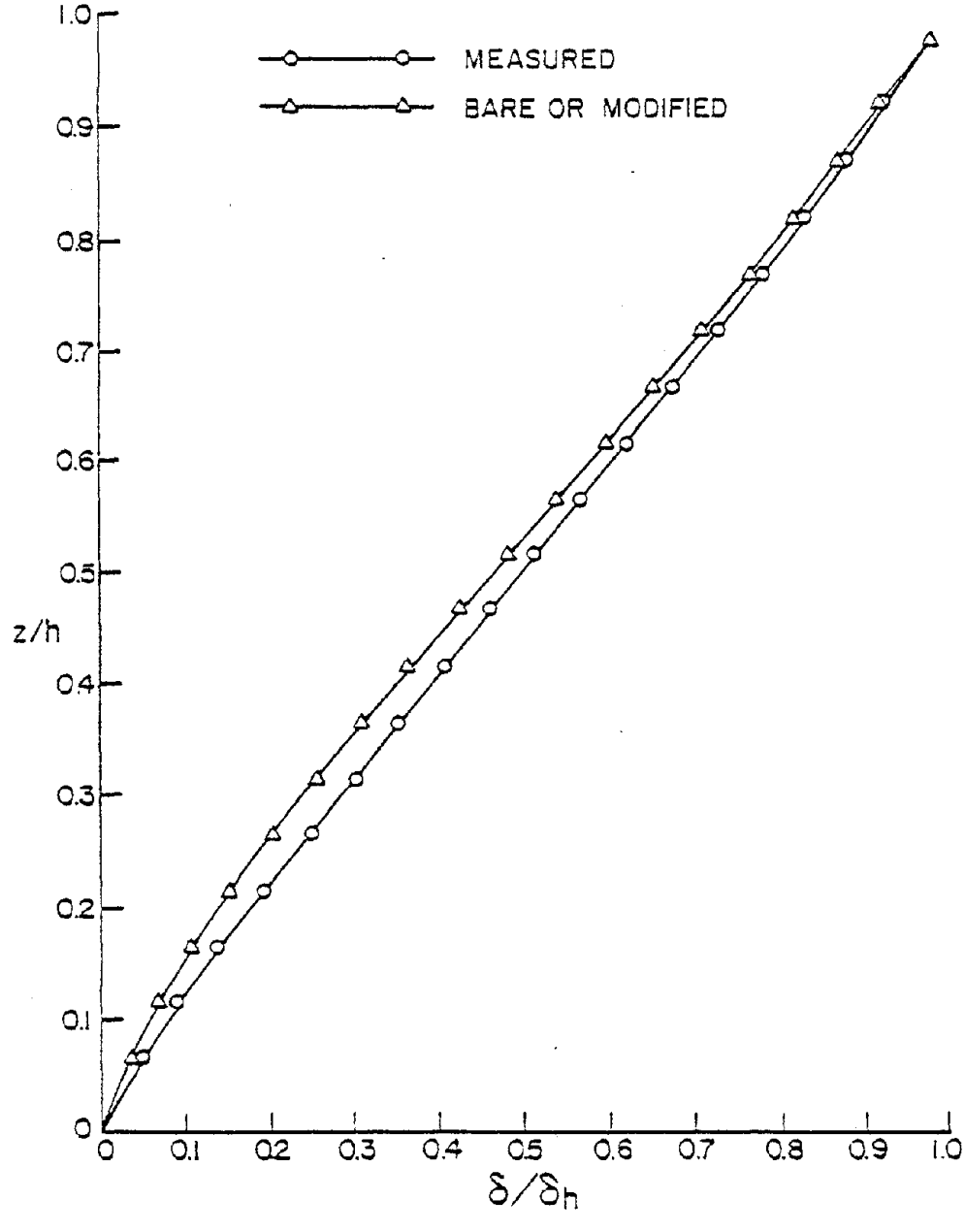

Figure 6.4. X Mode Shapes for the Arts Tower.

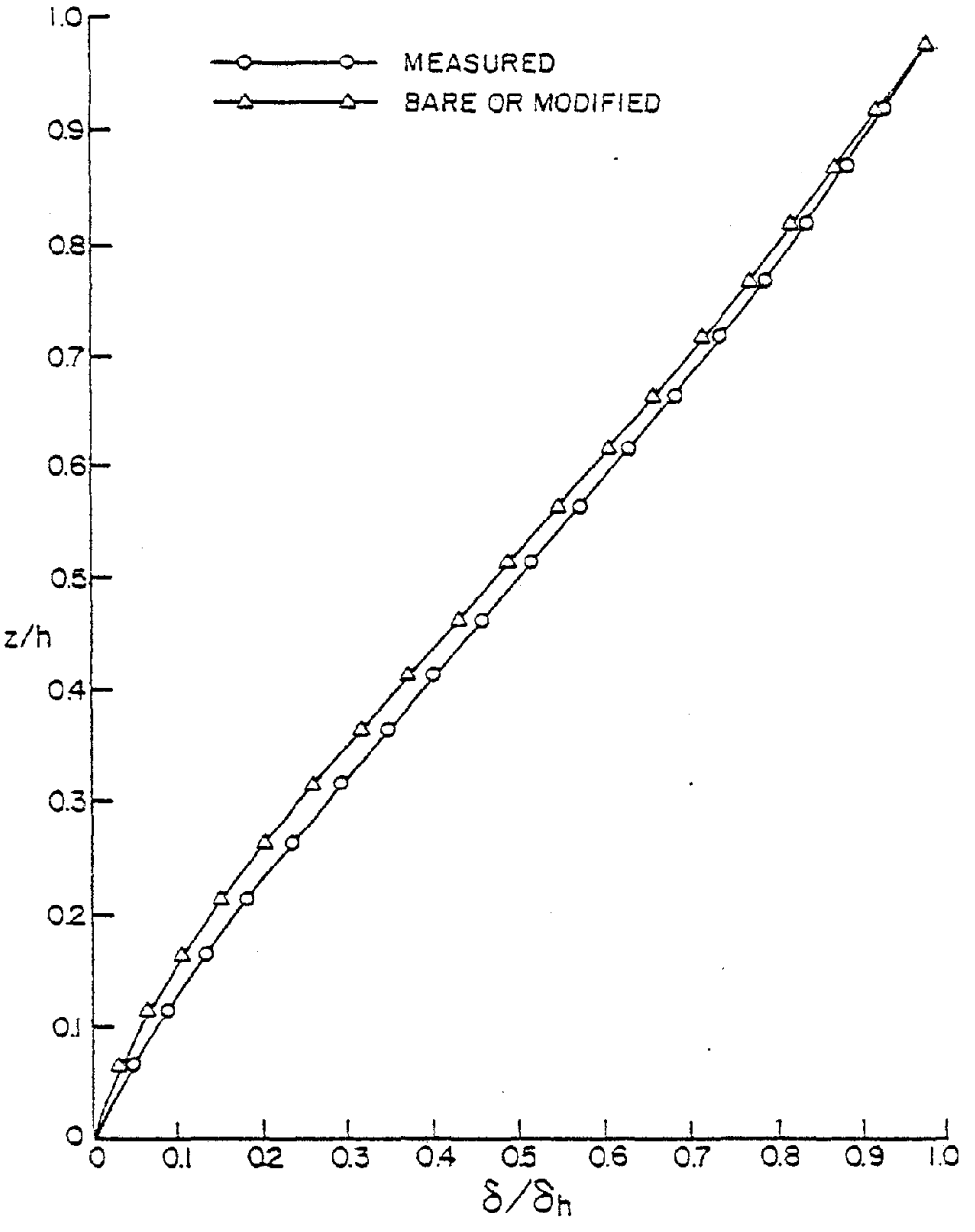

Figure 6.5. Y Mode Shape of the Arts Tower.

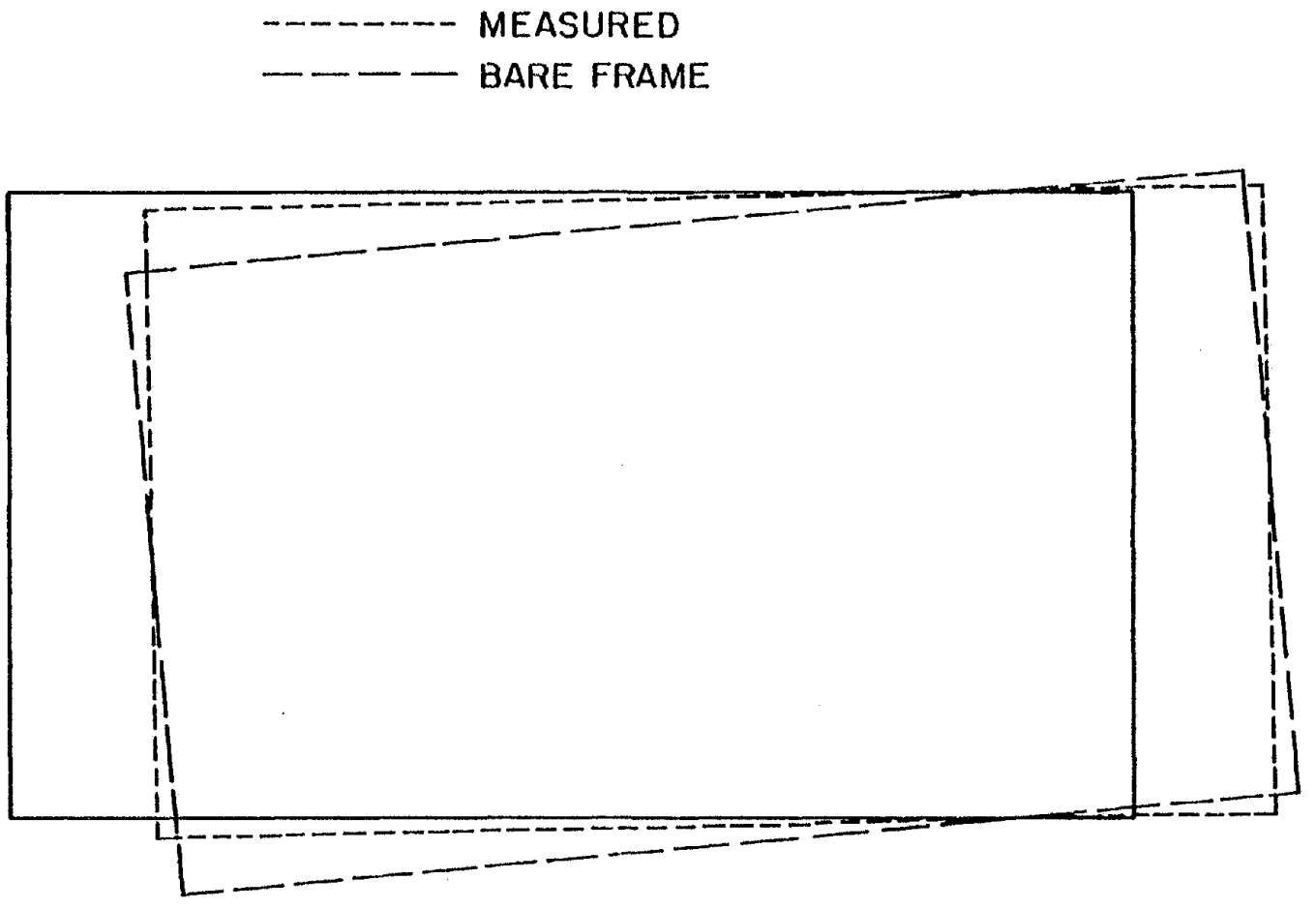

Figure 6.6. X Plan Mode Shapes for the Arts Tower.

important factors in proper modelling. There was no problem in logically accounting for the interior partitions nor was there any problem in adjusting for the effect of the glass in the exterior walls but there was a question of the proper treatment of the interior cores for shear lag effects. The Plymouth buildings each responded well to a reduction in stiffness to accomodate shear lag effects. But Derecho (22) has stated that in multiple cell tubes, connecting the internal cores to the exterior or perimeter grid lines, reduces the shear lag in the windward and leeward grids. Here it was assumed that the internal cores participated as central cells in a multiple cell tube being connected to the external columns through the action of the internal partitions. It is believed that Derecho's reasoning applies to the internal cores as well as to the exterior grid. Although Derecho was not dealing with a tube-in-tube system which best describes the Arts Tower with the interior partitions included as is shown in Figure 6.7, the Arts Tower strongly resembles the multiple cell tube. Therefore, for the modified frame no reduction for shear lag was permitted.

The modified frame thus consisted of two extra columns in column line B to accomodate the effects of the existing interior partitions in the x direction. In frame lines A and C the glass cladding was assumed to be structurally active since the windows use the exterior columns as mullions. The windows were therefore assumed to act as infill panels. According to Smith (2) these infill panels can be modelled as equivalent diagonal struts. The frames in the y direction were accorded a similar treatment, and this is indicated in Figure 6.7.

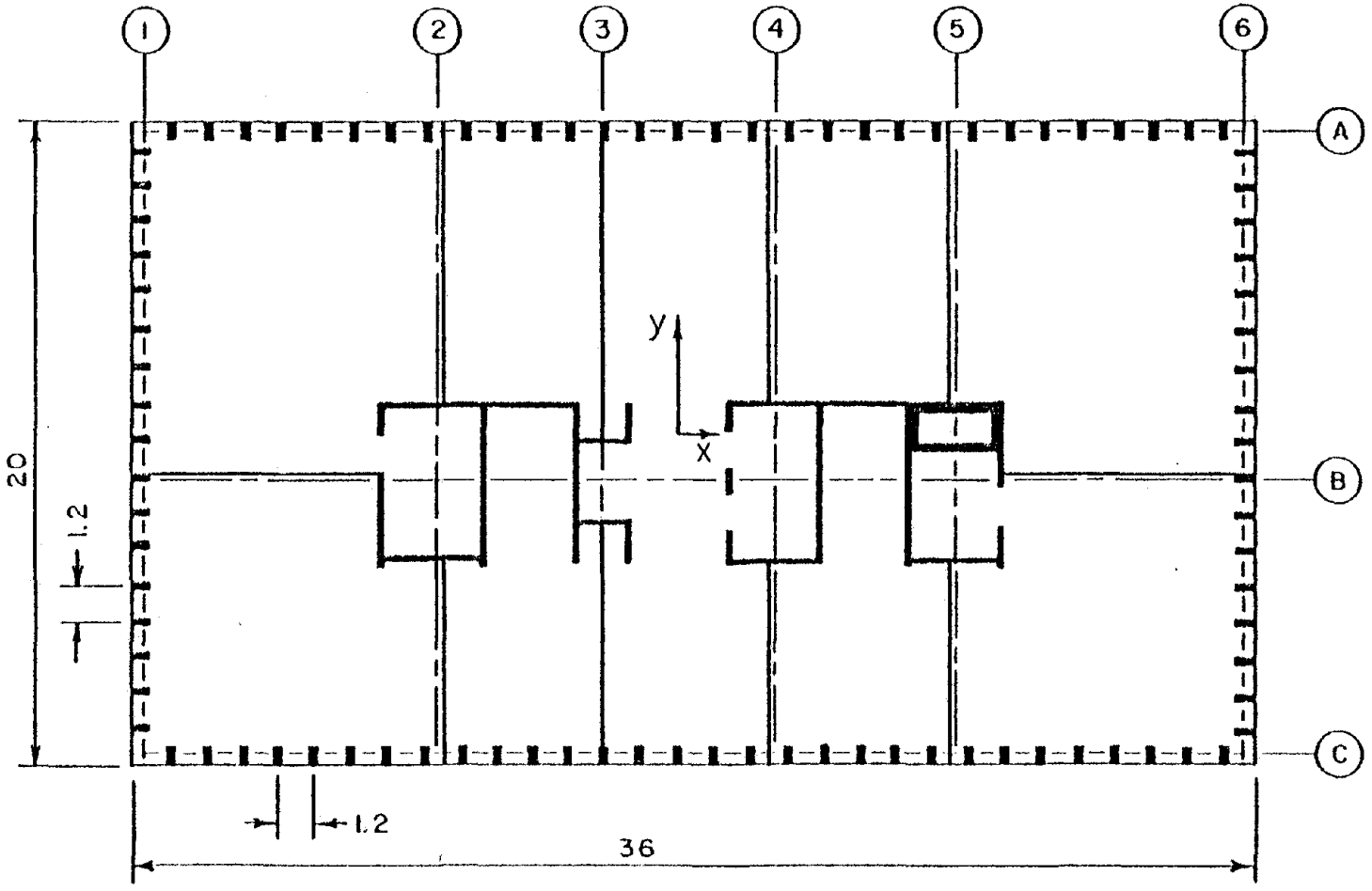

Figure 6.7. Location of the Internal Partitions for the Arts Tower.

The results of the analysis of the modified frames are shown in Table 6.2 below. As can be seen from this table, there is a reasonably good agreement between measured and computed translational frequencies but the computed torsional frequency diverges from the measured value by some 13 percent. Further, computations show that the elevation mode

TABLE 6.2 Measured and Predicted Fundamental Frequencies

Direction	Frequency (Hz) Bare Frame	Frequency (Hz) Experimental
x	0.84	0.87
y	0.64	0.68
θ	0.69	0.79

shapes remain unchanged from those developed for the bare frame model and they are thus adequate. However, the modified model produced a plan mode shape that was improved somewhat over the bare frame model but it is still considered to be an inadequate match with the measured plan mode shape. In other words, the measured amount of coupling is greater than that indicated by either the bare frame or the modified models. Figure 6.8 shows for comparison the plan mode shape for the x direction developed for each model and that which was measured experimentally.

No parametric study was made for the Arts Tower for it is believed that the TABS-77 program is not designed for a tube or a tube-in-tube structure and, further, since agreement between measured values and those produced by the TABS-77 program are questionable at best, then no meaningful parametric study can likely be done.

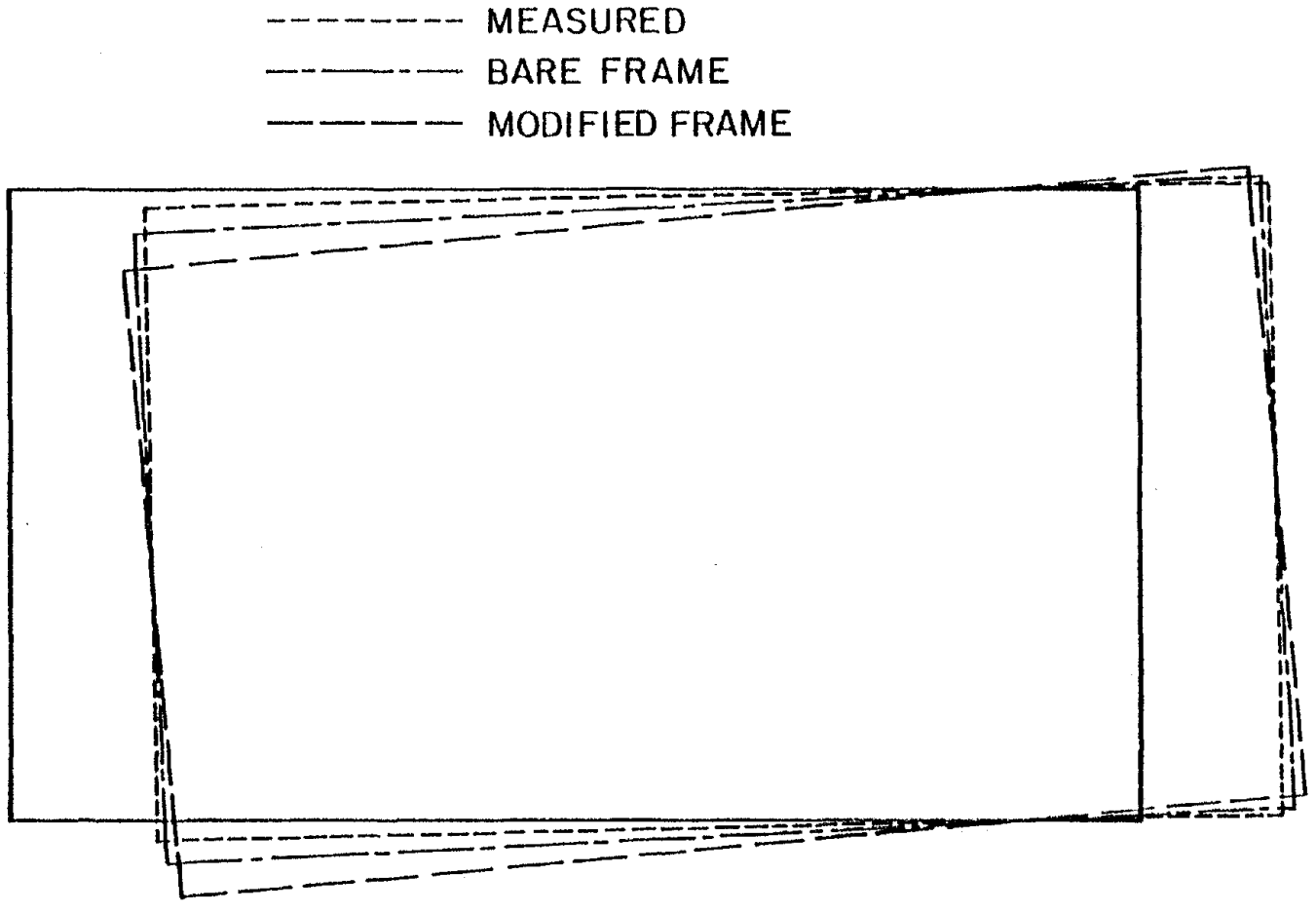

Figure 6.8. X Plan Model Shapes for the Arts Tower.

Forces and moments resulting from static and earthquake loadings were not calculated for the TABS-77 program is unable to cope with as many elements as the Arts Tower contains.

6.5 Concluding Comments

An examination of the results produced by the two models indicates that in this type of building the glazing can contribute to the overall lateral and torsional stiffness of the structure. Heretofore glazing was not considered to be an important stiffness element but in this case where the exterior columns act directly as mullions it is likely to be more effective.

The interior partitions as in all other buildings previously examined have an important role affecting the structural behavior. In the Arts Tower the partitions not only add to the stiffness of the column lines in which they occur but they also form a grid which forces the flange portions of the interior cores and the exterior columns to participate fully in providing stiffness and accordingly reduce shear lag effects. According to Sparks (27) these interior partition walls certainly take part in carrying some of the lateral load which the wind exerts on the Arts Tower. The walls are cracked and these cracks can be seen opening and closing during windy days.

The underestimation of the torsional frequency may be due to the fact that no account was taken of the warping restraint provided by the very stiff floors which effectively increase the torsional stiffness of the columns and cores.

In general the TABS-77 program was not designed to analyse the tube-in-tube type of structure and perhaps this accounts for the lack of adequate agreement between measured dynamic characteristics and calculated ones. Further, the program lacked the capacity to perform some of the computations that were made on the buildings in Plymouth.

According to Khan (23) there exists a need for special progams to cope with this type of structure. He thinks that attempting to apply any normal program to even preliminary design for this type of building of moderate size may prove too expensive. Certainly TABS-77 cannot cope adequately with the Arts Tower.

CHAPTER VII. THE GARSTON MODEL

7.1 Geometry and Location

The Garston model is not a full scale building. It is a quarter-scale model constructed in the laboratory of the Building Research Establishment of the Department of the Environment at the Building Research Station, Garston, Watford, England. This model is one of a large panel building. So far as is known no full-scale tests have been conducted on a structure of this type; this large model is the only known source of experimental data for this type of structural system.

This model is not small for it is very close to 12 m high and it represents an 18 story large panel buiding. It has six cross walls which are labeled walls 1 to 6 in Figure 7.1. There is a spine wall which is located through the center of the model parallel to the longer dimension of the rectangular structure. The combination of cross walls and spine wall divide the five bay areas of each story in ten sections. Figures 7.2 through 7.5 show four elevation views at the different sections shown in Figure 7.1. These views show the general arrangement of door and window openings in the model.

The walls and floors of the model were not cast as one piece and, as a result, they are not monolithic. Floors and walls were precast as panels with complex edge detailing so that the joints made during construction would be easily finished for each joint provided its own formwork. Each of the wall and floor panels were 45 mm thick except those of the central core which were 55 mm thick. The central core was designed to represent the elevator shaft.

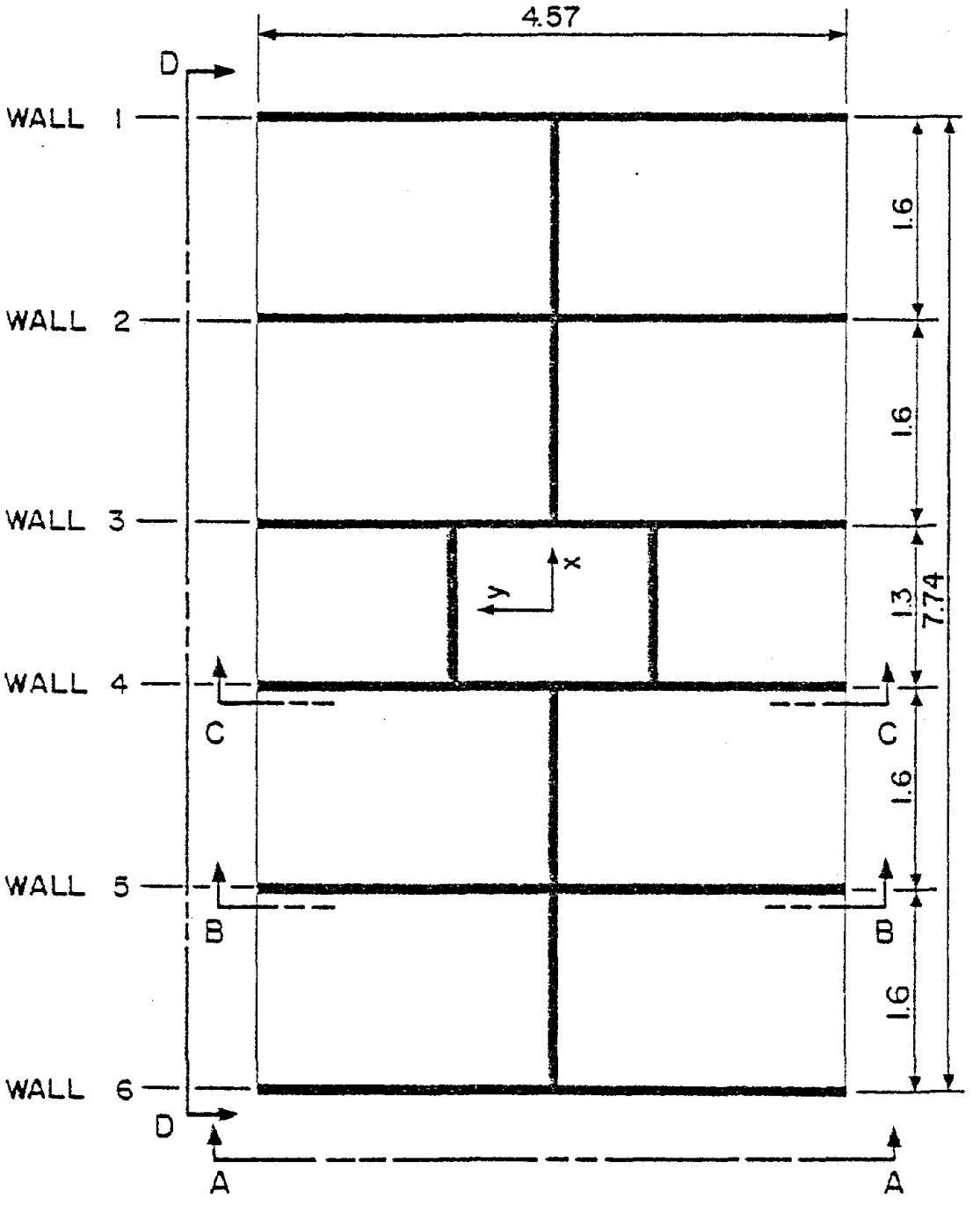

Figure 7.1. Typical Plan View of the Garston Model (All Dimensions in Meters).

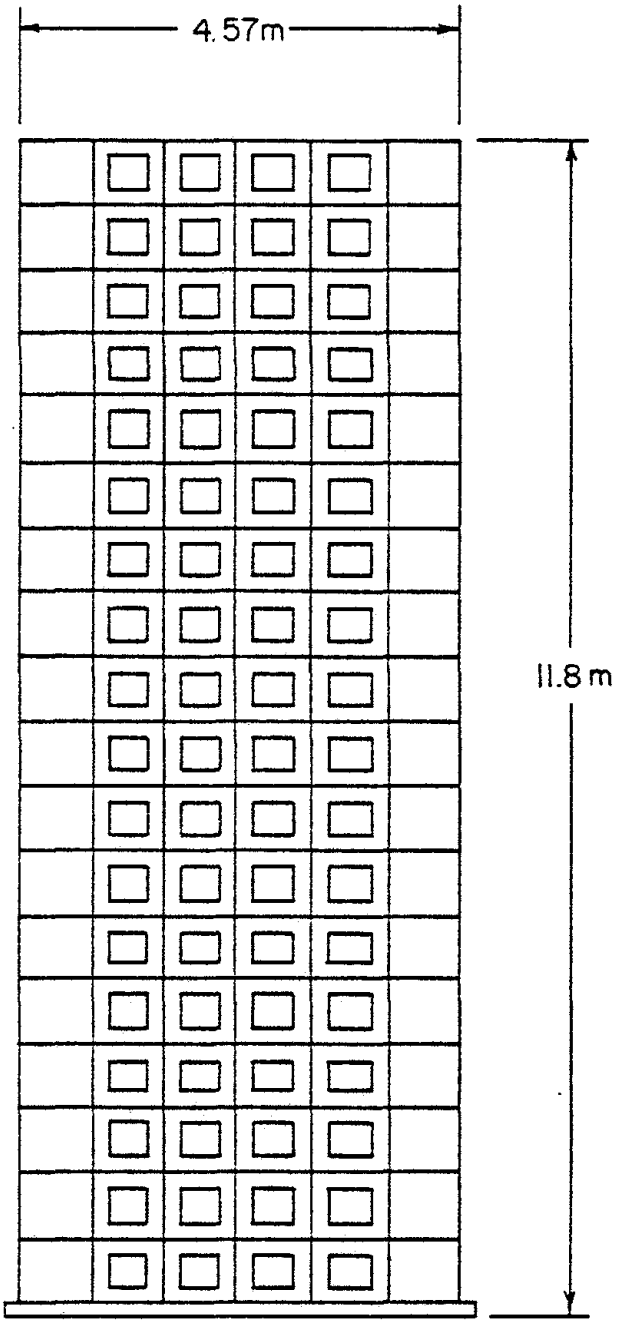

Figure 7.2. Elevation View of the Garston Model in the Short Direction.

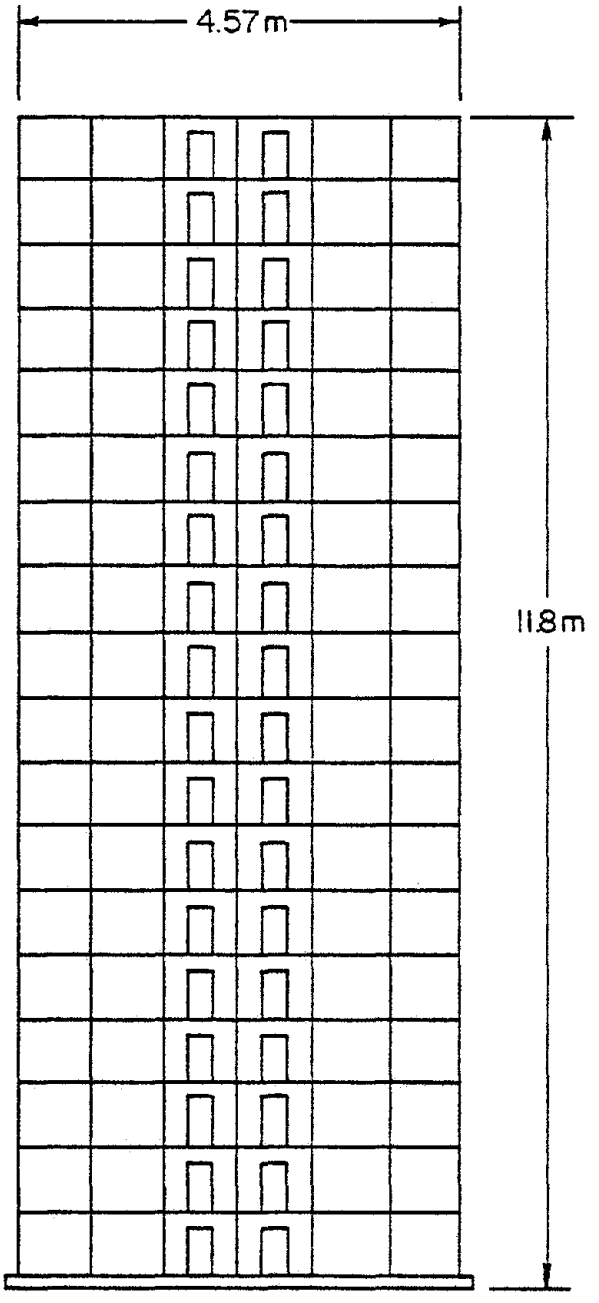

SECTION B-B

Figure 7.3. Elevation View of the Garston Model in the Short Direction.

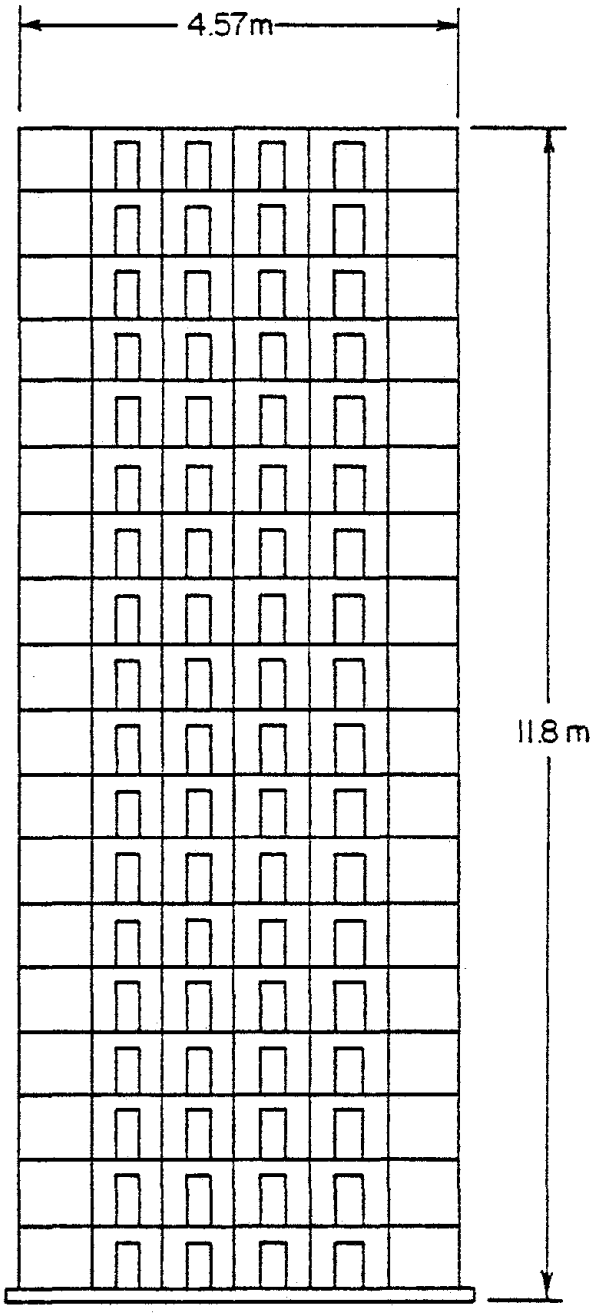

SECTION C-C

Figure 7.4. Elevation View of the Garston Model in the Short Direction.

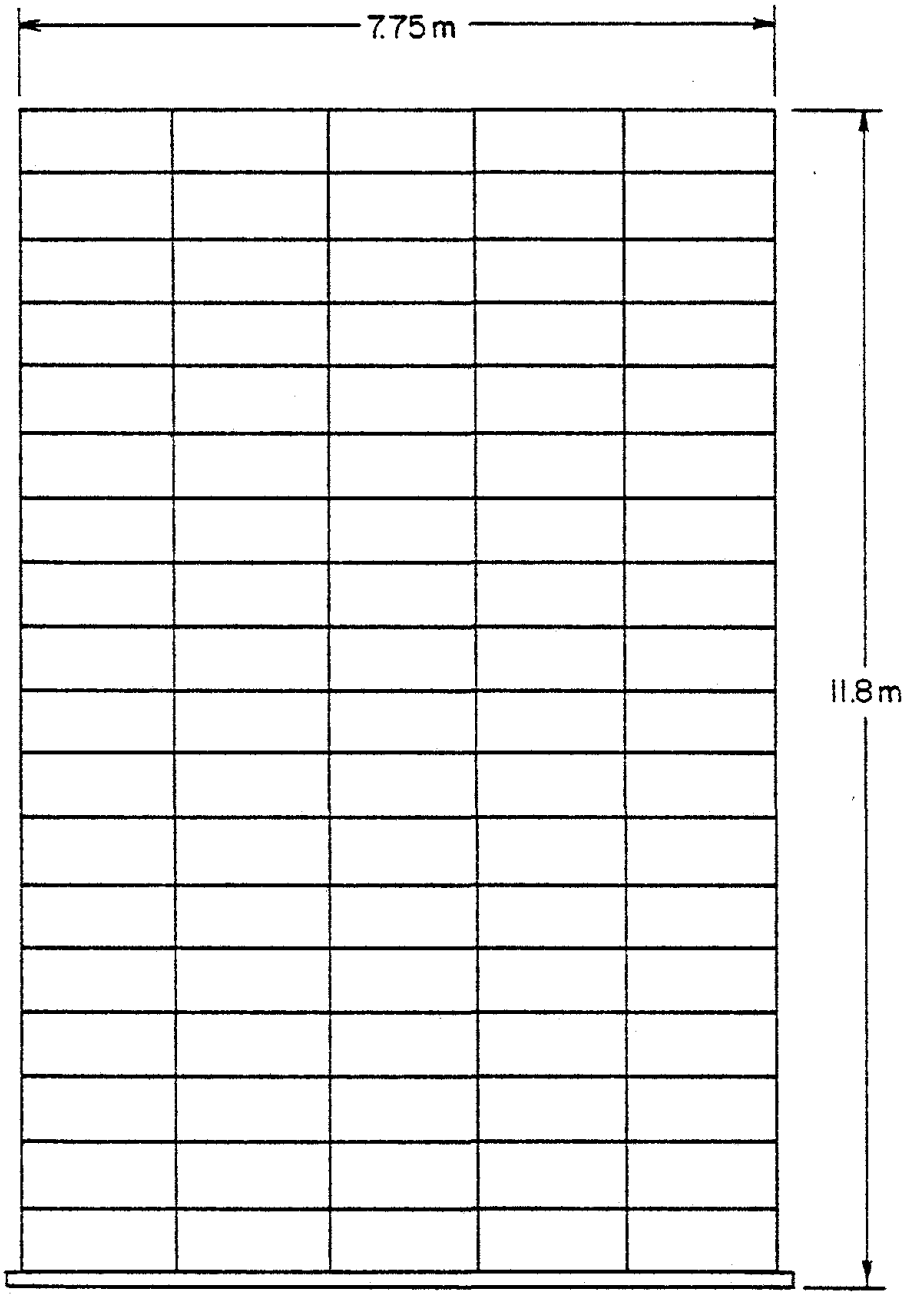

SECTION D-D

Figure 7.5. Elevation View of the Garston Model in the Long Direction.

A special feature of the Garston model was its foundation. It was built on a reinforced concrete foundation raft. All of the walls and the central core were provided with small stub walls, 150 mm by 100 mm, for attaching them to the foundation raft except wall 6 and the adjacent bay length of the spine wall. Wall 6 and its adjacent spine wall were constructed on specially prepared ground beams, one beam supporting wall 6 and the other, at right angles, supporting a bay length of the spine wall. These two beams were supported on a total of seven jacks which could be manipulated to simulate various foundation movements. The model and its foundations are described in detail by Kumar and Dupuch (24) and by Sparks, Jeary and deSouza (25).

7.2 Experimental Procedures

The Garston large panel model was tested using an omnidirectional vibrator mounted on top of the building core. Although this model was designed and constructed in a highly symmetrical manner, the x mode exhibited considerable torsional response, and the y mode was completely coupled with the torsional mode, apparently sharing the same natural frequency.

In addition to the dynamic tests a series of static tests were run with horizontal static loading applied directly to the model. This was intended to simulate wind loading. It was applied at each floor level through a series of hydraulic jacks. Further details of these tests are given in reference (24) and (25).

7.3 Structural Analysis

The Garston mdel was analyzed first in the y direction. Inspection of the views shown in Figures 7.2, 7.3, and 7.4 shows regularly patterned openings in each of the cross walls and some method of adjustment had to be devised to account for their effects on the wall panels. According to MacLeod (26) shear walls or any wall panel which contain rows of regular holes may be approximated by a beam and column system. His technique was applied to the cross walls in the Garston model, and they were taken as a series of parallel frames. The spine wall and core were taken as a monolithic unit and treated analytically as a single column. TABS-77 was used to compute the dynamic characteristics of the model.

The Garston model was found to have a computed frequency of 5.80 Hz in the y direction. This contrasts with a measured frequency of 3.85 Hz. Figure 7.6 shows that this beam and column idealization is inadequate for predicting mode shape in this direction. The predicted mode shape, as was expected, shows slight framing action which appears to be absent from the measured mode shape. This suggests that the cross walls really do act as shear walls and MacLeod's method is perhaps not the best in this situation. Thus another approach was attempted.

It seemed logical to treat the cross walls as solid walls each having its thickness reduced to approximate the effect of the holes. This was done. The new solid walls had the same volume as the original pierced walls, and the new thickness was computed to be 40 mm. The cross walls were modelled in the TABS-77 program as a series of parallel

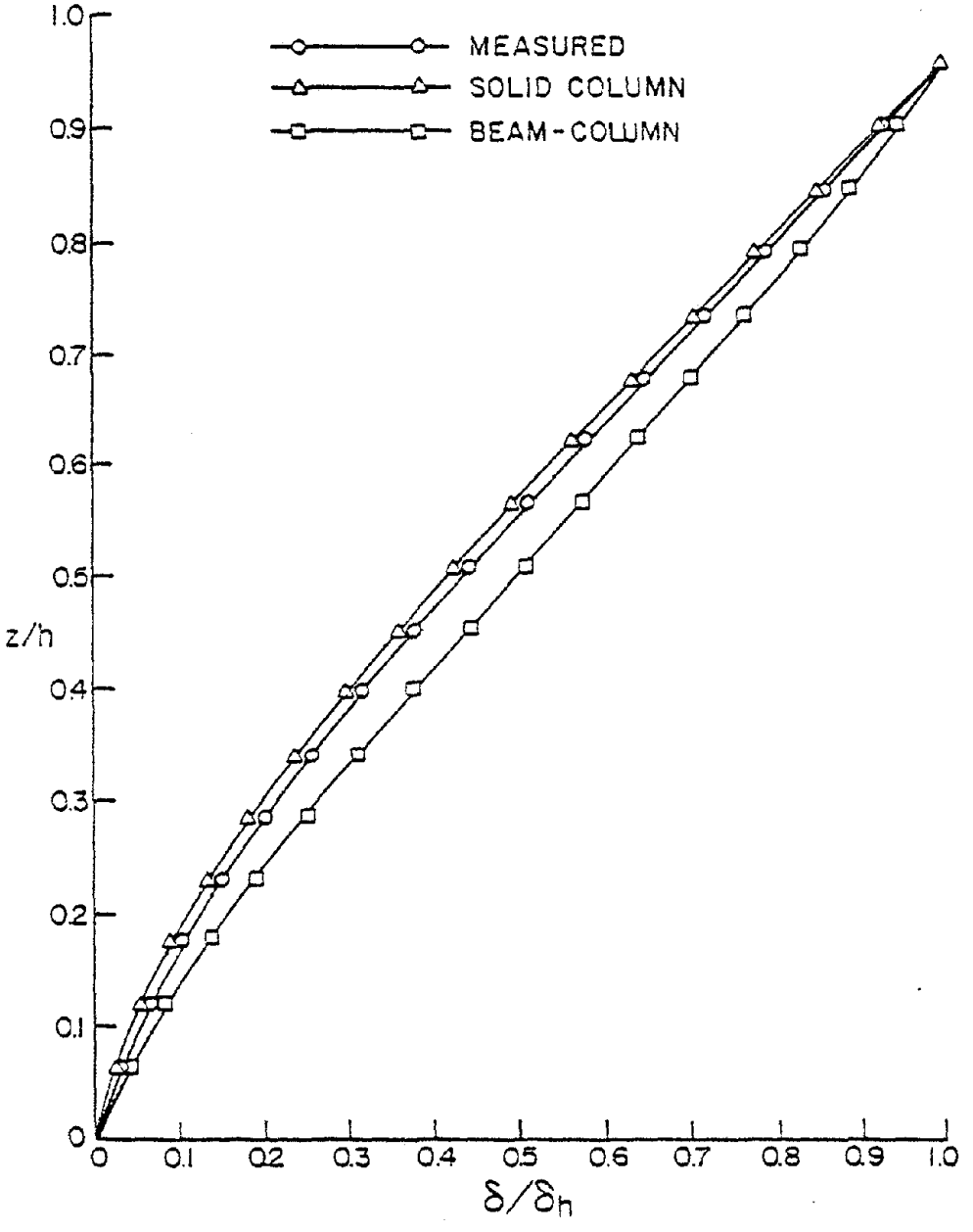

Figure 7.6. Y Mode Shapes of the Garston Model.

single columns. This resulted in a computed natural frequency of 5.60 Hz in the y direction which is not significantly different from the value computed using the MacLeod assumption. However the mode shape computed with this new approximation was in excellent agreement with the measured mode shape. Although the MacLeod approach predicts the overall lateral stiffness to be nearly the same as the solid wall approach, the distribution of the stiffness throughout the height of the structure as is manifest by the mode shape leaves something to be desired. The solid wall assumption is clearly superior.

Further, both MacLeod's assumption and the solid wall assumption were used to compute the displacement of the Garston model under the set of lateral loads shown in Figure 7.7. These loads were applied to the model in the Building Research Establishment laboratory and the displacements were measured. In addition, Kumar and Dupuch (24) reported the predicted lateral displacements of the model using a finite element approach. For the y direction the average measured displacement at the top floor was 0.70 mm with some rotation being detected. Each of the computational methods predicted a displacement very close to 0.31 mm without rotation. Thus each of the idealizations, MacLeod's as well as the solid wall and the finite element, predicted an overall lateral stiffness which was twice that of the tested structure. This is a fact of some significance.

In the x direction the Garston model was idealized as a very large monolithically connected unit such that the cross section could be described as being an outsized I-beam with intermediate flanges. For

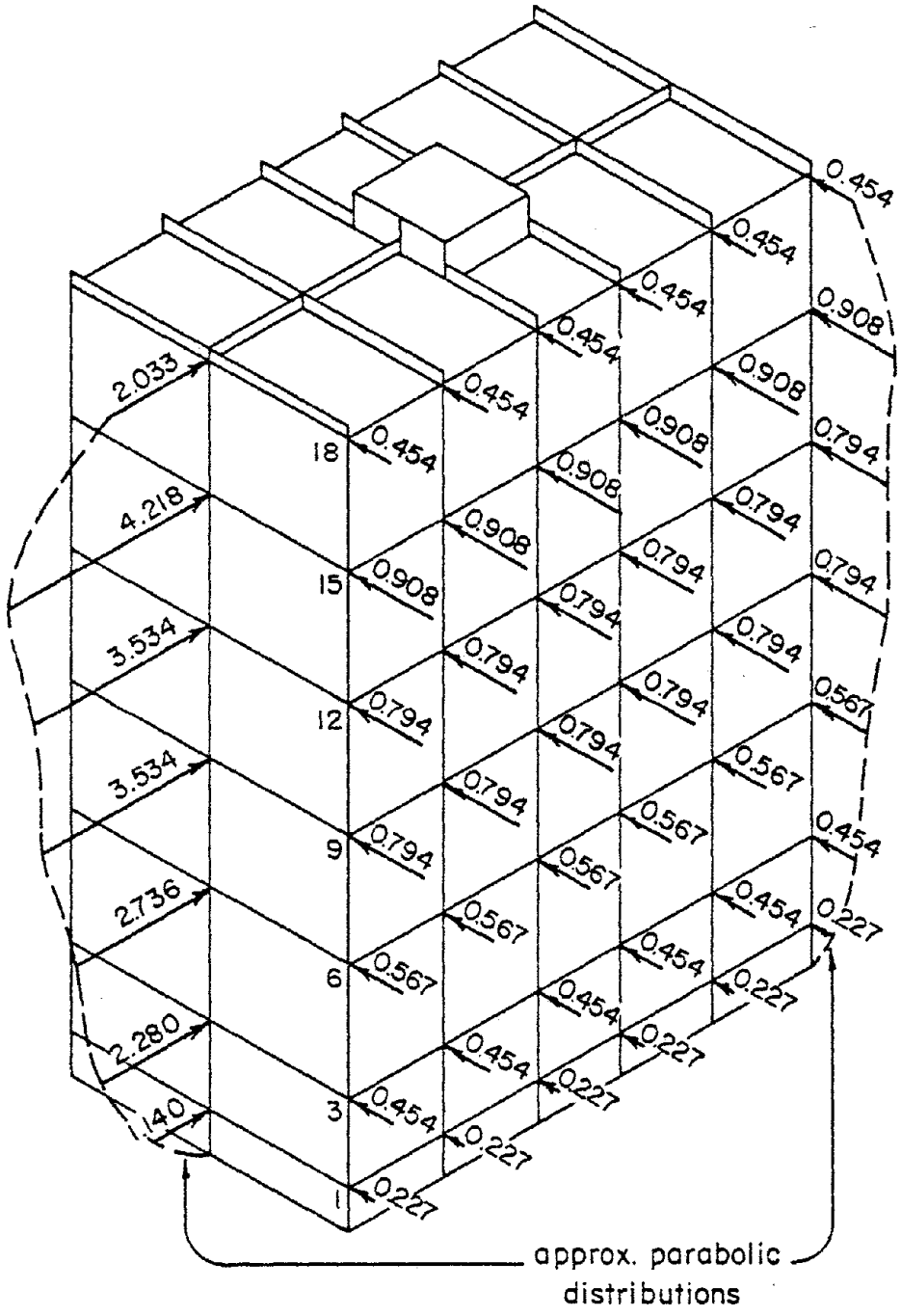

Figure 7.7. Applied Static Load to the Garston Model (Newton).

the first analysis it was assumed that the entire cross section was effective and no allowance was made for shear lag effects, even though experience with other buildings described in previous chapters indicated that this was not necessarily the best assumption. The no-shear-lag-effect idealization computed a frequency in the x direction of 8.10 Hz as compared to the measured frequency in this direction of 4.65 Hz. Figure 7.8 shows that this idealization produced a good match with the measured mode shape.

Then the section was modified to compensate for shear lag effects in accordance with Timoshenko's recommendation (19). The computed natural frequency was then found to be 6.50 Hz which is certainly an improvement over 8.10 Hz but it is still considerably higher than the measured value of 4.65 Hz. This idealization produced no detectable change in the mode shapes from that shown in Figure 7.8.

A computation was made for the lateral displacement under lateral static loading for the section corrected for shear lag effects. This was found to be 0.15 mm at the top floor level. The average measured displacement at this level under the same loading was 0.29 mm. Thus, even after modification for shear lag effects, the measured displacement was twice the computed value.

Choosing the idealization in each direction which best fitted the measured values, i.e. the solid walls in the y direction and the reduced stiffness in the x direction, computations were made of the dynamic characteristics in the Θ direction. The torsional frequency was computed as 5.82 Hz. This contrasts with a measured torsional frequency

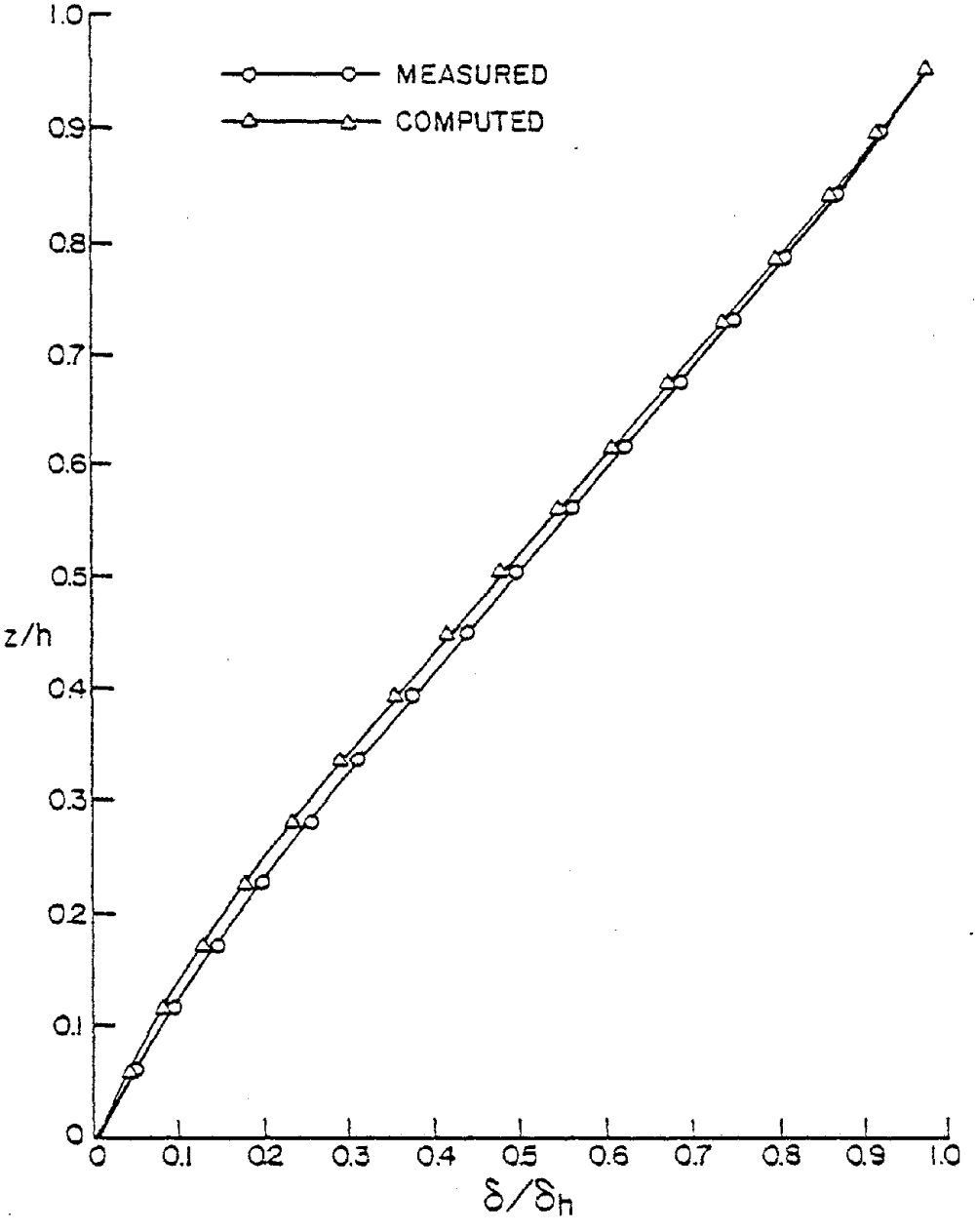

Figure 7.8. X Mode Shapes of the Garston Model.

of 3.85 Hz. Once more, this indicates that the computed torsional stiffness is about twice the measured stiffness.

The above analyses indicated that all fundamental frequencies had been overestimated by a factor of nearly 1.4 or that the best idealizations attempted resulted in the mathematical model being twice as stiff in all directions as the actual structure was measured to be. Since the translational and torsional stiffnesses had all been overestimated by the same factor, this was an indication of some discrepancy which was common to both translational and rotational computations. Obviously the stiffness of the mathematical model had to be reduced in some manner if the experimetnal results were to be matched. After close study of the published information concerning the design and construction of the Garston model, it appeared that the joints between the panels comprising the walls might allow some movement to occur in the form of rotation and shear between adjacent panels. Thus the walls and the structure as a whole were probably more flexible than was assumed in the mathematical modelling where the existence of the jointing was ignored.

The most logical way of introducing some flexibility throughout the walls of the structure was to operate on the modulus of elasticity although other stiffness factors could have been varied. The modulus of elasticity of the walls was reduced, in steps, until a computation matched the experimental results. As expected, both translational and rotational dynamic characteristics improved the same amount. The computed frequencies for all directions matched the measured ones when

the E value was reduced to 56 per cent of the actual E value. The elevation mode shapes remained unchanged.

Even though a model had now been made which matched all frequencies measured and the elevation mode shapes, the model did not yet reflect the coupling that was evident from the measured plan mode shapes. The measurements of plan mode shape indicated that some torsion existed in the x mode while the y mode was completely coupled with the torsional mode. The y mode and the torsional mode also had exactly the same natural frequency. Since there was coupling in both directions, there must have been a double eccentricity of the mass or stiffness centers. There was no obvious reason for these eccentricites in the symetrical layout of the Garston model.

As was mentioned in section 7.1, there was a special beam under wall 6 which permitted adjustment of wall 6 to simulate differential settlement. The jacking was activiated so that wall 6 was lowered somewhat to simulate settlement prior to testing the structure. This would have relieved wall 6 of some of its load and certainly introduced an element of assymmetry to the structure in the y direction, changing the distribution of stiffness in that direction. This was introduced to the mathematical model by reducing the stiffness of the wall over the beams. The new stiffness of wall 6 was taken as that which would match the measured rotation of the entire structure resulting from the lateral static load in the y direction. As was pointed out earlier, the symmetrical loading produced some rotation. The stiffness was reduced in steps until the calculated displacements under the static load

matched the observed values. This occurred when the stiffness of wall 6 was 80 per cent of its initial value.

The experimental results indicated that there was some eccentricity in the x direction. This could not be explained on the basis of the stiffness center being different than the center of geometry for the plan showed an axis of symmery about the x axis. Eccentricity therefore could not exist in the x direction unless the center of mass was different from the center of stiffness. Study of published information on the Garston model yielded absolutely no reason for the center of stiffness to have been different from the center of geometry in the x direction. The only remaining possibility was that the center of mass was different from the center of stiffness and, in this case, different from the center of geometry. It was noted that superimposed loads were added to the Garston model prior to dynamic testing. It might have been possible that the placement of these small masses throughout the structure was not strictly symmetrical.

In attempting to improve the idealization so that coupling in the x direction could be properly calculated that there was some guidance available from the measured plan mode shapes. The plan mode shapes suggested the direction in which the center of mass should be moved but offered no help in deciding how far the mass center should be moved. This was determined by trail and error until the computed plan mode shape approximately matched the measured one. This was quite time consuming for changing a parameter in one direction resulting in changing dynamic characteristics in all directions; the parameters were

not independent. Coupling upset results in the y direction and then this had to be compensated for by moving the mass center again. It is believed that the fact that torsional frequency was apparently identical to the y translational frequency complicated the problem. Figures 7.9 and 7.10 show a comparison between the measured and computed plan mode shapes for the x and y directions.

The discovery of only two fundamental natural frequencies had caused considerable concern at the time the dynamic tests were carried out. In an attempt to identify a third mode the model was excited by the random loading caused by air turbulence generated by the laboratory air conditioning system. Recordings were made of signals from accelerometers mounted on the model roof in such a way that they would respond to both translation and torsion. Analysis of these results showed only two peaks in the acceleration spectrum. If a third peak existed at the third fundamental frequency, it could not be resolved.

It was first thought surprising that the building appeared to twist about a point between the center and the weak wall 6. Careful consideration of the problem during this project provided an explanation. If it is assumed that the center of stiffness was in fact on the other side of the center of the model to wall 6 then if the y translational mode was excited and its frequency was slightly higher than the torsional mode. The initial torque applied by the center of mass about the center of stiffness, would be applied above resonance and twisting would occur in antiphase to the translation. The resulting mode shape would then appear to consist of rotation about a point on the

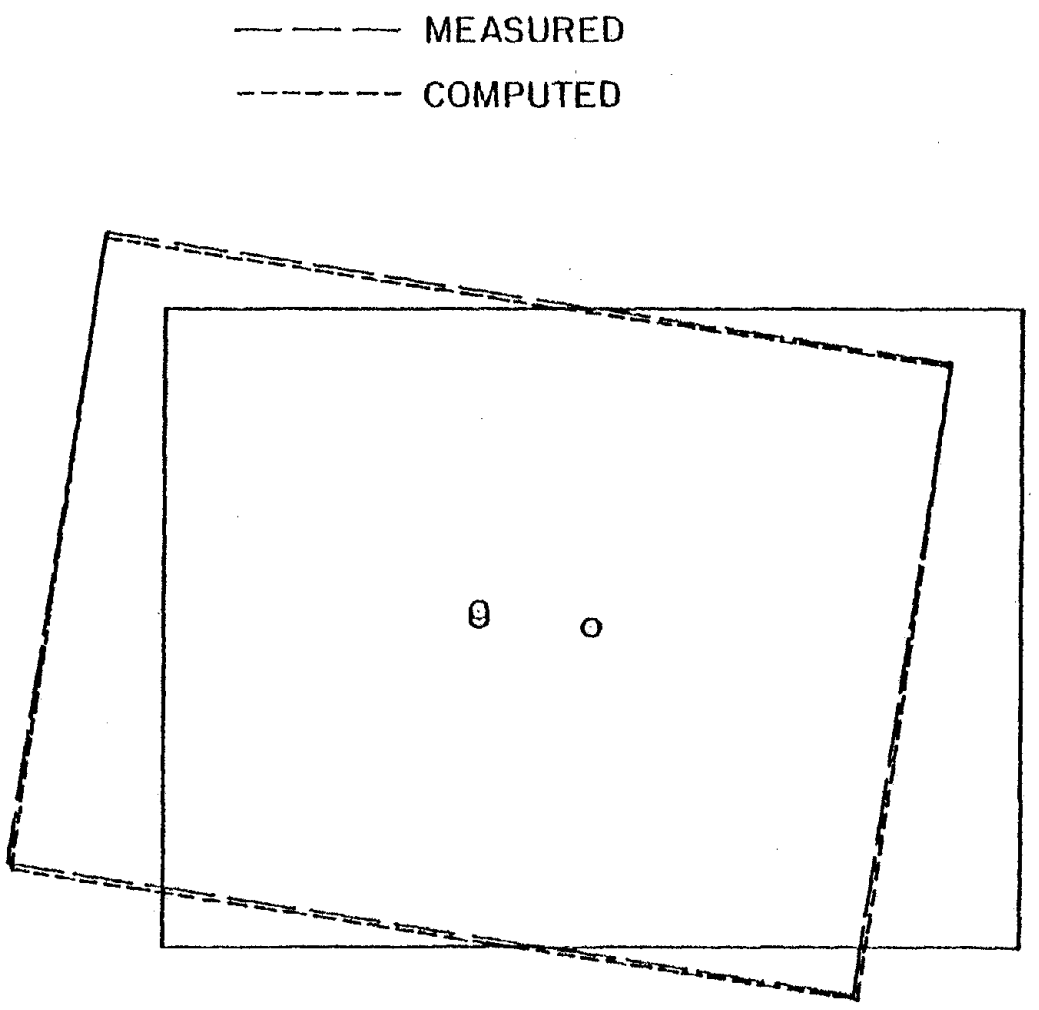

Figure 7.9. X Plan Mode Shapes for the Garston Model

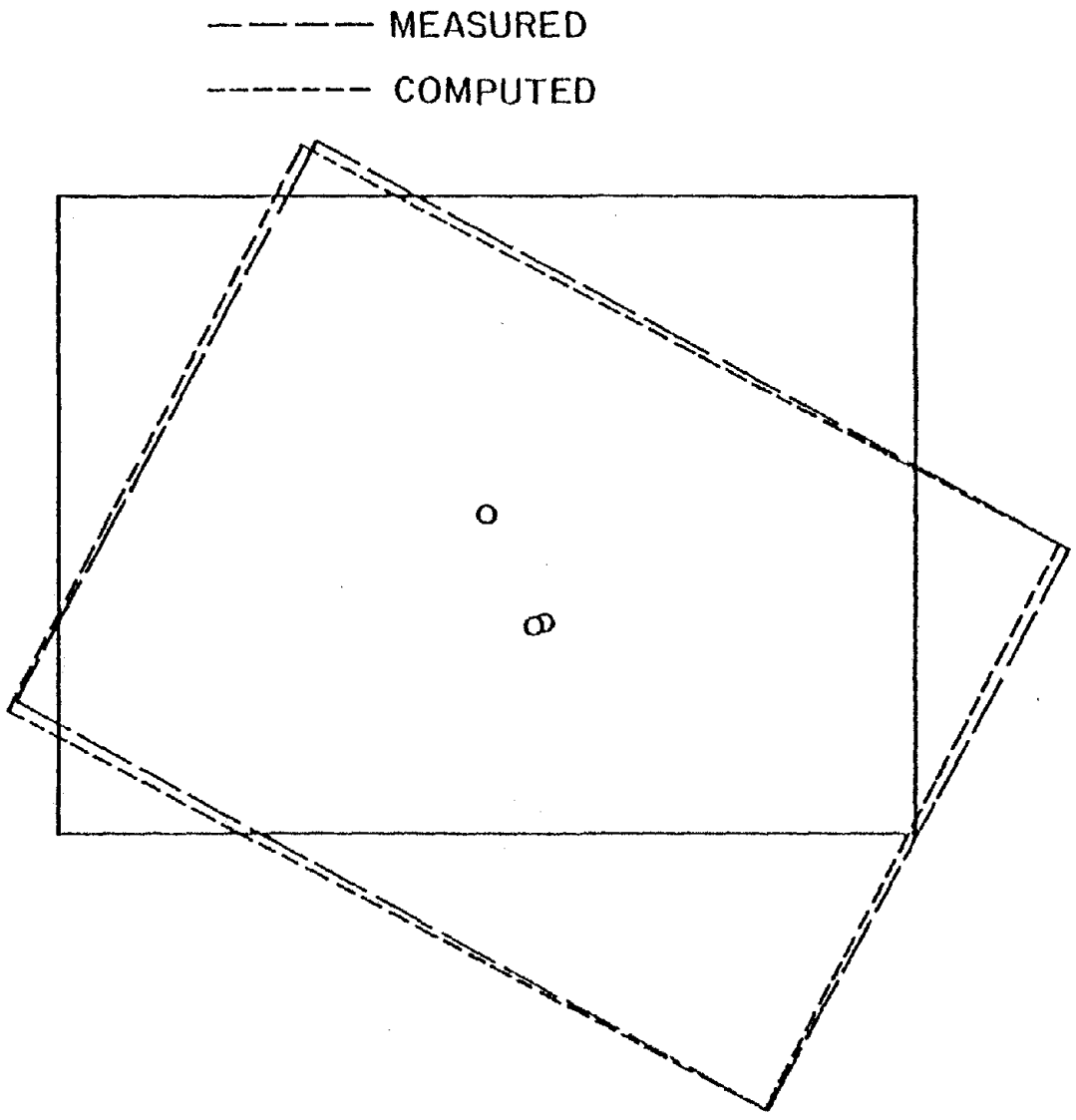

Figure 7.10. θ Plan Mode Shapes for the Garston Model

wall 6 side of the center line. This effect would be very pronounced since the frequencies were apparently very close.

So apparently the second and third fundamental frequencies had been observed and any matching of three dimensional mode shapes had to reflect that fact.

7.5 Concluding Comments

The Garston model was a large panel structure and joints existed wherever two panels met. Joint rotation is likely to make this type of structural system more flexible than that normally predicted by standard structural computer programs or by standard finite element programs which do not make allowances for this. In this instance the stiffness of the structure was overestimated by a factor of 2.

In analysing large panels acting as shear walls containing regular rows of openings it was shown that the beam-column system of approximation does not adequately predict building performance while a simple reduction in the thickness of the walls, making the walls solid but equivalent in volume to that of the actual walls, yielded excellent results.

Shear lag effects exist in this large panel structure. However no cladding was used along the faces comprising the long dimension of the Garston model nor were nonstructural partitions included. Partitions and cladding, had they been modelled, probably would have made the cross wall and its flanges more efficient but this would, at the same time, have introduced considerable load into these nonstructural members,

possibly causing damage and, in the case of cladding, lack of weather tightness.

The Garston model exhibited a high degree of coupling. This was attributed to a small differential settlement of one end of the structure. Even symmetrically applied dynamic loading, given this type of coupling, would have caused a very severe torsional response.

CHAPTER VIII. CONCLUSIONS AND RECOMMENDATIONS

Proper mathematical modelling of structural performance under lateral static and dynamic loading is both an art and a science. The most rigorous theoretical model existing today requires some idealization, and the application of engineering judgement is necessary in evaluating input parameters. A major purpose of this study has been to improve these input parameters. This has been done by successively refining analytical models to take account of the effects of partitions and cladding and the inefficiency of structural members, until a match was achieved between the predicted and observed dynamic characteristics of five concrete buildings.

Previous work in this area has concerned itself mainly with matching frequencies in the analytical model and concluding that when the computed frequencies matched the experimental frequencies, then an accurate evaluation of building performance was possible. This study shows that not only frequency matching is important but mode shapes must be matched as well. Mode shape is a manifestation of the stiffness distribution throughout the height of the building. Inappropriate modelling of this can seriously alter the evaluation of loads carried by the structural elements.

Internal partitions and cladding not only add stiffness to the structure but also change the mode shape. This study indicates that these 'nonstructural' elements, as commonly placed and fastened to the frame, do attempt to carry load and thus provide stiffening for frames and floors.

While shear walls and elevator cores are very effective elements in providing lateral stiffness, this study has pointed out that not all of the cross section is effective in bending. This is a shear lag effect. The traditional assumption that cores are fully effective leads to an overestimation of the load carried by them and to an underestimation of the load carried by other elements in frames containing cores. This could result in serious damage to a building under severe loading conditions.

Previous work has shown that the interaction between a frame and a shearwall is such that increasing the shear wall stiffness relative to the frame does not produce a proportional increase in the overall lateral stiffness of the structure. Since the frequency is proportional only to the square root of the overall stiffness, large changes in shear wall stiffness produce relatively small changes in frequency. This study confirms that this is indeed the case. However, this study also shows that mode shape, along with everything implied by mode shape, is extremely sensitive to changes in stiffnesses of shear walls and cores. Since shear lag has a significant effect on the stiffness of cores, reducing their stiffnesses, it follows that while the resulting inaccurate modelling may not affect frequency very much, it can have a great effect on mode shape.

In large panel types of structures there is an indication from this study that the stiffness is overestimated. This is probably due to the assumption of no joint rotation. Apparently, in the large panel structure studied, there was considerable joint rotation.

It may be concluded that certain changes in current practice ought to adopted by designers. The following recommendations are made:

1. Wherever possible building plans should be symmetrical. This applies to partitions and cladding as well as columns and all forms of shear walls.

2. If a frame line is stiffened by any means, it must be recognized that its members will carry more load.

3. Partitions and cladding should either be designed to carry loads or they must be designed and fastened so that they do not carry loads.

4. Recognition should be given to the fact that stiffening the floor slab in a flat slab type of construction is an efficient and effective means of providing overall lateral stiffness.

5. The inefficiency of thin walled members formed by shear walls should be recognized. This inefficiency is a result of shear lag effects.

In conclusion, using a standard computer program in conjunction with the results of some relatively simple vibration tests has enabled a great deal of information to be gleaned about the behavior of various types of buildings. Since this has shown that there are considerable inaccuracies in present design practice this type of work ought to be extended to other buildings so that better guidance can be provided for designers. In addition, some of the aspects discovered in this investigation ought to be studied in more detail with the aid of physical models and finite element analytical models, using the present results to establish accurate initial models. This investigation has

also been restricted to linear performance of buildings. Clearly if such buildings were subjected to a severe earthquake they would not continue to perform in the manner predicted by these matched analyses. Their inelastic behavior is likely to be quite different from that considered possible by the designer. Future work should consider the likely implications of incorrect structural modelling on the nonlinear performance of buildings.

REFERENCES

1. Holmes, M. "Steel Frames with Brickwork and Concrete Infillings," Institution of Civil Engineers, Vol. 19, 1961, pp. 473-478.

2. Smith, B. S. "Lateral stiffness of infilled frames," Journal of Structural Division Proceeding of American Society of Civil Engineers, December 1962, pp. 183-198.

3. Mallick, D. V. and Garg, R. P. "Effect of Openings on the lateral stiffness of infilled frames," Institution of Civil Engineers, Vol. 48-49, 1971, pp. 193-210.

4. Raggett, J. D., "Influence of Nonstructural Partitions on the Dynamic Response Characteristics of Structures," John A. Blume & Associates Research Division, San Francisco, California, July 1972.

5. Gjelsvik, A. "Interaction Between Frames and Precast Panel Walls," Journal of the Structural Division American Society of Civil Engineers, February 1974, pp. 405-426.

6. El-Dakhakhni, W. M. "Shear of Light-Gage Partitions," Journal of the Structural Division American Society of Civil Engineers, July 1976, pp. 1431-1445.

7. El-Dakhakhni, W. M. "Effect of Light-Gage Partitions on Multistory Buildings," Journal of the Structural Division American Society of Civil Engineering, January 1977, pp. 119-132.

8. Oppenheim, I. J., "Dynamic Behavior of Tall Buildings with Cladding," Fifth World Conference on Earthquake Engineering, Rome, Italy, June 1973, pp. 2769-2773.

9. Khan, F. R. and Sbarounis, J. A., "Interaction of Shear Walls and Frames," Journal of the Structural Division Proceeding of the American Society of Civil Engineers, June 1964, pp. 285-335.

10. Coull, A. and Smith, B. S., "Analysis of Shear Wall Structures," Tall Buildings, Proceeding of Symposium on Tall Buildings with Particular Reference to Shear Wall Structures, Pergamon Press, New York, 1967, pp. 139-155.

11. Williams, C., "The Real Performance of Some Civil Engineering Structures," Ph.D. Dissertation, Construction Studies Group, School of Engineering Science, Plymouth Polytechnic, March 1979.

12. Baruh, H., "Parameter Identification and Control of Distributed-Parameter Systems," Ph.D. Dissertation, Virginia Polytechnic Institute and State University, August 1981.

13. Goodno, B. J. and Will, K. M., "Dynamic Analysis of a Highrise Building Including Cladding-Structure Interaction Effects," Proceedings American Society of Civil Engineers, Specialty Conference on Computing in Civil Engineering, Atlanta, Georgia, June 1978, pp. 623-638.

14. Will, K. M. and Goodno, B. J. and Saurer, G., "Dynamic Analysis of Buildings with Precast Cladding," Conference on Electronic Computers, Publication by American Society of Civil Engineers, New York, New York, 1979, pp. 251-264.

15. Wilson, E. L., Dovey, H. H. and Hobibullah, A., TABS-77, Three Dimensional Analysis of Building Systems, University of California, Berkeley, California, February 1977.

16. Jeary, A. P. and Sparks, P. R., "Some Observations on the Dynamic Sway Characteristics of Concrete Structures," Vibrations of Concrete Structures, Publications SP-60, American Concrete Institute, Detroit, Michigan, 1979, pp. 155-180.

17. American National Standards Institute, "Building Code Requirement for Minimum Design Loads on Buildings and Other Structures," A58.1-1972.

18. Clark, W. J. and MacGregor, J. G., "Analysis of Reinforced Concrete Shear Wall-Frame Structure," Structural Eng. Report No. 16, University of Alberta, Nov. 1968.

19. Timoshenko, S. P. and Goodier, J. N., Theory of Elasticity, McGraw-Hill, 1951, pp. 171-177.

20. Brotchie, J. F. and Russell, J. J., "Flat Plate Structures," ACI Journal, August 1964.

21. Jeary, A. P., "The Dynamic Behavior of the Arts Tower, University of Sheffield, and Its Implications to Wind Loading and Occupant Reaction," Building Research Establishment, Garston, Watford, Current Paper, CP48178, 1978.

22. Derecho, A. T., "Frames and Frame-Shear Wall Systems," Response of Multistory Concrete Structures to Lateral Forces, Publication SP-36, American Concrete Institute, Detroit, Michigan, 1973, pp. 13-40.

23. Khan, F. R., "Analysis and Design of Framed Tube Structures for Tall Concrete Buildings," Response of Multistory Concrete Structures to Lateral Forces," Publication SP-36, American Concrete Institute, Detroit, Michigan, 1973, pp. 39-60.

24. Kumar, S. and Dupuch, G. W., "Design Details and Pseudo-Wind Loading Tests on an 18 Story Quarter Scale Panel Structure," Building Research Establishment, Garston, Watford, N150176, 1976.

25. Sparks, P. R., Jeary, A. P. and deSouza, V. C., "A Study of the Use of Ambient Vibration Measurements to Detect Changes in the Structural Characteristics of a Building," Proceeding of the Second A.S.C.E. Specialty Conference on Dynamic Response of Structures: Experimentation, Observation, Prediction and Control, ASCE, Atlanta, Georgia, January 1981, pp. 189-216.

26. MacLeod, I. A., "Lateral Stiffness of Shear Walls with Openings," Tall Buildings, Proceeding of Symposium on Tall Buildings with Particular Reference to Shear Wall Structures, Pergamon Press, New York, New York, 1967, pp. 223-244.

27. Private communication with P. R. Sparks.